2015

Cellular function and structure of primary cilia

Ashraf M. Mohieldin
University of Toledo

A Dissertation

entitled

Cellular Function and Structure of Primary Cilia

by

Ashraf M. Mohieldin

Submitted to the Graduate Faculty as partial fulfillment of the requirements for the

Doctor of Philosophy Degree in Medicinal Chemistry

_____

Dr. Surya M. Nauli, Committee Chair

_____

Dr. Youssef Sari, Committee Member

_____

Dr. Zahoor A. Shah, Committee Member

_____

Dr. Hermann Von Grafenstein, Committee Member

_____

Dr. Marcia McInerney, Committee Member

_____

Dr. Patricia R. Komuniecki, Dean

College of Graduate Studies

The University of Toledo

August 2015

An Abstract of

Cellular Function and Structure of Primary Cilia

by

Ashraf M. Mohieldin

Submitted to the Graduate Faculty as partial fulfillment of the requirements for the Doctor of Philosophy Degree in Medicinal Chemistry

The University of Toledo
August 2015

The dysfunction of primary cilia has been linked to a list of diseases, now known as ciliopathy disorders. As a result, the primary cilia have been the focus of intense research and clinical studies for the past years. Even though many ciliary proteins of primary cilia have been identified, there are still many to be recognized. Therefore, we were interested in studying the primary cilia in depth to fully understand their function and structure. Here we report that primary cilia exhibit a swelling membrane structure, which based on their unique ultrastructure and motility, and could be mechanically regulated by fluid-shear stress. In addition, we for the first time reported that monosialodihexosylganglioside (GM3S) and bicaudal-c1 (Bicc1) were members of the primary ciliary proteins localized particularly on the ciliary swelling membrane structure. In doing so, we have developed a new differential side-view imaging technique and called it "The formvar-folding technique" where cells were grown on a flexible substratum. The technique allowed us to record and measure cilioplasm calcium signals, as well as performs ciliary protein localization and immunofluorescence studies.

However, the main challenge in studying the ultrastructure of primary cilia is particularly due to the high sensitivity of cilium to chemical fixation, which is required by many imaging techniques. To come over this issue, we have developed other techniques and used the combined freeze fracture transmission electron microscopy (FFTEM) and high pressure freezing (HPF) techniques to study the ultrastructure of primary cilia. We showed that the FFTEM/HPF is an inexpensive procedure that can be used to reveal the ultrastructure of primary cilia without the use of any chemical fixation and allows maintenance of the cilia morphology in its best natural form.

To further investigate the ciliary membrane proteins of primary cilia, we used a sensitive multidimensional protein identification technique (MudPIT) to generate a ciliary protein database. In this study, we reported 19 new ciliary proteins. Overall, our studies provided important steps to better understand the importance of primary cilia and how they play a role in ciliopathy disorders.

To my family and to the soul of my father, the first teacher, I dedicate this dissertation.

Acknowledgements

I owe my deepest gratitude to my mentor Dr. Surya Nauli. Without his help and support, it would not have been possible to conduct this study. I thank him for his encouragement, guidance, and support from the initial to the last level. I would also like to thank Dr. Abou-Alaiwi for his comments and Makiko Takahashi for the initial training. I offer my regards and blessing to all of my colleagues for providing a stimulating, and fun environment in which to learn and produce. I'm especially thankful to Dr. Shakila, Dr. Brian, Dr. Jin, Dr. Shao, Blair, Ali and Alzahra for their comments, suggestions and mutual friendship. Lastly, I would like to thank my family, especially my parents, and my siblings, Dr. Mohieldin, Dr. Shimaa, Dr. Marwa and my lovely wife Dr. Walla for their ultimate support and care.

Table of Contents

List of Tables

List of Figures

List of Abbreviations

ACE.....Angiotensin-converting enzyme
ADPKD.....Autosomal dominant polycystic kidney disease
ARPKD.....Autosomal recessive polycystic kidney disease
AT1 .....Angiotensin receptor

Bicc1 .....Bicaudal-c1

cAMP .....Cyclic adenosine monophosphate
CEMOVIS .....Cryo-electron microscopy of vitreous sections
CFTR .....Cystic fibrosis transmembrane conductance regulator

DIC.....Differential interference contrast

EGFR .....Epidermal growth factor
eNOS.....Endothelial nitric oxide synthase
ESRD .....End Stage Renal Disease
ET-1 .....Endothelin-1

FFTEM.....Freeze Fracture Transmission Electron Microscopy

GFP .....Green fluorescent protein
GM3 .....Monosialodihexosylganglioside
GM3S.....Monosialodihexosylganglioside synthase

HPF .....High pressure freezing

LLC-PK1.....Porcine kidney epithelial cells
LVH .....Left ventricular hypertrophy
LVMI .....Left ventricular mass index

MAPK.....Mitogen-activated protein kinases
MRI.....Magnetic resonance imaging
MS.....Mass spectrometer
mTOR .....Mammalian target of rapamycin
MudPIT.....Multidimensional protein identification technology

NO.....Nitric oxide

PKD1 .....Polycystin-1
PKD2 .....Polycystin-2
PKHD1.....Polycystic kidney and hepatic disease 1
RAAS.....Renin-angiotensin-aldosterone system

RPS-BLAST .....Reversed Position Specific BLAST

SCX.....Strong cation-exchange
SEM .....Scanning electron microscopy
SSTR3 .....Somatostatin receptor 3

TEM .....Transmission electron microscope
TRP .....Transient receptor potential

V2R.....Vasopressin receptor 2

List of Symbols

M .....Molar
μM.....Micromolar

μl .....Microlitter
ml .....Milliliter
μg .....Microgram

nm .....Nanometer
mm .....Millimeter

α .....Alpha

C.....Degrees Celsius
KV.....Kilovolt

Chapter 1

Autosomal Polycystic Kidney Disease: Pathophysiology and Treatment

Ashraf M. Mohieldin[1], Viralkumar S. Upadhyay[2], Albert C. M. Ong[3], Surya M. Nauli[1,2]

[1]Department of Medicinal and Biological Chemistry, The University of Toledo, Toledo, Ohio [2]Department of Pharmacology, The University of Toledo, Toledo, Ohio [3]Academic Unit of Nephrology, University of Sheffield Medical School, Sheffield S10 2RX, UK

Running title: ADPKD and Primary Cilium

Corresponding author:
Surya M. Nauli, Ph.D.
The University of Toledo
Department of Pharmacology; MS 1015
Health Education building; Room 274
3000 Arlington Ave
Toledo, OH 43614

Phone: 419-383-1910
Fax: 419-383-1909
Email: Surya.Nauli@UToledo.Edu

Abstract

Autosomal dominant polycystic kidney disease (ADPKD) is an inherited genetic disorder that results in progressive renal cyst formation and ultimately loss of renal function. Mutation in either *PKD1* or *PKD2*, which are the genes coding for polycystin-1 and polycystin-2, respectively, is the main cause of the disease. The mutation in *PKD1* accounts for 85% of all ADPKD cases, whereas only 15% of ADPKD cases result from *PKD2* mutations. ADPKD is a systemic disorder associated with cardiovascular, portal, pancreatic and gastrointestinal systems. ADPKD is a ciliopathy, a disease associated with abnormal primary cilia. Non-motile primary cilia, functioning as mechanosensory organelles, have been an intense research topic in ADPKD. It has been shown that both structural and functional defects in primary cilia result in cystic kidney and vascular hypertension. In particular, polycystin-1 and polycystin-2 are co-localized to primary cilia and are responsible for mechanosensory induced calcium influx in response to fluid-shear stress. Based on the multiple signaling pathways in ADPKD, different molecular targets have been developed for potential therapies.

Introduction

Polycystic kidney disease (PKD) is a group of renal cyst diseases that are characterized by the formation of fluid-filled cysts. PKD is classified into acquired and hereditary forms. The acquired form of polycystic kidney disease is characterized by long standing chronic renal failure and subsequent dialysis. However, most forms of polycystic kidney disease are hereditary, including nephronophthisis and medullary cystic kidney diseases. The most common hereditary forms of PKD are autosomal dominant PKD (ADPKD) and autosomal recessive PKD (ARPKD). The pathophysiological presentation of these diseases starts from birth in ARPKD and in the adult years in ADPKD. While the key feature of ARPKD is elongated cysts due to collecting duct dilatation, the hallmark of ADPKD is large focal cysts arising from the rapidly dividing tubular epithelial cells. An important difference between the two is that cysts in ADPKD become isolated, while cysts remain in contact with their tubular origin (*1*) in ARPKD.

The estimated prevalence of ADPKD is one in every 500 to 1,000 individuals (*2, 3*). ADPKD is caused by mutation in either *PKD1* or *PKD2*, encoding polycystin-1 or polycystin-2, respectively (*4-6*). Mutations in *PKD1* are responsible for more than 85% of ADPKD whereas mutations in *PKD2* account for 15%. On the other hand, ARPKD is caused by mutations in *PKHD1* gene, with a prevalence of one in 20,000 live births (*7*). In ADPKD, cysts can form not only in the kidney but also in other organs such as the liver, seminal vesicles, pancreas, and arachnoid membrane (*8-10*). Clinically, ADPKD is also characterized by vascular abnormalities such as intracranial aneurysms, dilatation of the aortic root, dissection of the aortic thoracic aorta, mitral valve prolapse, and

abdominal wall hernias. Imaging studies are primarily used to diagnose ADPKD. Magnetic resonance imaging (MRI) is used to determine kidney volume as well as to exclude intracranial aneurysms, particularly in patients at high risk. Genetic testing is clinically available for both *PKD1* and *PKD2*.

1.1. Primary cilia and cystic kidney

Primary cilia are found on almost all mammalian cell types including renal epithelia where they act as mechanosensory organelles, sensing and responding to urinary flow in the nephron (*11, 12*). Previous studies have showed that primary cilia contain polycystin-1 and polycystin-2 (*11-13*). Polycystin-1 and polycystin-2 are glycoproteins widely expressed in various tissues, including renal epithelia, vascular endothelia and cardiac myocytes. Polycystin-1, with 11 transmembrane domains, is developmentally regulated (*14, 15*). Subcellular localization of polycystin-1 seems to depend on the stage of development and cell polarization of the tubular epithelium (*16, 17*). Polycystin-2 is a calcium channel with six transmembrane domains (*6, 18*). The transmembrane region of polycystin-2 is homologous to polycystin-1, voltage-activated and transient receptor potential (TRP) channel subunits (*19*).

Ultrastructurally, the cilium is a hair-like structure filled with microtubules and enclosed by the ciliary membrane. Primary cilia contains the outer nine microtubule doublets, but lack the inner pair of microtubules, and that is why it is known as a "9+0" axoneme. The outer microtubule doublet is connected by a structural protein nexin to form a ring in the primary cilium (*20*). The basal body or mother centriole is a region in which doublet

microtubules rise from the triplet microtubules and is known as the transition zone. The basal body and centriole join together and form a centrosome, which serves as the cell's main microtubule organization. The ciliary necklace, which is made of a series of membrane proteins at the transition zone, helps differentiate the ciliary membrane from the cell's plasma membrane (*21*). The primary cilium also has ciliary pockets on each side of the plasma membrane (*22*). These are invaginations into the cell membrane adjacent to the ciliary necklace common to many species. The semi-enclosed area is created by apertures at the transition zone, known as the ciliary sheath, and is thought to restrict protein and lipid entry into the cilium; this area is formed during ciliogenesis (*23, 24*).

Within an epithelial cilium, the polycystin complex has been proposed to have a role in sensing and mediating flow dependent mechanosensory calcium signaling (*11, 12, 25-28*). The involvement of polycystins in primary cilia has further provided that ciliary dysfunction results in abnormal planar cell polarity (*29, 30*).

Figure 1.1. Hypothetical model of cytogenesis.

The diagram depicts the mechanosensory function of a renal tubular cilium and how cilia dysfunction can lead to cyst formation. The cilium plays an important role as a mechanosensory organelle that transmits extracellular signals such as urine and blood flow into the cell. These signals may provide critical messages to the cell regarding the direction of cell division along the tubule. A mutation in either *PKD1* and/or *PKD2* will result in ciliary dysfunction in sensing fluid movement. The abnormality in ciliary sensing could result in the loss of many signals, including those regulating planar cell polarity. As a result, the direction of cell division becomes randomized, resulting in increased tubular diameter rather than tubular elongation. Consequently, cyst growth will occur in isolated focal manner along the renal tubules. More cysts illustrated from the neighboring nephrons are depicted on the bottom left corner. The diagram was modified from the original (*152*).

Within the kidney anatomy, planar cell polarity is defined as an organized arrangement of cells in a plane of tissue perpendicular to the apical-basal axis as a direction for the orientation of cell division. Using cystic kidney mouse models, defects in cilia function have been shown to cause abnormal spindle pole orientation during cell division (*31*). It is therefore thought that inactivation of ciliary protein would result in abnormal planar cell polarity, which in turn triggers an increase in renal tubular diameter. It is hypothesized that the net result is the initiation of cyst formation (**Figure 1.1**).

1.2. Liver cysts

The most common extrarenal manifestation of ADPKD is the formation of liver cysts, the severity and frequency of which increase with age. Polycystic liver also occurs as a genetically distinct disease in the absence of renal cysts. The prevalence of liver cysts is between 75 to 90% among ADPKD patients (*32*). Their prevalence by magnetic resonance imaging is 58% in patients 15 to 24 years old, 85% in 25- to 34-year-olds, and 94% in 35- to 46-year-old subjects (*33*). Hepatic cysts are more prevalent and cyst volumes larger in women than in men (*34*). In addition, women who have had multiple pregnancies or have used oral contraceptive drugs or estrogen replacement therapy have worse disease outcomes suggesting an estrogen effect on hepatic cyst growth.

1.3. Pancreatic cysts

The pancreas, involved in secretion of hormones and gastric enzymes, contains a maze of tubules and ducts involved in carrying the enzymes to the intestinal lumen. Ductal epithelial cells secrete bicarbonate to neutralize the acidic chime from the stomach (*35*).

True congenital cysts of the pancreas are rare. Multiple congenital pancreatic cysts are mostly associated with ADPKD, although they are also found in cystic fibrosis, von Hippel-Lindau disease, Ivemark syndrome, and Meckel Gruber syndrome (*36*). In the case of ADPKD, a connection between cilia defects and pancreatic pathologies suggested a link with pancreatic lesions. In some cases, remnants of chronic pancreatitis are found in approximately 10% of patients with ADPKD (*37, 38*). In addition, other studies in mutant mice with defects in cilia formation have shown several pancreatic abnormalities, including exocrine cell atrophy, ductal dilation, and collagen deposition (*39, 40*). Moreover, another mutant mouse study demonstrated that the absence of cilia in pancreatic cells produces pancreatic lesions that resemble those found in patients with chronic pancreatitis or cystic fibrosis (*41*).

1.4. Diverticulitis

Patients with ESRD due to ADPKD have a higher prevalence (20%) of colon diverticulitis than do those with ESRD due to other etiologies (3%) (*41*). Not only do ADPKD-ESRD patients have a higher incidence of diverticulitis, they also have a higher complication rate associated with colon diverticulitis (*42*). Colon perforation, fistula formation, intra-abdominal abscess, and generalized peritonitis are frequently diagnosed in ADPKD patients (*43, 44*). However, colonic diverticula are usually asymptomatic. Major complications of diverticulitis, including perforation-related peritonitis, sepsis and shock, occur in only a small percentage of patients.

1.5. Pain

Pain is the most frequent complaint among ADPKD patients. A recent study of 171 ADPKD patients reported that 71.3% of the patients had lower back pain, the most common site of pain in this group (*45*). About 30% of this group had radiculopathy symptoms. The second most common site for pain was reported to be the abdominen. Abdominal pain was reported by 61% of ADPKD patients. The character of pain described by these patients varied from a dull ache (49.5%), uncomfortable fullness (42.7%), stabbing pain (40.4%), and cramping pain (33.0%). Chronic headache and chest pain were also reported in these patients. Pain in ADPKD can occur acutely or persist becoming chronic. Cyst rupture or hemorrhage, infected cysts and renal stones are considered the most common phases of acute pain (*32*). Progressive kidney enlargement may cause dull, chronic pain by stretching of the renal capsule. Larger renal volumes accompanied by asymmetric, hypertrophic lumbosacral muscle spasm are likely to be the basis of back pain.

1.6. Hypertension

With the availability of renal replacement therapies for patients reaching ESRD, cardiovascular complications have emerged as the major cause of death in patients with ADPKD (*46, 47*). Hypertension is diagnosed in 50–70% of patients usually before any substantial reduction in glomerular filtration rate is observed (*48*). Hypertension relates to progressive kidney enlargement and to ESRD, but in some studies has been reported to be an independent risk factor for progression to ESRD (*49*). In addition, hypertension occurs at a much earlier age in ADPKD patients than in the general population (*50*).

About 10-20% of children with ADPKD develop hypertension, and the majority of adults are hypertensive before any loss of kidney function. The median age for diagnosis of hypertension in ADPKD was 32 years for males and 34 years for females, compared to a median age of 45-55 years in patients with essential hypertension (*50, 51*). Not surprisingly, the occurrence of hypertension is greater in both male and female ADPKD patients when their affected parents are hypertensive (*32*). The pathogenesis of hypertension in ADPKD patients is complex and multifactorial (*52*).

1.6.1. Endothelin

Endothelin-1 (ET-1) has been reported to exert multiple effects on renal physiology (*53*). In addition, there is good evidence that many renal cell types, including tubular cells, synthesize and are affected by ET-1, indicating its role as an autocrine or a paracrine factor (*54, 55*). ET-1 has also been demonstrated to play a significant role in human renal tubular cells, and it can stimulate collagen I gene expression in human renal interstitial fibroblasts (*56, 57*). Moreover, tubular cell proliferation has been reported to be an early feature of precystic tubules in human ADPKD and many rodent PKD models (*58*).

Several studies have shown that patients with ADPKD have high expression of ET-1 in the renal cystic epithelium (*57, 59*). ET-1 is also found to be present in cyst fluid (*60*). Another study demonstrated that patients with ADPKD have increased plasma levels of ET-1 compared with healthy controls and patients with essential hypertensive (*61*). Moreover, endothelium-dependent relaxation is impaired and endothelial nitric oxide synthase activity is decreased in normotensive patients with ADPKD (*62*). These

alterations cause up-regulation of ET-1 and dysfunction of the NO system, resulting in arterial vasoconstriction (*63*).

Other studies have demonstrated a physiological role for ET-1 acting via tubular ET_B receptor to regulate sodium and water excretion in kidney collecting ducts (*64, 65*). Activation of tubular ET_B receptors inhibits vasopressin action, thereby promoting diuresis and sodium excretion by inhibiting Na^+/K^+ ATPase and /or epithelial sodium channels (*66*). As a result, ET_B inhibition can potentiate vasopressin action in cysts derived from the collecting duct and consequently stimulate cyst growth (*67, 68*). It is also noteworthy that the increased sympathetic activity and circulating ET-1 levels could result from the stimulation of intrarenal renin-angiotensin-aldosterone system due to progressive cyst enlargement, thereby leading to systemic hypertension (*69*).

1.7.2. Primary cilia and nitric oxide

Primary cilia regulated nitric oxide (NO) production play an important role in the regulation of vascular tone (*70, 71*). In a blood vessel, an abrupt increase in blood pressure or shear stress can be detected by mechanosensory proteins localized in the cilia (*72, 73*). Extracellular fluid mechanics can then be transduced and translated into a complex of intracellular signaling, which in turn activates endothelial nitric oxide synthase (eNOS), an endothelial enzyme that synthesizes NO. The released NO diffuses from endothelial cells to neighboring smooth muscle cells, thus promoting vasodilation.

Both polycystin-1 and polycystin-2 are expressed in the endothelial and vascular smooth muscle cells of all major vessels (*74, 75*) . Mutations in both *PKD1* and *PKD2* have been shown to contribute to hypertension (*76, 77*), in part by the failure to convert an increase in mechanical blood flow into cellular NO biosynthesis (*72, 73*). It has been shown that impaired endothelial dependent relaxation from aorta cells of *PKD1* knockout mice, due to a defect in (NO) release from the endothelium (**Figure 2**), correlates with a decrease in Ca^{2+} dependent endothelial NO synthesis activity (*78*). We also previously reported the loss of response to fluid-shear stress in mouse endothelial cells with knockdown or knockout of *PKD2* (*72*). In addition to the mouse data, polycystin-2 null endothelial cells generated from *PKD2* patients that do not show polycystin-2 in the cilia are unable to sense fluid flow. This further indicates that overall major effect of endothelial cilia function is to decrease total peripheral resistance, thereby lowering the blood pressure through the production of NO.

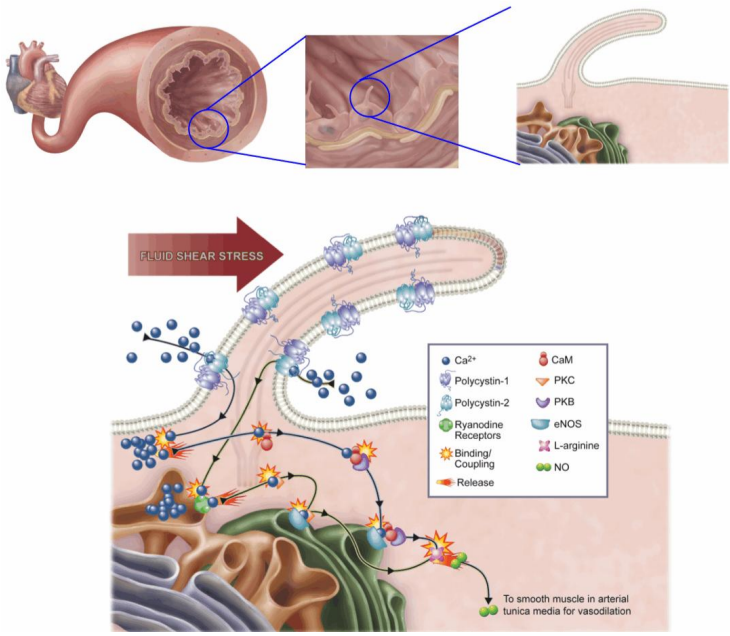

Figure 1.2. The role of mechanosensory cilia and nitric oxide production in ADPKD.

The biochemical production and release of nitric oxide (NO) is dependant on the function of endothelial cilia in the vasculature. In ADPKD, dysfunctional cilia are not able to mechanically sense blood flow, and NO is not produced, resulting in increased blood pressure. The bending of cilia by fluid-shear stress activates the mechanosensory polycystins complex and initiates biochemical synthesis and release of NO. This biochemical cascade involves extracellular calcium influx (Ca^{2+}), followed by the activation of various calcium-dependent proteins including calmodulin (CaM), protein kinase C (PKC) andAkt/PKB). This illustration was modified from the original (*153*).

A final contributor to loss of vascular tone regulation could be reduction in NO bioavailability secondary to increased reactive oxygen species at least in *PKD2* heterozygous smooth muscle cells (*79*).

1.6.3. Angiotensin

Changes in renal structure may play an important role in the pathogenesis of hypertension in ADPKD patients (**Figure 1.3**). Cyst enlargement in ADPKD is associated with medial vascular changes and compression of the adjacent parenchyma with resultant areas of renal ischemia and activation of the renin-angiotensin-aldosterone system (RAAS).

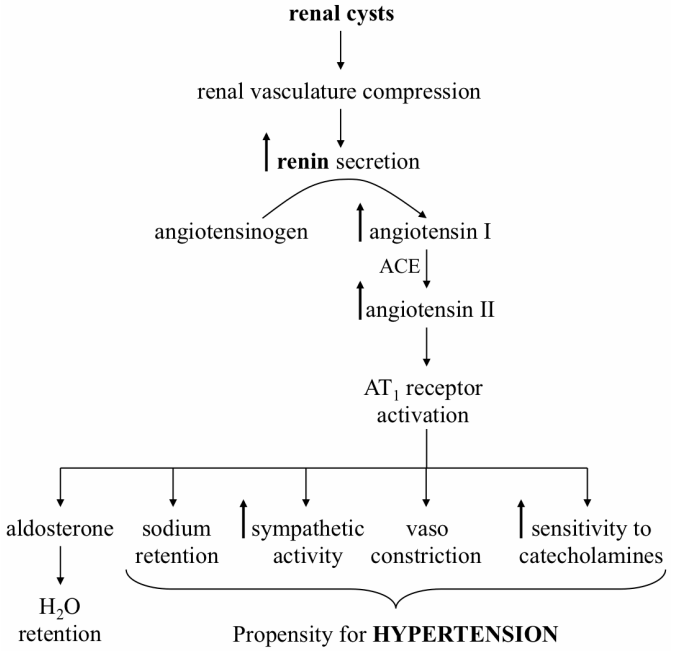

Figure 1.3. RAAS regulation in ADPKD. Renal cysts compress and disrupt the vascular network in the kidney, which leads to ischemic kidney. It was proposed that this would increase the release of renin from the juxtaglomerular apparatus. The increase in renin secretion would eventually accelerate the conversion of angiotensinogen to angiotensin I, which is further converted by angiotensin-converting enzyme (ACE) to angiotensin II. As a result, the angiotensin receptor (AT1) is activated initiating cascades of responses resulting in hypertension. This illustration was modified from the original (*154*).

In support of this, hypertensive patients with ADPKD demonstrate significantly greater renal volumes than patients with normal blood pressure (*32, 80*). Other components of the RAAS, including angiotensinogen, angiotensin converting enzyme (ACE), angiotensin II receptor and angiotensin II peptide, have also been detected in cysts and dilated tubules in ADPKD kidneys (*81*). Activation of the RAAS has been found in normotensive and hypertensive PKD patients, regardless of their blood pressure and renal function (*82*). Not surprisingly, the high levels of circulating angiotensin II in PKD patients have been shown to contribute to the development of vascular hypertrophy, which is further implicated in vascular remodeling (*83*). In addition, changes in the vasculature during the course of the PKD progression have been observed in both human (*84, 85*) and animal studies (*86, 87*).

Increased sympathetic activity has been reported in hypertensive patients with ADPKD, regardless of renal function (*88, 89*), suggesting that sympathetic hyperactivity could contribute to the pathogenesis of hypertension in ADPKD patients. ACE-I ramipril and the beta-blocker metoprolol are both effective as first-line therapies in hypertensive PKD patients (*90*). It is recommended that more aggressive blood pressure control with these agents is necessary in order to be beneficial for ADPKD patients (*32*). It should be noted that angiotensin can stimulate the sympathetic nervous system and vice-versa.

1.7. Left ventricular hypertrophy

Left ventricular hypertrophy (LVH) is well known as a powerful independent risk factor for cardiovascular morbidity and mortality (*91*). Increased left ventricular mass index

(LVMI) is associated with worse renal and patient outcomes in ADPKD (*92*). Chapman and colleagues further reported in their study that LVH was found in 48% of hypertensive subjects with ADPKD (*93*). Their study also showed a significant correlation between hypertension and LVMI, which has been demonstrated in both children and adults with ADPKD. In addition, children whose blood pressure was within the upper quartile of the normal range were found to have a significantly greater LVMI than those with lower blood pressure (*94*).

Bardaji and colleagues showed that young normotensive ADPKD patients and preserved renal function had increased LVMIs and Doppler abnormalities consistent with early diastolic dysfunction in a cross-sectional study of three different groups of ADPKD patients (*95*). Another study by Oflaz and colleagues showed that biventricular diastolic dysfunction was present in both hypertensive and normotensive ADPKD patients with well-preserved renal function (*96*).

Verdecchia et al. reported that hypertensive patients whose nocturnal blood pressure remains elevated demonstrate higher LVMI compared to those whose blood pressure falls at night (*97*). Furthermore, Li Kam et al. demonstrated that hypertensive patients with ADPKD who have normal renal function or mild renal impairment have significantly lower nocturnal decreases in blood pressure compared to patients with essential hypertension (*98*). Another study has shown that the nocturnal fall in blood pressure was attenuated even in young normotensive ADPKD patients (*99*). In this study, a higher LVMI was closely related to the ambulatory systolic blood pressure in normotensive patients.

It has also been shown that insulin resistance is significantly associated with LVMI in healthy relatives and patients with *PKD1* mutations independent of other factors known to increase LVMI such as age, body weight, systolic blood pressure and albuminuria (*100*). Thus, the stimulation of angiotensin II and the sympathetic nervous system due to hyperinsulinemia may contribute to increased LVMI in *PKD1* patients (*100, 101*). However, other factors besides hypertension, including anemia, obesity, and sodium intake, as well as increased activity of the renin-angiotensin-aldosterone system and other genetic factors, may be associated with LVH, in both hypertensive and normotensive ADPKD patients (*93*). The etiology of LVH is likely to be multifactorial but hypertension still plays a major role in its development (*102*).

1.8. Aneurysm

ADPKD patients have a higher prevalence (4.0-11.7%) of intracranial aneurysms than the general population (1.0%) (*103, 104*). In addition, four to seven percent of patients with ADPKD die from intracranial aneurysm rupture, and such deaths occur at a younger age than in sporadic cases (*105*). Intracranial aneurysm rupture seems to be more common in certain families with ADPKD (*106, 107*). This indicates that a family history can be an important tool in assessing the risk of aneurysm rupture in ADPKD. Extracranial aneurysm, such as in coronary arteries, abdominal aorta, renal artery and splenic artery, has been reported in ADPKD patients suggesting that these are primary abnormalities (*108, 109*). Other potential cardiovascular features reported in patients with ADPKD include biventricular diastolic dysfunction, endothelial dysfunction, increased carotid intima-media thickness, impaired coronary flow and cardiac valvular defects.

1.9. Therapeutic treatments for cardiovascular complications

Early and effective treatment of hypertension is highly recommended for the prevention of cardiovascular complications in ADPKD patients. Since LVH and hypertension contribute significantly to cardiovascular morbidity and mortality, controlling these factors can positively impact patient health and sruvival. Antihypertensive treatment with an ACE inhibitor has been shown to reverse LVH over a seven-year follow-up period, thus decreasing an important risk factor for cardiovascular death in ADPKD patients (*110*). A seven-year prospective, randomized study in 75 hypertensive patients with ADPKD and LVH compared the effects of rigorous and standard blood pressure control (<120/80 mmHg versus 135–140/85–90 mmHg) on LVH and renal function. Ecder and Schrier suggest that both strategies decreased LVH significantly (*46*). In addition, rigorous blood pressure control was considerably more effective in decreasing LVMI than was standard blood pressure control. More patients in the rigorous-control group (71%) achieved normal LVMI than in the standard group (44%). A subgroup analysis showed that patients who received the ACE inhibitor enalapril experienced a significantly greater decrease in LVH than patients who received the calcium-channel blocker amlodipine, despite similar blood pressure control. On this basis, a blood pressure goal of less than 120/80 mmHg has been recommended that patients with ADPKD with hypertension and LVH (*46*).

1.10. Modern therapy to halt progression of renal cysts

Since ADPKD accounts for up to 10% of patients on renal replacement therapy, an effective disease-modifying drug would have significant implications. The identification

of *PKD1* and *PKD2* has led to an explosion in knowledge identifying new disease mechanisms and testing new drugs. Currently, there are three major treatment strategies to treat or reduce progression of kidney failure in ADPKD: to reduce cAMP levels, inhibit cell proliferation, and reduce fluid secretion (*111, 112*).

1.10.1. cAMP

Cyclic AMP (cAMP) elevation has an inhibitory effect on cell growth in normal kidney epithelial cells, while it stimulates cell proliferation in ADPKD cells (*113*). The molecular basis of this may be Protein kinase-A activation of the B-Raf/MEK/ERK signaling pathway (*114*). It has also been proposed that hyper-phosphorylation of polycystin-2 by protein kinase-A can contribute to cystic kidney formation by loss of PC2 inhibition of cell cycle progression (*115*). Elevated cAMP also results in increased fluid secretion and cyst enlargement by stimulating the apical CFTR channel and specific basolateral transporters (*114, 116*).

Vasopressin V2 receptor (V2R) is a major regulator of cAMP production and adenylyl cyclase activity in the principal cells lining the collecting ducts (*116*). Nagao et al. showed that high water intake can suppress vasopressin and decrease cyst and renal volumes in PCK rats, with a reduced activity of the cAMP dependent B-Raf/MEK/ERK pathway (*117*). The strongest evidence for a pathogenic role of vasopressin in cyst growth comes from a study which demonstrated that deletion of vasopressin in PCK rats by breeding these with Brattleboro rats results in lower renal cAMP levels and near complete inhibition of cystogenesis (*118*).

The V2R antagonist OPC-31260 substantially reduced cAMP concentrations and inhibited cyst development in several rodent cystic kidney models (*119-121*). Tolvaptan, an analogue with higher potency and selectivity for the human V2R, was equally effective in reducing renal cysts in PCK rats (*122*). In a recently concluded phase III clinical trial, Tolvaptan slowed the increase in total kidney volume and the decline in GFR over a three-year period in patients with ADPKD (*123*). There was however a significant drop-out rate in the treated group and a few patients developed liver enzyme abnormalities which reversed on cessation of treatment. It is worth mentioning that these drugs had no effect on liver cysts, due to the absence of VPV2R in the liver (*34*).

1.10.2. mTOR

The mTOR pathway was shown to be directly regulated by primary cilia (*124*). In addition, mTOR signaling can be regulated by different signaling inputs and leads to changes in activity of many cellular processes that drive cyst growth (*125*). The polycystin-1 protein directly interacts with the Tuberous Sclerosis Complex-2 (TSC2) protein. TSC2 and Tuberous Sclerosis Complex-1 (TSC1) protein are normally found together in a complex. Bonnet et al. demonstrated that combined mutations in *PKD1* and either *Tsc1* or *Tsc2* in compound heterozygous mice was associated with a more severe renal cystic phenotype than in mice with either mutation alone (*126*). mTOR activity is regulated by TSC1-TSC2 complex through several cellular inputs (*124, 127*). Thereafter, mTOR regulates protein synthesis, lipid biosynthesis, hypoxia response, *de novo* ceramide synthesis, PKC, AKT, fluid secretion, glycosphingolipid metabolism and ion balance, all of which are dysregulated in PKD. Particularly, the activity of mTORC1,

mTORC2, PKC, AKT, ERK, IGF-1, CFTR and EGF-1 are all increased in ADPKD patients (*124*). It has therefore been proposed that mTOR inhibition can delay cystic growth and expansion in ADPKD kidneys. More specifically, mTOR kinase activity is aberrantly increased in ADPKD patients (*128*). Treatments with mTOR inhibitor, such as rapamycin, sirolimus or everolimus, decrease renal cyst size and improve kidney function in cystic kidney models (*129, 130*) although not in humans (*131, 132*)

1.10.3. EGFR

Members of the epidermal growth factor (EGF)-family bind to ErbB (EGFR)-family receptors, which play an important role in the regulation of various fundamental cell processes including cell proliferation and differentiation (*133*). Although ErbB2 and ErbB4 have been detected in developing ureteric buds, EGFR is the predominant ErbB receptor expressed in normal adult mammalian kidney tubules (*134, 135*). In addition, EGF-ErbB receptor-mediated interaction is a key element in renal tubular cell proliferation, not only in normal kidneys but also in cyst formation and enlargement. EGF is a well-known mitogen for normal renal epithelia and has been shown to stimulate hyperproliferation in renal cystic epithelia (*136, 137*). As mentioned above, EGF and EGF-immunoreactive peptide species are secreted into the apical medium of cultured ADPKD epithelia, and high mitogenic concentrations of EGF have been measured in ADPKD cyst fluids (*1*). Interestingly, the increase of EGF-1 can result in ERK activation through Ras and (B-Raf) Raf signaling pathways, which could in turn regulate the TSC1-TSC2 complex in ADPKD patients (*125*).

Administration of EGFR inhibitors, such as EKI-785 and EKB-569, in some renal cystic models decreases kidney weights and cyst volumes, suggesting a therapeutic potential of EGFR inhibition in ADPKD treatment (*138*). In addition, EGF-like growth factors such as TGF-α and heparin-binding EGF have been found to be abnormally expressed in human ADPKD epithelial cells (*133, 139*).

1.10.4. Other potential targets

Besides cAMP, mTOR and EGF, there are other potential drugs targeting other signaling pathways such as SR, AP-1, c-Src, Raf, MEK, ERK, A3AR, CFTR and IGF-1(*113, 125*), all of which are abnormally regulated in patients with ADPKD (**Figure 1.4.**). A number of drugs showing promise in preclinical models have been or are being tested in clinical trials (Table 1.1).

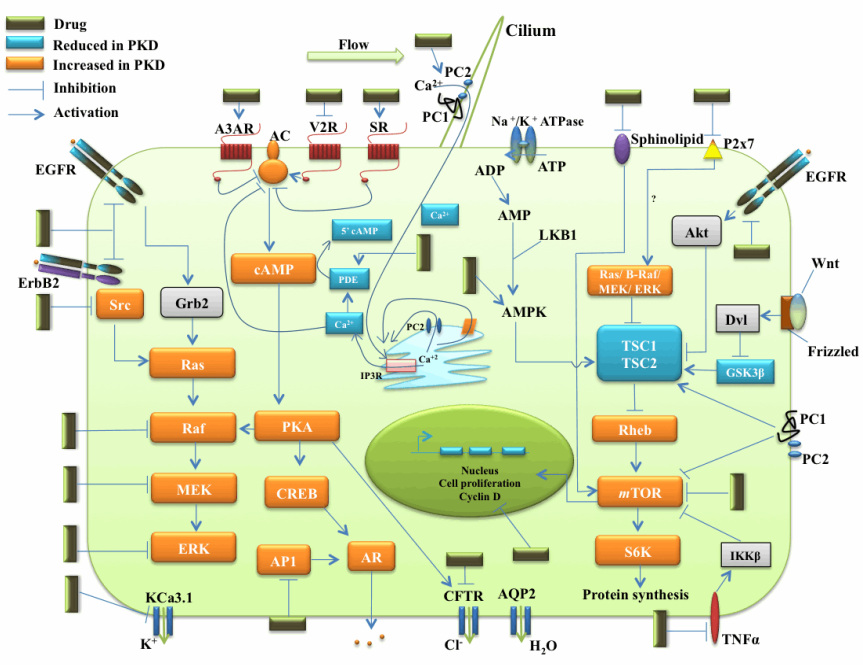

Figure 1.4. The signaling pathway and drug targets in ADPKD cystic cells.

The diagram illustrates the mechanism that polycystin-1 (PC1), polycystin-2 (PC2), signaling proteins, molecules, receptors and drugs exert on signaling pathways leading to cyst formation. The green box indicates drug targets proposed for ADPKD. The blue box indicates the reduced molecules and signaling proteins in ADKPD. The orange box indicates the increased signaling proteins in ADPKD, which are thought to be responsible for an increase in cell proliferation including cAMP, EGFR, Ras/Raf/ERK, Src, CFTR, AC, and mTOR activity. In addition, EGFR activation is also enhanced by amphiregulin (AR) that is abnormally expressed in cystic cells through cAMP, CREB and AP1 signaling. Furthermore, altered EGFR and cAMP signaling stimulate mTOR activity by activation of Akt and Ras/Raf/ERK, which inhibit the TSC1/TSC2 complex. The sphonigolipid, Na^+/K^+ ATPase, Wnt and P2x7 purinergic receptors are also involved in the regulation of mTOR activity. Na^+/K^+ ATPase also regulates the KCa3.1 receptor. However, the abnormal cAMP accumulation contributes to the activation of the Ras/Raf/ERK signaling pathway directly or by the activation of Src, which is able to interact with EGFR in its EGFR/ErbB2 heterodimer form. Other receptors that are involved in ADPKD include adenosine receptor-3A (A3AR), vasopressin receptor-2 (V2R) and somatostatin receptor (SR), which regulate activity of adenylate cyclase (AC). This illustration was adapted from the original (*112*).

TABLE 1.1. Current clinical trials in ADPKD

	Drugs	Signaling pathway	Study design	Treatment duration (months)	Clinical phase trial	Clinical trial status	Clinical trials Gov. identifier	Ref.
1	Octreotide	Analogue of somatostatin known to inhibit cAMP pathway in ADKPD and ADPLD	Randomized, double-blind, Placebo controlled and crossover	12	phase 2/3	Completed /failed	NCT00426153	(*140, 141*)31
2	Lanreotide	Analogue of somatostatin known to inhibit cAMP pathway in ADKPD and ADPLD	Randomized, double-blind and placebo controlled	6	phase 2/3	Completed	NCT00565097	(*142*)
3	Sirolimus	mTOR inhibitor	Randomized and penlabel	18	phase 2/3	Completed/failed	NCT00346918	(*132*)
4	Sirolimus (SIRENA study)	mTOR inhibitor	Randomized, open-label and crossover	6	phase 2	Completed	NCT00491517	(*143*)
5	Everolimus	mTOR inhibitor	Multicenter, randomized, double-blind, placebo-controlled	24	phase 3	Completed/failed	NCT00414440	(*131*)
6	Tolvaptan	V2-receptor antagonist	parallel-arm, double blind and placebo controlled	36	phase 3	Ongoing	NCT00428948	(*123*)
7	Lisinopril and Telmisartan (HALT PKD)1	ACE inhibitor [lisinopril] and angiotensin II receptor blocker (ARB) [telmisartan]	Randomized, double-blind and placebo controlled	72	phase 3	Ongoing	NCT00283686	(*144, 145*)
8	Pravastatin1	A (HMG coA) reductase inhibitors	Randomized, doubleblind, placebo-controlled	36	phase 3	Ongoing	NCT00456365	(*146, 147*)
9	Somatostatin	cAMP inhibitor pathway in ADKPD and ADPLD	Randomized, single-blind and placebo controlled	36	phase 3	Ongoing	NCT00309283	not available
10	Bosutinib	c-Src inhibitor	Randomized, double-blind and placebo controlled	24	phase 2	Ongoing	NCT01233869	(*148*)
12	Triptolide	Restore intracellular Ca2+ signaling and inhibit cell proliferation	Randomized and open-label	36	phase 2	Ongoing	NCT00801268	(*149-151*)

1.11. Summary

Since the discovery of *PKD1* and *PKD2*, there has been tremendous progress in studying disease pathophysiology. As a result, many promising drugs have been and are being developed to slow halt or reverse the progression of cystic disease. Given the complexity of disease and the important extrarenal features, it is likely that a range of specific drugs will be needed to treat patients with ADPKD.

References

1. P. D. Wilson, Polycystic kidney disease. *The New England journal of medicine* **350**, 151 (Jan 8, 2004).

2. W. E. Braun, Autosomal dominant polycystic kidney disease: emerging concepts of pathogenesis and new treatments. *Cleve Clin J Med* **76**, 97 (Feb, 2009).

3. US Renal Data System: USRDS 2008 Annual Data Report. *The National Institutes of Health, National Institute of Diabetes and Digestive and Kidney Disease* **Bethesda, MD**, (2008).

4. Polycystic kidney disease: the complete structure of the PKD1 gene and its protein. The International Polycystic Kidney Disease Consortium. *Cell* **81**, 289 (Apr 21, 1995).

5. The polycystic kidney disease 1 gene encodes a 14 kb transcript and lies within a duplicated region on chromosome 16. The European Polycystic Kidney Disease Consortium. *Cell* **77**, 881 (Jun 17, 1994).

6. T. Mochizuki *et al.*, PKD2, a gene for polycystic kidney disease that encodes an integral membrane protein. *Science* **272**, 1339 (May 31, 1996).

7. C. J. Ward *et al.*, The gene mutated in autosomal recessive polycystic kidney disease encodes a large, receptor-like protein. *Nature genetics* **30**, 259 (Mar, 2002).

8. V. E. Torres, P. C. Harris, Polycystic kidney disease in 2011: Connecting the dots toward a polycystic kidney disease therapy. *Nature reviews. Nephrology* **8**, 66 (Feb, 2012).

9. P. C. Harris, V. E. Torres, in *GeneReviews,* R. A. Pagon, T. D. Bird, C. R. Dolan, K. Stephens, M. P. Adam, Eds. (Seattle (WA), 1993).

10. P. C. Harris, V. E. Torres, Polycystic kidney disease. *Annual review of medicine* **60**, 321 (2009).

11. S. M. Nauli *et al.*, Loss of polycystin-1 in human cyst-lining epithelia leads to ciliary dysfunction. *Journal of the American Society of Nephrology : JASN* **17**, 1015 (Apr, 2006).

12. S. M. Nauli *et al.*, Polycystins 1 and 2 mediate mechanosensation in the primary cilium of kidney cells. *Nature genetics* **33**, 129 (Feb, 2003).

13. B. K. Yoder, X. Hou, L. M. Guay-Woodford, The polycystic kidney disease proteins, polycystin-1, polycystin-2, polaris, and cystin, are co-localized in renal cilia. *Journal of the American Society of Nephrology : JASN* **13**, 2508 (Oct, 2002).

14. R. Sandford *et al.*, Comparative analysis of the polycystic kidney disease 1 (PKD1) gene reveals an integral membrane glycoprotein with multiple evolutionary conserved domains. *Human molecular genetics* **6**, 1483 (Sep, 1997).

15. J. Hughes *et al.*, The polycystic kidney disease 1 (PKD1) gene encodes a novel protein with multiple cell recognition domains. *Nature genetics* **10**, 151 (Jun, 1995).

16. J. Van Adelsberg, S. Chamberlain, V. D'Agati, Polycystin expression is temporally and spatially regulated during renal development. *The American journal of physiology* **272**, F602 (May, 1997).

17. L. Geng *et al.*, Distribution and developmentally regulated expression of murine polycystin. *The American journal of physiology* **272**, F451 (Apr, 1997).

18. S. Gonzalez-Perrett *et al.*, Polycystin-2, the protein mutated in autosomal dominant polycystic kidney disease (ADPKD), is a Ca2+-permeable nonselective cation channel. *Proceedings of the National Academy of Sciences of the United States of America* **98**, 1182 (Jan 30, 2001).

19. P. Koulen *et al.*, Polycystin-2 is an intracellular calcium release channel. *Nature cell biology* **4**, 191 (Mar, 2002).

20. B. S. Muntean, S. Jin, S. M. Nauli, Primary Cilia are Mechanosensory Organelles with Chemosensory Roles. *Mechanical Stretch and Cytokines, Mechanosensitivity in Cells and Tissues* **5**, 201 (2012).

21. N. B. Gilula, P. Satir, The ciliary necklace. A ciliary membrane specialization. *The Journal of cell biology* **53**, 494 (May, 1972).

22. A. Molla-Herman *et al.*, The ciliary pocket: an endocytic membrane domain at the base of primary and motile cilia. *Journal of cell science* **123**, 1785 (May 15, 2010).

23. H. L. Kee *et al.*, A size-exclusion permeability barrier and nucleoporins characterize a ciliary pore complex that regulates transport into cilia. *Nature cell biology* **14**, 431 (Apr, 2012).

24. R. Rohatgi, W. J. Snell, The ciliary membrane. *Current opinion in cell biology* **22**, 541 (Aug, 2010).

25. S. Wang *et al.*, Fibrocystin/polyductin, found in the same protein complex with polycystin-2, regulates calcium responses in kidney epithelia. *Molecular and cellular biology* **27**, 3241 (Apr, 2007).

26. C. Xu *et al.*, Human ADPKD primary cyst epithelial cells with a novel, single codon deletion in the PKD1 gene exhibit defective ciliary polycystin localization and loss of flow-induced Ca2+ signaling. *American journal of physiology. Renal physiology* **292**, F930 (Mar, 2007).

27. S. H. Low *et al.*, Polycystin-1, STAT6, and P100 function in a pathway that transduces ciliary mechanosensation and is activated in polycystic kidney disease. *Developmental cell* **10**, 57 (Jan, 2006).

28. V. Chauvet *et al.*, Mechanical stimuli induce cleavage and nuclear translocation of the polycystin-1 C terminus. *The Journal of clinical investigation* **114**, 1433 (Nov, 2004).

29. E. Fischer *et al.*, Defective planar cell polarity in polycystic kidney disease. *Nature genetics* **38**, 21 (Jan, 2006).

30. V. Patel *et al.*, Acute kidney injury and aberrant planar cell polarity induce cyst formation in mice lacking renal cilia. *Human molecular genetics* **17**, 1578 (Jun 1, 2008).

31. W. A. AbouAlaiwi, S. Ratnam, R. L. Booth, J. V. Shah, S. M. Nauli, Endothelial cells from humans and mice with polycystic kidney disease are characterized by polyploidy and chromosome segregation defects through survivin down-regulation. *Human molecular genetics* **20**, 354 (Jan 15, 2011).

32. A. Masoumi, B. Reed-Gitomer, C. Kelleher, M. R. Bekheirnia, R. W. Schrier, Developments in the management of autosomal dominant polycystic kidney disease. *Therapeutics and clinical risk management* **4**, 393 (Apr, 2008).

33. K. T. Bae *et al.*, Magnetic resonance imaging evaluation of hepatic cysts in early autosomal-dominant polycystic kidney disease: the Consortium for Radiologic Imaging Studies of Polycystic Kidney Disease cohort. *Clinical journal of the American Society of Nephrology : CJASN* **1**, 64 (Jan, 2006).

34. V. E. Torres, P. C. Harris, Y. Pirson, Autosomal dominant polycystic kidney disease. *Lancet* **369**, 1287 (Apr 14, 2007).

35. S. Abdul-Majeed, S. M. Nauli, Polycystic diseases in visceral organs. *Obstetrics and gynecology international* **2011**, 609370 (2011).

36. J. H. Grendell, T. H. Ermak, Anatomy, histology, embryology, and developmental anomalies ofthe pancreas. *Sleisenger and Fordtran's Gastrointestinal and Liver Disease*, 761 (1998).

37. O. Basar *et al.*, Recurrent pancreatitis in a patient with autosomal-dominant polycystic kidney disease. *Pancreatology* **6**, 160 (2006).

38. R. Torra *et al.*, Ultrasonographic study of pancreatic cysts in autosomal dominant polycystic kidney disease. *Clinical nephrology* **47**, 19 (Jan, 1997).

39. D. A. Cano, N. S. Murcia, G. J. Pazour, M. Hebrok, Orpk mouse model of polycystic kidney disease reveals essential role of primary cilia in pancreatic tissue organization. *Development* **131**, 3457 (Jul, 2004).

40. J. H. Moyer *et al.*, Candidate gene associated with a mutation causing recessive polycystic kidney disease in mice. *Science* **264**, 1329 (May 27, 1994).

41. D. A. Cano, S. Sekine, M. Hebrok, Primary cilia deletion in pancreatic epithelial cells results in cyst formation and pancreatitis. *Gastroenterology* **131**, 1856 (Dec, 2006).

42. S. Y. Li *et al.*, Recurrent retroperitoneal abscess due to perforated colonic diverticulitis in a patient with polycystic kidney disease. *Journal of the Chinese Medical Association : JCMA* **72**, 153 (Mar, 2009).

43. E. D. Lederman, G. McCoy, D. J. Conti, E. C. Lee, Diverticulitis and polycystic kidney disease. *The American surgeon* **66**, 200 (Feb, 2000).

44. E. D. Lederman, D. J. Conti, N. Lempert, T. P. Singh, E. C. Lee, Complicated diverticulitis following renal transplantation. *Diseases of the colon and rectum* **41**, 613 (May, 1998).

45. Z. H. Bajwa, K. A. Sial, A. B. Malik, T. I. Steinman, Pain patterns in patients with polycystic kidney disease. *Kidney international* **66**, 1561 (Oct, 2004).

46. T. Ecder, R. W. Schrier, Cardiovascular abnormalities in autosomal-dominant polycystic kidney disease. *Nature reviews. Nephrology* **5**, 221 (Apr, 2009).

47. G. M. Fick, A. M. Johnson, W. S. Hammond, P. A. Gabow, Causes of death in autosomal dominant polycystic kidney disease. *Journal of the American Society of Nephrology : JASN* **5**, 2048 (Jun, 1995).

48. A. B. Chapman, R. W. Schrier, Pathogenesis of hypertension in autosomal dominant polycystic kidney disease. *Seminars in nephrology* **11**, 653 (Nov, 1991).

49. A. B. Chapman, K. Stepniakowski, F. Rahbari-Oskoui, Hypertension in autosomal dominant polycystic kidney disease. *Advances in chronic kidney disease* **17**, 153 (Mar, 2010).

50. C. L. Kelleher, K. K. McFann, A. M. Johnson, R. W. Schrier, Characteristics of hypertension in young adults with autosomal dominant polycystic kidney disease compared with the general U.S. population. *American journal of hypertension* **17**, 1029 (Nov, 2004).

51. R. W. Schrier, A. M. Johnson, K. McFann, A. B. Chapman, The role of parental hypertension in the frequency and age of diagnosis of hypertension in offspring with autosomal-dominant polycystic kidney disease. *Kidney international* **64**, 1792 (Nov, 2003).

52. S. M. Nauli, X. Jin, B. P. Hierck, The mechanosensory role of primary cilia in vascular hypertension. *International journal of vascular medicine* **2011**, 376281 (2011).

53. M. Y. Chang, A. C. Ong, Endothelin in polycystic kidney disease. *Contributions to nephrology* **172**, 200 (2011).

54. Y. Kawanabe *et al.*, Cilostazol prevents endothelin-induced smooth muscle constriction and proliferation. *PloS one* **7**, e44476 (2012).

55. Y. Kawanabe, S. M. Nauli, Endothelin. *Cellular and molecular life sciences : CMLS* **68**, 195 (Jan, 2011).

56. A. C. Ong *et al.*, An endothelin-1 mediated autocrine growth loop involved in human renal tubular regeneration. *Kidney international* **48**, 390 (Aug, 1995).

57. A. C. Ong *et al.*, Human tubular-derived endothelin in the paracrine regulation of renal interstitial fibroblast function. *Experimental nephrology* **2**, 134 (Mar-Apr, 1994).

58. M. Y. Chang *et al.*, Haploinsufficiency of Pkd2 is associated with increased tubular cell proliferation and interstitial fibrosis in two murine Pkd2 models. *Nephrology, dialysis, transplantation : official publication of the European Dialysis and Transplant Association - European Renal Association* **21**, 2078 (Aug, 2006).

59. B. Hocher *et al.*, Renal endothelin system in polycystic kidney disease. *Journal of the American Society of Nephrology : JASN* **9**, 1169 (Jul, 1998).

60. C. Munemura, J. Uemasu, H. Kawasaki, Epidermal growth factor and endothelin in cyst fluid from autosomal dominant polycystic kidney disease cases: possible evidence of heterogeneity in cystogenesis. *American journal of kidney diseases : the official journal of the National Kidney Foundation* **24**, 561 (Oct, 1994).

61. R. Giusti *et al.*, Plasma concentration of endothelin and arterial pressure in patients with ADPKD. *Contributions to nephrology* **115**, 118 (1995).

62. D. Wang, J. Iversen, S. Strandgaard, Endothelium-dependent relaxation of small resistance vessels is impaired in patients with autosomal dominant polycystic kidney disease. *Journal of the American Society of Nephrology : JASN* **11**, 1371 (Aug, 2000).

63. M. A. Al-Nimri *et al.*, Endothelial-derived vasoactive mediators in polycystic kidney disease. *Kidney international* **63**, 1776 (May, 2003).

64. Y. Ge, P. K. Stricklett, A. K. Hughes, M. Yanagisawa, D. E. Kohan, Collecting duct-specific knockout of the endothelin A receptor alters renal vasopressin responsiveness, but not sodium excretion or blood pressure. *American journal of physiology. Renal physiology* **289**, F692 (Oct, 2005).

65. Y. Ge *et al.*, Collecting duct-specific knockout of endothelin-1 alters vasopressin regulation of urine osmolality. *American journal of physiology. Renal physiology* **288**, F912 (May, 2005).

66. D. E. Kohan, The renal medullary endothelin system in control of sodium and water excretion and systemic blood pressure. *Current opinion in nephrology and hypertension* **15**, 34 (Jan, 2006).

67. V. E. Torres, P. C. Harris, Autosomal dominant polycystic kidney disease: the last 3 years. *Kidney international* **76**, 149 (Jul, 2009).

68. M. Y. Chang, E. Parker, M. El Nahas, J. L. Haylor, A. C. Ong, Endothelin B receptor blockade accelerates disease progression in a murine model of autosomal dominant polycystic kidney disease. *Journal of the American Society of Nephrology : JASN* **18**, 560 (Feb, 2007).

69. R. W. Schrier, Renal volume, renin-angiotensin-aldosterone system, hypertension, and left ventricular hypertrophy in patients with autosomal dominant polycystic kidney disease. *Journal of the American Society of Nephrology : JASN* **20**, 1888 (Sep, 2009).

70. S. Abdul-Majeed, S. M. Nauli, Dopamine receptor type 5 in the primary cilia has dual chemo- and mechano-sensory roles. *Hypertension* **58**, 325 (Aug, 2011).

71. S. Abdul-Majeed, B. C. Moloney, S. M. Nauli, Mechanisms regulating cilia growth and cilia function in endothelial cells. *Cellular and molecular life sciences : CMLS* **69**, 165 (Jan, 2012).

72. W. A. AbouAlaiwi *et al.*, Ciliary polycystin-2 is a mechanosensitive calcium channel involved in nitric oxide signaling cascades. *Circulation research* **104**, 860 (Apr 10, 2009).

73. S. M. Nauli *et al.*, Endothelial cilia are fluid shear sensors that regulate calcium signaling and nitric oxide production through polycystin-1. *Circulation* **117**, 1161 (Mar 4, 2008).

74. A. C. Ong *et al.*, Coordinate expression of the autosomal dominant polycystic kidney disease proteins, polycystin-2 and polycystin-1, in normal and cystic tissue. *The American journal of pathology* **154**, 1721 (Jun, 1999).

75. S. Abdul-Majeed, S. M. Nauli, Calcium-mediated mechanisms of cystic expansion. *Biochimica et biophysica acta* **1812**, 1281 (Oct, 2011).

76. N. Hateboer *et al.*, Location of mutations within the PKD2 gene influences clinical outcome. *Kidney international* **57**, 1444 (Apr, 2000).

77. N. Hateboer *et al.*, Comparison of phenotypes of polycystic kidney disease types 1 and 2. European PKD1-PKD2 Study Group. *Lancet* **353**, 103 (Jan 9, 1999).

78. S. Hassane *et al.*, Pathogenic sequence for dissecting aneurysm formation in a hypomorphic polycystic kidney disease 1 mouse model. *Arteriosclerosis, thrombosis, and vascular biology* **27**, 2177 (Oct, 2007).

79. Z. L. Brookes *et al.*, Pkd2 mesenteric vessels exhibit a primary defect in endothelium-dependent vasodilatation restored by rosiglitazone. *American journal of physiology. Heart and circulatory physiology* **304**, H33 (Jan 1, 2013).

80. P. A. Gabow *et al.*, Renal structure and hypertension in autosomal dominant polycystic kidney disease. *Kidney international* **38**, 1177 (Dec, 1990).

81. M. Loghman-Adham, C. E. Soto, T. Inagami, L. Cassis, The intrarenal renin-angiotensin system in autosomal dominant polycystic kidney disease. *American journal of physiology. Renal physiology* **287**, F775 (Oct, 2004).

82. A. B. Chapman, P. A. Gabow, Hypertension in autosomal dominant polycystic kidney disease. *Kidney international. Supplement* **61**, S71 (Oct, 1997).

83. E. A. McPherson *et al.*, Chymase-like angiotensin II-generating activity in end-stage human autosomal dominant polycystic kidney disease. *Journal of the American Society of Nephrology : JASN* **15**, 493 (Feb, 2004).

84. P. J. Azurmendi *et al.*, Early renal and vascular changes in ADPKD patients with low-grade albumin excretion and normal renal function. *Nephrology, dialysis, transplantation : official publication of the European Dialysis and Transplant Association - European Renal Association* **24**, 2458 (Aug, 2009).

85. C. T. Itty, A. Farshid, G. Talaulikar, Spontaneous coronary artery dissection in a woman with polycystic kidney disease. *American journal of kidney diseases : the official journal of the National Kidney Foundation* **53**, 518 (Mar, 2009).

86. C. Boulter *et al.*, Cardiovascular, skeletal, and renal defects in mice with a targeted disruption of the Pkd1 gene. *Proceedings of the National Academy of Sciences of the United States of America* **98**, 12174 (Oct 9, 2001).

87. M. A. Arnaout, Molecular genetics and pathogenesis of autosomal dominant polycystic kidney disease. *Annual review of medicine* **52**, 93 (2001).

88. J. Neumann, G. Ligtenberg, I. H. Klein, P. J. Blankestijn, Pathogenesis and treatment of hypertension in polycystic kidney disease. *Current opinion in nephrology and hypertension* **11**, 517 (Sep, 2002).

89. I. H. Klein, G. Ligtenberg, P. L. Oey, H. A. Koomans, P. J. Blankestijn, Sympathetic activity is increased in polycystic kidney disease and is associated with hypertension. *Journal of the American Society of Nephrology : JASN* **12**, 2427 (Nov, 2001).

90. R. Zeltner, R. Poliak, B. Stiasny, R. E. Schmieder, B. D. Schulze, Renal and cardiac effects of antihypertensive treatment with ramipril vs metoprolol in autosomal dominant polycystic kidney disease. *Nephrology, dialysis, transplantation : official publication of the European Dialysis and Transplant Association - European Renal Association* **23**, 573 (Feb, 2008).

91. M. J. Koren, R. B. Devereux, P. N. Casale, D. D. Savage, J. H. Laragh, Relation of left ventricular mass and geometry to morbidity and mortality in uncomplicated essential hypertension. *Annals of internal medicine* **114**, 345 (Mar 1, 1991).

92. P. A. Gabow *et al.*, Factors affecting the progression of renal disease in autosomal-dominant polycystic kidney disease. *Kidney international* **41**, 1311 (May, 1992).

93. A. B. Chapman *et al.*, Left ventricular hypertrophy in autosomal dominant polycystic kidney disease. *Journal of the American Society of Nephrology : JASN* **8**, 1292 (Aug, 1997).

94. M. A. Cadnapaphornchai, K. McFann, J. D. Strain, A. Masoumi, R. W. Schrier, Increased left ventricular mass in children with autosomal dominant polycystic kidney disease and borderline hypertension. *Kidney international* **74**, 1192 (Nov, 2008).

95. A. Bardaji *et al.*, Cardiac involvement in autosomal-dominant polycystic kidney disease: a hypertensive heart disease. *Clinical nephrology* **56**, 211 (Sep, 2001).

96. H. Oflaz *et al.*, Biventricular diastolic dysfunction in patients with autosomal-dominant polycystic kidney disease. *Kidney international* **68**, 2244 (Nov, 2005).

97. P. Verdecchia *et al.*, Circadian blood pressure changes and left ventricular hypertrophy in essential hypertension. *Circulation* **81**, 528 (Feb, 1990).

98. T. C. Li Kam Wa, A. M. Macnicol, M. L. Watson, Ambulatory blood pressure in hypertensive patients with autosomal dominant polycystic kidney disease. *Nephrology, dialysis, transplantation : official publication of the European Dialysis and Transplant Association - European Renal Association* **12**, 2075 (Oct, 1997).

99. F. A. Valero *et al.*, Ambulatory blood pressure and left ventricular mass in normotensive patients with autosomal dominant polycystic kidney disease. *Journal of the American Society of Nephrology : JASN* **10**, 1020 (May, 1999).

100. A. Lumiaho *et al.*, Insulin resistance is related to left ventricular hypertrophy in patients with polycystic kidney disease type 1. *American journal of kidney diseases : the official journal of the National Kidney Foundation* **41**, 1219 (Jun, 2003).

101. G. Lembo *et al.*, Abnormal sympathetic overactivity evoked by insulin in the skeletal muscle of patients with essential hypertension. *The Journal of clinical investigation* **90**, 24 (Jul, 1992).

102. T. Ecder, R. W. Schrier, Hypertension and left ventricular hypertrophy in autosomal dominant polycystic kidney disease. *Expert review of cardiovascular therapy* **2**, 369 (May, 2004).

103. P. M. Ruggieri *et al.*, Occult intracranial aneurysms in polycystic kidney disease: screening with MR angiography. *Radiology* **191**, 33 (Apr, 1994).

104. A. P. Rocchini, C. Moorehead, S. DeRemer, T. L. Goodfriend, D. L. Ball, Hyperinsulinemia and the aldosterone and pressor responses to angiotensin II. *Hypertension* **15**, 861 (Jun, 1990).

105. S. Graf *et al.*, Intracranial aneurysms and dolichoectasia in autosomal dominant polycystic kidney disease. *Nephrology, dialysis, transplantation : official*

publication of the European Dialysis and Transplant Association - European Renal Association **17**, 819 (May, 2002).

106. M. M. Belz *et al.*, Recurrence of intracranial aneurysms in autosomal-dominant polycystic kidney disease. *Kidney international* **63**, 1824 (May, 2003).
107. M. M. Belz *et al.*, Familial clustering of ruptured intracranial aneurysms in autosomal dominant polycystic kidney disease. *American journal of kidney diseases : the official journal of the National Kidney Foundation* **38**, 770 (Oct, 2001).

108. H. Hadimeri, C. Lamm, G. Nyberg, Coronary aneurysms in patients with autosomal dominant polycystic kidney disease. *Journal of the American Society of Nephrology : JASN* **9**, 837 (May, 1998).

109. R. Torra *et al.*, Abdominal aortic aneurysms and autosomal dominant polycystic kidney disease. *Journal of the American Society of Nephrology : JASN* **7**, 2483 (Nov, 1996).

110. T. Ecder *et al.*, Reversal of left ventricular hypertrophy with angiotensin converting enzyme inhibition in hypertensive patients with autosomal dominant polycystic kidney disease. *Nephrology, dialysis, transplantation : official publication of the European Dialysis and Transplant Association - European Renal Association* **14**, 1113 (May, 1999).

111. M. Y. Chang, A. C. Ong, Mechanism-based therapeutics for autosomal dominant polycystic kidney disease: recent progress and future prospects. *Nephron. Clinical practice* **120**, c25 (2012).

112. M. Y. Chang, A. C. Ong, New treatments for autosomal dominant polycystic kidney disease. *British journal of clinical pharmacology*, (Apr 18, 2013).

113. G. Aguiari, L. Catizone, L. Del Senno, Multidrug therapy for polycystic kidney disease: a review and perspective. *American journal of nephrology* **37**, 175 (2013).

114. T. Yamaguchi, G. A. Reif, J. P. Calvet, D. P. Wallace, Sorafenib inhibits cAMP-dependent ERK activation, cell proliferation, and in vitro cyst growth of human ADPKD cyst epithelial cells. *American journal of physiology. Renal physiology* **299**, F944 (Nov, 2010).

115. A. J. Streets, O. Wessely, D. J. Peters, A. C. Ong, Hyperphosphorylation of polycystin-2 at a critical residue in disease reveals an essential role for polycystin-1-regulated dephosphorylation. *Human molecular genetics* **22**, 1924 (May 15, 2013).

116. S. Terryn, A. Ho, R. Beauwens, O. Devuyst, Fluid transport and cystogenesis in autosomal dominant polycystic kidney disease. *Biochimica et biophysica acta* **1812**, 1314 (Oct, 2011).

117. S. Nagao *et al.*, Increased water intake decreases progression of polycystic kidney disease in the PCK rat. *Journal of the American Society of Nephrology : JASN* **17**, 2220 (Aug, 2006).

118. X. Wang, Y. Wu, C. J. Ward, P. C. Harris, V. E. Torres, Vasopressin directly regulates cyst growth in polycystic kidney disease. *Journal of the American Society of Nephrology : JASN* **19**, 102 (Jan, 2008).

119. V. H. Gattone, 2nd, X. Wang, P. C. Harris, V. E. Torres, Inhibition of renal cystic disease development and progression by a vasopressin V2 receptor antagonist. *Nature medicine* **9**, 1323 (Oct, 2003).

120. V. E. Torres *et al.*, Effective treatment of an orthologous model of autosomal dominant polycystic kidney disease. *Nature medicine* **10**, 363 (Apr, 2004).

121. V. H. Gattone, 2nd, R. L. Maser, C. Tian, J. M. Rosenberg, M. G. Branden, Developmental expression of urine concentration-associated genes and their altered expression in murine infantile-type polycystic kidney disease. *Developmental genetics* **24**, 309 (1999).

122. X. Wang, V. Gattone, 2nd, P. C. Harris, V. E. Torres, Effectiveness of vasopressin V2 receptor antagonists OPC-31260 and OPC-41061 on polycystic kidney disease development in the PCK rat. *Journal of the American Society of Nephrology : JASN* **16**, 846 (Apr, 2005).

123. V. E. Torres *et al.*, Tolvaptan in patients with autosomal dominant polycystic kidney disease. *The New England journal of medicine* **367**, 2407 (Dec 20, 2012).

124. C. Boehlke *et al.*, Primary cilia regulate mTORC1 activity and cell size through Lkb1. *Nature cell biology* **12**, 1115 (Nov, 2010).

125. O. Ibraghimov-Beskrovnaya, T. A. Natoli, mTOR signaling in polycystic kidney disease. *Trends in molecular medicine* **17**, 625 (Nov, 2011).

126. C. S. Bonnet *et al.*, Defects in cell polarity underlie TSC and ADPKD-associated cystogenesis. *Human molecular genetics* **18**, 2166 (Jun 15, 2009).

127. J. Huang, C. C. Dibble, M. Matsuzaki, B. D. Manning, The TSC1-TSC2 complex is required for proper activation of mTOR complex 2. *Molecular and cellular biology* **28**, 4104 (Jun, 2008).

128. J. M. Shillingford *et al.*, The mTOR pathway is regulated by polycystin-1, and its inhibition reverses renal cystogenesis in polycystic kidney disease. *Proceedings of the National Academy of Sciences of the United States of America* **103**, 5466 (Apr 4, 2006).

129. M. Wu *et al.*, Everolimus retards cyst growth and preserves kidney function in a rodent model for polycystic kidney disease. *Kidney & blood pressure research* **30**, 253 (2007).

130. P. R. Wahl *et al.*, Inhibition of mTOR with sirolimus slows disease progression in Han:SPRD rats with autosomal dominant polycystic kidney disease (ADPKD). *Nephrology, dialysis, transplantation : official publication of the European Dialysis and Transplant Association - European Renal Association* **21**, 598 (Mar, 2006).

131. G. Walz *et al.*, Everolimus in patients with autosomal dominant polycystic kidney disease. *The New England journal of medicine* **363**, 830 (Aug 26, 2010).

132. A. L. Serra *et al.*, Sirolimus and kidney growth in autosomal dominant polycystic kidney disease. *The New England journal of medicine* **363**, 820 (Aug 26, 2010).

133. N. N. Zheleznova, P. D. Wilson, A. Staruschenko, Epidermal growth factor-mediated proliferation and sodium transport in normal and PKD epithelial cells. *Biochimica et biophysica acta* **1812**, 1301 (Oct, 2011).

134. F. Zeng, A. B. Singh, R. C. Harris, The role of the EGF family of ligands and receptors in renal development, physiology and pathophysiology. *Experimental cell research* **315**, 602 (Feb 15, 2009).

135. F. Zeng, M. Z. Zhang, A. B. Singh, R. Zent, R. C. Harris, ErbB4 isoforms selectively regulate growth factor induced Madin-Darby canine kidney cell tubulogenesis. *Molecular biology of the cell* **18**, 4446 (Nov, 2007).

136. J. Du, P. D. Wilson, Abnormal polarization of EGF receptors and autocrine stimulation of cyst epithelial growth in human ADPKD. *The American journal of physiology* **269**, C487 (Aug, 1995).

137. P. D. Wilson, J. Du, J. T. Norman, Autocrine, endocrine and paracrine regulation of growth abnormalities in autosomal dominant polycystic kidney disease. *European journal of cell biology* **61**, 131 (Jun, 1993).

138. V. E. Torres *et al.*, EGF receptor tyrosine kinase inhibition attenuates the development of PKD in Han:SPRD rats. *Kidney international* **64**, 1573 (Nov, 2003).

139. G. Aguiari *et al.*, Polycystin-1 regulates amphiregulin expression through CREB and AP1 signalling: implications in ADPKD cell proliferation. *J Mol Med (Berl)* **90**, 1267 (Nov, 2012).

140. M. C. Hogan *et al.*, Randomized clinical trial of long-acting somatostatin for autosomal dominant polycystic kidney and liver disease. *Journal of the American Society of Nephrology : JASN* **21**, 1052 (Jun, 2010).

141. T. V. Masyuk, A. I. Masyuk, V. E. Torres, P. C. Harris, N. F. Larusso, Octreotide inhibits hepatic cystogenesis in a rodent model of polycystic liver disease by reducing cholangiocyte adenosine 3',5'-cyclic monophosphate. *Gastroenterology* **132**, 1104 (Mar, 2007).

142. L. van Keimpema *et al.*, Lanreotide reduces the volume of polycystic liver: a randomized, double-blind, placebo-controlled trial. *Gastroenterology* **137**, 1661 (Nov, 2009).

143. N. Perico *et al.*, Sirolimus therapy to halt the progression of ADPKD. *Journal of the American Society of Nephrology : JASN* **21**, 1031 (Jun, 2010).

144. V. E. Torres *et al.*, Analysis of baseline parameters in the HALT polycystic kidney disease trials. *Kidney international* **81**, 577 (Mar, 2012).

145. A. M. Sengul, Y. Altuntas, A. Kurklu, L. Aydin, Beneficial effect of lisinopril plus telmisartan in patients with type 2 diabetes, microalbuminuria and hypertension. *Diabetes research and clinical practice* **71**, 210 (Feb, 2006).

146. M. A. Cadnapaphornchai *et al.*, Effect of statin therapy on disease progression in pediatric ADPKD: design and baseline characteristics of participants. *Contemporary clinical trials* **32**, 437 (May, 2011).

147. R. W. Schrier, Optimal care of autosomal dominant polycystic kidney disease patients. *Nephrology (Carlton)* **11**, 124 (Apr, 2006).

148. J. Elliott, N. N. Zheleznova, P. D. Wilson, c-Src inactivation reduces renal epithelial cell-matrix adhesion, proliferation, and cyst formation. *American journal of physiology. Cell physiology* **301**, C522 (Aug, 2011).

149. S. J. Leuenroth, N. Bencivenga, H. Chahboune, F. Hyder, C. M. Crews, Triptolide reduces cyst formation in a neonatal to adult transition Pkd1 model of ADPKD. *Nephrology, dialysis, transplantation : official publication of the European Dialysis and Transplant Association - European Renal Association* **25**, 2187 (Jul, 2010).

150. S. J. Leuenroth, N. Bencivenga, P. Igarashi, S. Somlo, C. M. Crews, Triptolide reduces cystogenesis in a model of ADPKD. *Journal of the American Society of Nephrology : JASN* **19**, 1659 (Sep, 2008).

151. S. J. Leuenroth *et al.*, Triptolide is a traditional Chinese medicine-derived inhibitor of polycystic kidney disease. *Proceedings of the National Academy of Sciences of the United States of America* **104**, 4389 (Mar 13, 2007).

152. R. J. Kolb, S. M. Nauli, Ciliary dysfunction in polycystic kidney disease: an emerging model with polarizing potential. *Frontiers in bioscience : a journal and virtual library* **13**, 4451 (2008).

153. W. A. Abou Alaiwi, S. T. Lo, S. M. Nauli, Primary cilia: highly sophisticated biological sensors. *Sensors (Basel)* **9**, 7003 (2009).

154. S. Ratnam, S. M. Nauli, Hypertension in Autosomal Dominant Polycystic Kidney Disease: A Clinical and Basic Science Perspective. *Int J Nephrol Urol* **2**, 294 (2010).

Chapter 2

Protein Composition and Movements of Membrane Swellings Associated with Primary Cilia

Ashraf M. Mohieldin[1,2], Hanan S. Haymour[2], Shao T. Lo[2], Wissam A. AbouAlaiwi[2], Kimberly F. Atkinson[3], Christopher J. Ward[4], Min Gao[5], Oliver Wessely[6], Surya M. Nauli[1,2,3]

[1]Department of Medicinal & Biological Chemistry, University of Toledo, Health Science Building, Toledo, OH 43614. [2]Department of Pharmacology & Experimental Therapeutics, University of Toledo, Health Science Building, Toledo, OH 43614. [3]Department of Biomedical & Pharmaceutical Sciences, Chapman University, Irvine, CA 92618. [4]Department of Medicine, The Kidney Institute, University of Kansas Medical Center, Kansas City, KS 66160. [5]Liquid Crystal Institute, Kent State University, 1425 University Esplanade, Kent, OH 44242. [6]Department of Cellular and Molecular Medicine, Lerner Research Institute, Cleveland Clinic Foundation, Cleveland, OH 44195.

Corresponding:
Surya Nauli
Chapman University
Harry and Diane Rinker Health Science Campus
9401 Jeronimo Road.
Irvine, CA 92618-1908
Tel: 714-516-5485
Email: nauli@chapman.edu; nauli@uci.edu

Co-corresponding:
Wissam AbouAlaiwi
The University of Toledo
3000 Arlington Ave
Toledo, OH 43614
Tel: 419-383-1949
Email: Wissam.Abou-Alaiwi@UToledo.Edu

Abstract

Dysfunction of many ciliary proteins has been linked to a list of diseases, from cystic kidney to obesity and from hypertension to mental retardation. We previously proposed that primary cilia are unique communication organelles that function as microsensory compartments to house mechanosensory molecules. Here we report that primary cilia exhibit bulb-like structures, which based on their unique ultrastructure and motility, could be mechanically regulated by fluid-shear stress. Together with the ultastructure analysis of the bulb, which contained monosialodihexosylganglioside (GM3), our results showed that ciliary bulb has a distinctive set of functional proteins, including GM3 synthase (GM3S), bicaudal-c1 (Bicc1) and polycystin-2 (PC2). In fact, cilia isolation demonstrated for the first time that GM3S and Bicc1 were members of the primary cilia proteins. Although bulb formation was independent from these proteins under static condition, fluid-shear stress induced bulb formation was partially modulated by GM3S. We therefore propose ciliary bulb has a sensory function within the mechano-ciliary structure. Overall, our studies provided an important step toward understanding the ciliary bulb function and structure.

2.1. Introduction

Primary cilia have been intensively studied over the last few years, because they are relevant to a group of diseases, called ciliopathies. Ciliopathyies include Bardet-Biedl syndrome, nephronophthisis Senior-Loken syndrome, Alstrom syndrome, Meckel syndrome, Joubert syndrome, Oral-facial-digital Type I, Jeune asphyxiating thoracic dystrophy, Ellis van Creveld, Leber congenital amaurosis and polycystic kidney diseases both the recessive and dominant forms (Tobin and Beales, 2009).

Ultrastructurally, primary cilia have hair-like structures supported by microtubules and enclosed by the ciliary membrane. These microtubules are arranged circumferentially, without a central pair "9+0" unlike the one that is seen in motile cilia. The basal body and centriole join together to form a centrosome, which serves as the cell's main microtubule organization. The ciliary necklace, which is made up by a distinct set of membrane proteins at the transition zone, helps differentiate the ciliary membrane from the cell's plasma membrane and cilia membrane (Gilula and Satir, 1972). In addition, receptors, ion channels, transporters and sensory proteins that serve different functions reside on the ciliary membrane. Furthermore, the cilioplasm of a primary cilium is enriched with many signaling intermediates.

In early 2000s, the Spring and Zhou laboratories independently demonstrated that primary cilia play a crucial role in sensing mechanical fluid-shear stress (Nauli et al., 2003; Praetorius and Spring, 2001). Both laboratories showed that activation of primary

cilia by micropipette- or fluid-bending resulted in an increase in cytosolic calcium in renal epithelial cells. Since then, these results have been extended to other cell types, such as endothelial (AbouAlaiwi et al., 2009; Nauli et al., 2008), bone (Delaine-Smith et al., 2014; Qiu et al., 2012), liver (Masyuk et al., 2006), nodal (McGrath et al., 2003; Yoshiba et al., 2012), fibroblast (Su et al., 2013), kidney (Liu et al., 2005; Nauli et al., 2006; Rydholm et al., 2010; Siroky et al., 2006; Xu et al., 2007), and pancreatic cells (Cano et al., 2004; Cano et al., 2006).

Primary cilium has a bulging structure, known as bulb, which was initially observed in 1977 by Dilly et al (Dilly, 1977b). They proposed that ciliary bulb region is the result of material transport within the cilia. Another group (Roth et al., 1988) suggested that the ciliary bulb or swelling is associated with the ciliary shaft and may represent a circumscribed region of the ciliary membrane which is sensitive to environmental osmatic pressure. In this study, we now show for the first time that the bulb of the primary cilium is actually a dynamic structure. We further identified biomechanical properties of the bulb and proteins that are present in the bulb.

2.2. Results

2.2.1. Ciliary bulb is a dynamic structure that can be modulated by fluid-shear stress.

We previously designed an experimental set-up that allowed us to examine primary cilia from the side (Jin et al., 2014). We noticed that when a cell population was roughly handled, the ciliary bulbs seemed to appear more often and was preferentially located

closer to the proximal tip of cilia. On the other hand, in gently handled cells, fewer bulbs were observed and located at the middle of the cilia. Based on this observation, we hypothesized that the ciliary bulb is a dynamic structure and that its dynamic movement can be regulated by the surrounding microenvironment.

To test our hypothesis, we used LLCPK cells grown on flexible substratum (formvar). Ciliary bulbs were studied during absence (static) and presence of fluid-shear stress. In line with our initial observation under static conditions, ciliary bulb tended to oscillate up and down along the ciliary shaft and was never able to reach the tip of the cilium (**Figure 2.1a; SuppMovie A.6**). To examine the sensitivity of a cilium in response to mechanical stimulus, we provided an abrupt pulse of fluid flow, enough to generate small movement of the cilium. To our surprise, this induced the appearance of another bulb (**Figure 2.1b; SuppMovie A.7**). However, one of the bulbs was reabsorbed into the cilia seconds after cessation of fluid flow. In some instances, especially when the additional bulb appeared earlier, an extended fluid flow tended to cause the cilium to maintain an additional bulb longer, even after the flow was stopped (**Figure 2.1c**). One of the bulbs was always maintained at the proximal tip of the cilium, while the second bulb seems to move very close to the tip of the cilium during fluid flow. In some cases, bulb appearance induced by fluid flow was observed from the middle of ciliary shaft (**Figure 2.1d; SuppMovie A.8**). When a new bulb appears, it always traveled to the proximal tip of cilia.

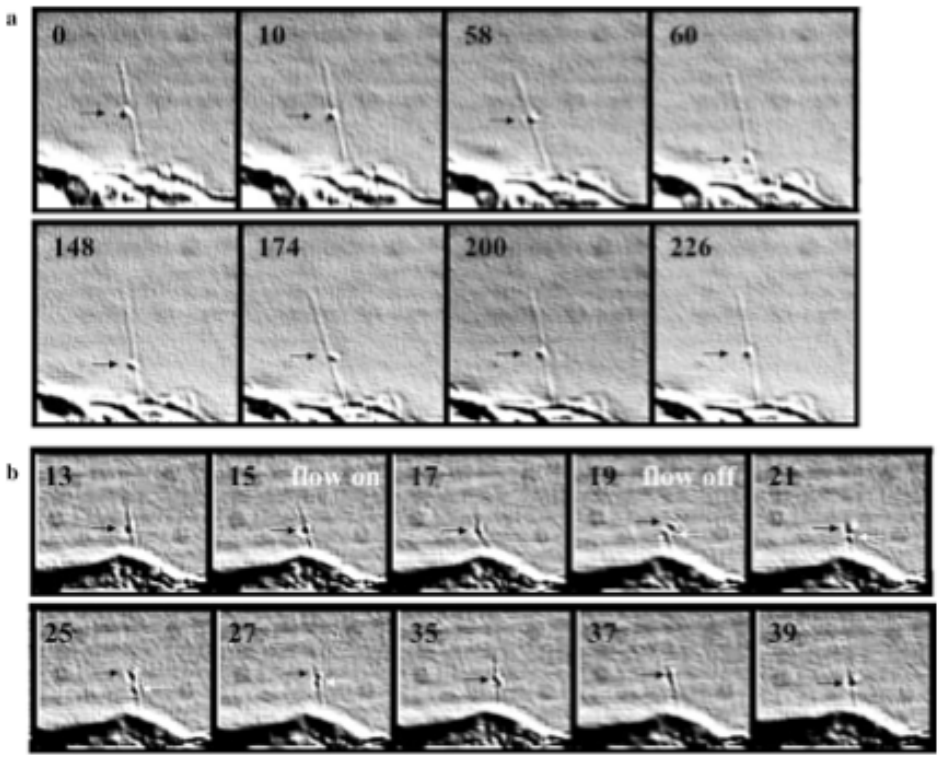

Figure 2.1. The ciliary bulb had a dynamic movement in both static and shear stress conditions. Representative time-lapse images are shown with time in seconds in the panels. Under static conditions, a bulb of a cilium moves along the ciliary shaft but never reaches the proximal tip of cilium (**a**). A very gentle fluid movement (~0.78 dyne/cm^2) was initiated at 2 seconds and stopped at 6 seconds. The new bulb formation was observed immediately (2 seconds). The cilium eventually retained only one bulb when shear stress was ceased (**b**). Fluid flow-induced cilia bending promoted ciliary bulb movement to the tip of cilium. Fluid flow was initiated immediately after the baseline image was taken at 2 seconds (**c**). A fluid movement was initiated at 2 seconds and stopped after 282 seconds (**d**). Formation of a new bulb in the middle of the ciliary shaft was seen at 170 seconds, and the bulb immediately migrated to the distal tip of the cilium (176 seconds). This bulb was reabsorbed when shear stress was ceased, and the physical swelling along the cilia is thus no longer observed. Black arrows indicate the positions of ciliary bulbs, and white arrows indicate newly formed ciliary bulbs.

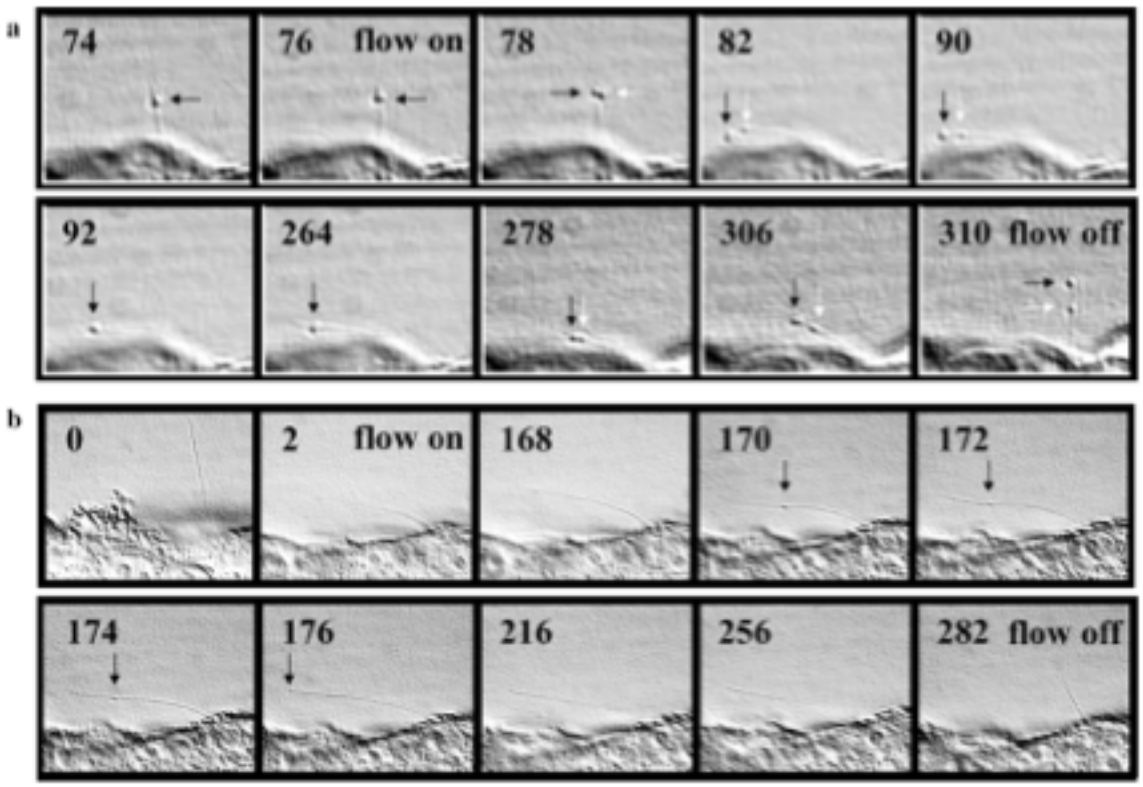

Fig. 2.2. The ciliary bulb could be induced by shear stress.

Representative time-lapse images are shown with time in seconds in each panel. Fluid flow-induced cilia bending promoted the movement of the ciliary swelling to the tip of cilium. Fluid flow was initiated immediately at 76 s (flow on) after the baseline and terminated at 310 s (flow off) (a). Two swelling structures were observed at the tip of the cilium. In a different experiment, a fluid movement was initiated at 2 s (flow on) and stopped after 282 s (flow off) (b). Formation of a new swelling in the middle of the ciliary shaft was seen at 170 s, and the bulb immediately migrated to the tip of the cilium (176 s). This swelling was reabsorbed when shear stress was ceased, and the physical swelling along the cilia is thus no longer observed. Black arrows indicate the positions of ciliary swellings, and white arrows indicate newly formed ciliary swellings

Quantifying these events, we found that ciliary bulb formation was significantly increased from static conditions (30.1%) to mechanical inductions (85.2%; **Figure 2.2a**).

The average cilia length in LLCPK cells was about 6 mm (**Figure 2.2b**). The position of the bulbs was about 4 and 6 mm away from the apical cell surface under static and mechanically-induced conditions, respectively. Regardless of a new or pre-existing bulb, the bulb always moved to the ciliary tip under fluid-shear stress (**Figure 2.2c**). This supported our hypothesis that the ciliary bulb was a dynamic structure and could be modulated by the physical force of fluid movement.

a.

	bulb formation	total observation (N)	% bulb formation
static	274	892	30.72
flow	524	615	85.20

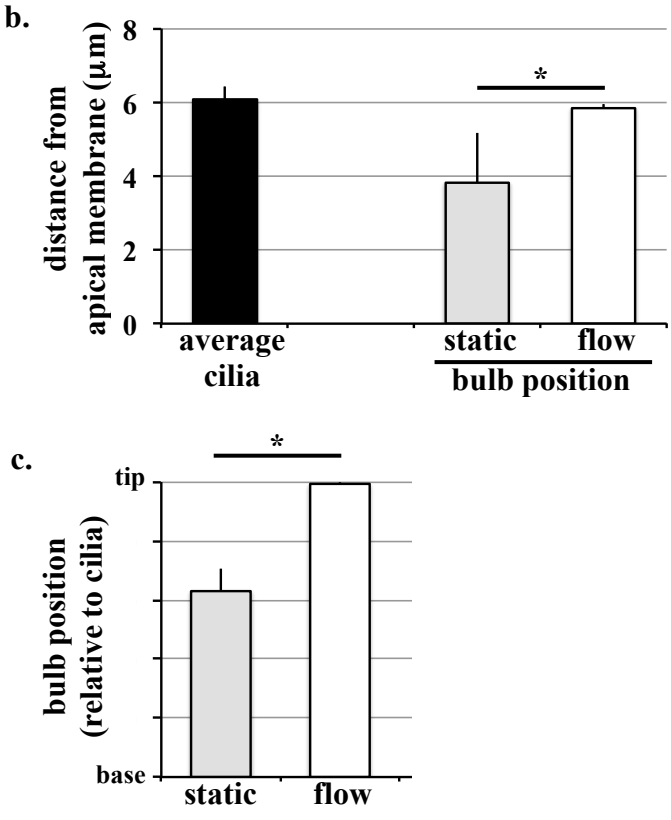

Figure 2.3. Fluid-shear stress modulated position and formation of bulb along the cilium.

Total number of observations on individual cilium was tabulated, and the number of the ciliary bulb was seen more frequently under fluid-shear stress than static condition (**a**). Average ciliary length was shown, and ciliary bulbs significantly moved away from the apical membrane under fluid-shear stress (**b**). When individual bulb was normalized to its own ciliary length, ciliary bulb significantly moved toward the ciliary tip (**c**). Asterisks denote significant difference between groups ($p<0.05$; $n>615$ for each group).

2.2.2. Ultrastructure studies indicated that bulb was part of a cilium embedded with integral proteins.

The ultrastructure of the ciliary bulb had never been studied. Therefore, we confirmed that the ciliary bulb was part of a cilium *in vitro* (**Figure 2.3a**) and *in vivo* (**Figure 2.3b**) by scanning electron microscopy (SEM). Furthermore, more than one bulb could be seen along the ciliary shaft. However, due to the chemical fixations that were required in the SEM studies, we decided to use a second technique to visualize the ciliary bulb to exclude the possibility of chemically-induced artifacts. To this end, we prepared the samples for freeze fracture transmission microscopy (FFTM) by treating cilia with an abrupt high-pressure freezing. The FFTM showed that ciliary membrane, including membrane around the bulb, contained particle indentions, which could be the result of integral proteins (**Figure 3c**). This indicated that ciliary bulb had protein moiety along the ciliary membrane. Furthermore, ciliary bulb structure was conjunct with the ciliary membrane.

2.2.3. Ciliary bulb was glycosylated and contained GM3S, PC2 and Bicc-1.

Because cilia have been shown to have specific lipid and carbohydrate moiety (Janich and Corbeil, 2007), we investigated the presence of monosialodihexosylganglioside (GM3) in the ciliary bulb. To our surprise, we found that GM3 specifically localized only on the ciliary bulb of a cilium (**Figure 2.4a**). As GM3 is synthesized by GM3 synthase (GM3S) (Ishii et al., 1998), we further investigated the presence of GM3S in ciliary bulb. Like GM3, GM3S was specifically localized in the ciliary bulb (**Figure 2.4b**). Because ciliary bulb could be modulated by fluid-shear stress, we next

investigated if polycystin-2 (PC2) known as a mechanosensory protein was localized to the bulb (AbouAlaiwi et al., 2009; Masyuk et al., 2006; Nauli et al., 2003; Nauli et al., 2008; Yoshiba et al., 2012).

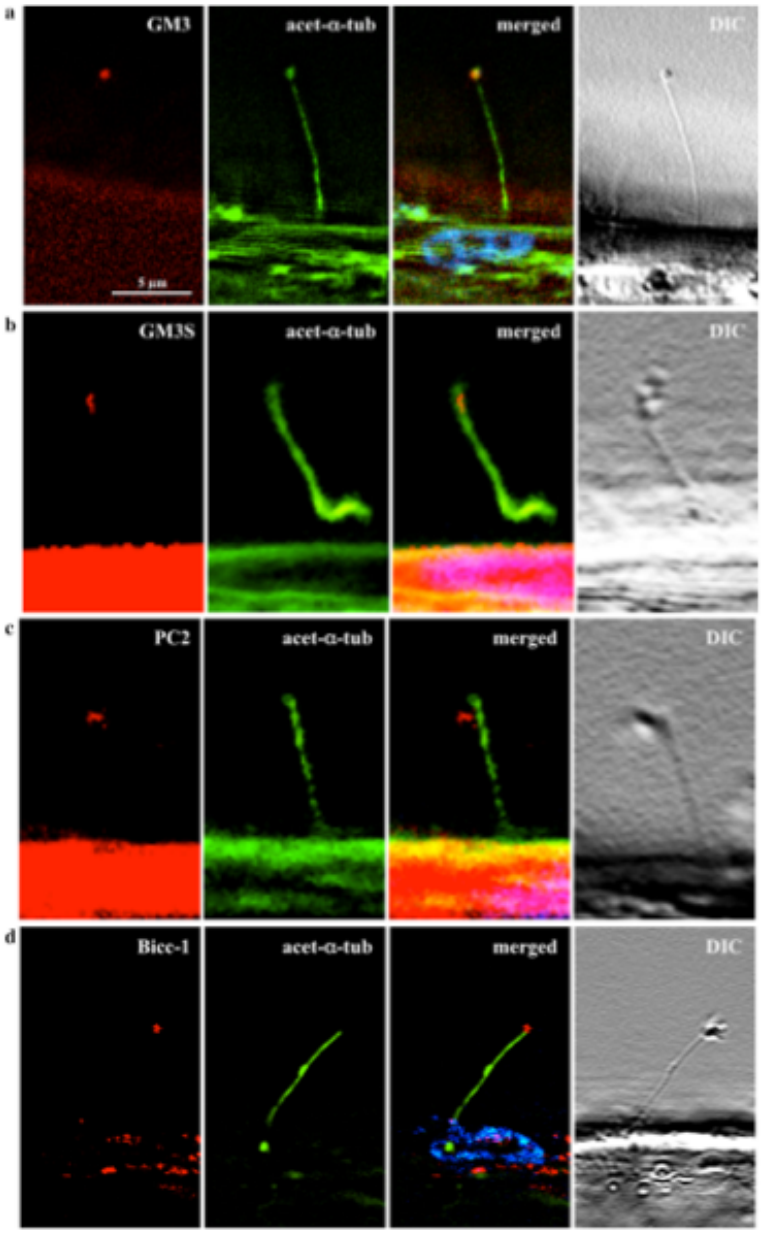

Figure 2.4. GM3, GM3S, PC2 and BICC-1 were localized to ciliary bulb.

Monosialodihexosylganglioside (GM3; **a**), GM3 synthase (GM3S; **b**), polycystin-2 (PC2; **c**) and bicaudal-C (Bicc-1; **d**) were localized to ciliary bulb (red). Acetylated-a-tubulin (acet- a -tub; green) and DAPI (blue) were used as ciliary and nuclear markers, respectively. High resolution differential interference contrast (DIC) images are shown to visualize and confirm the presence of ciliary bulbs. N>65 for each study.

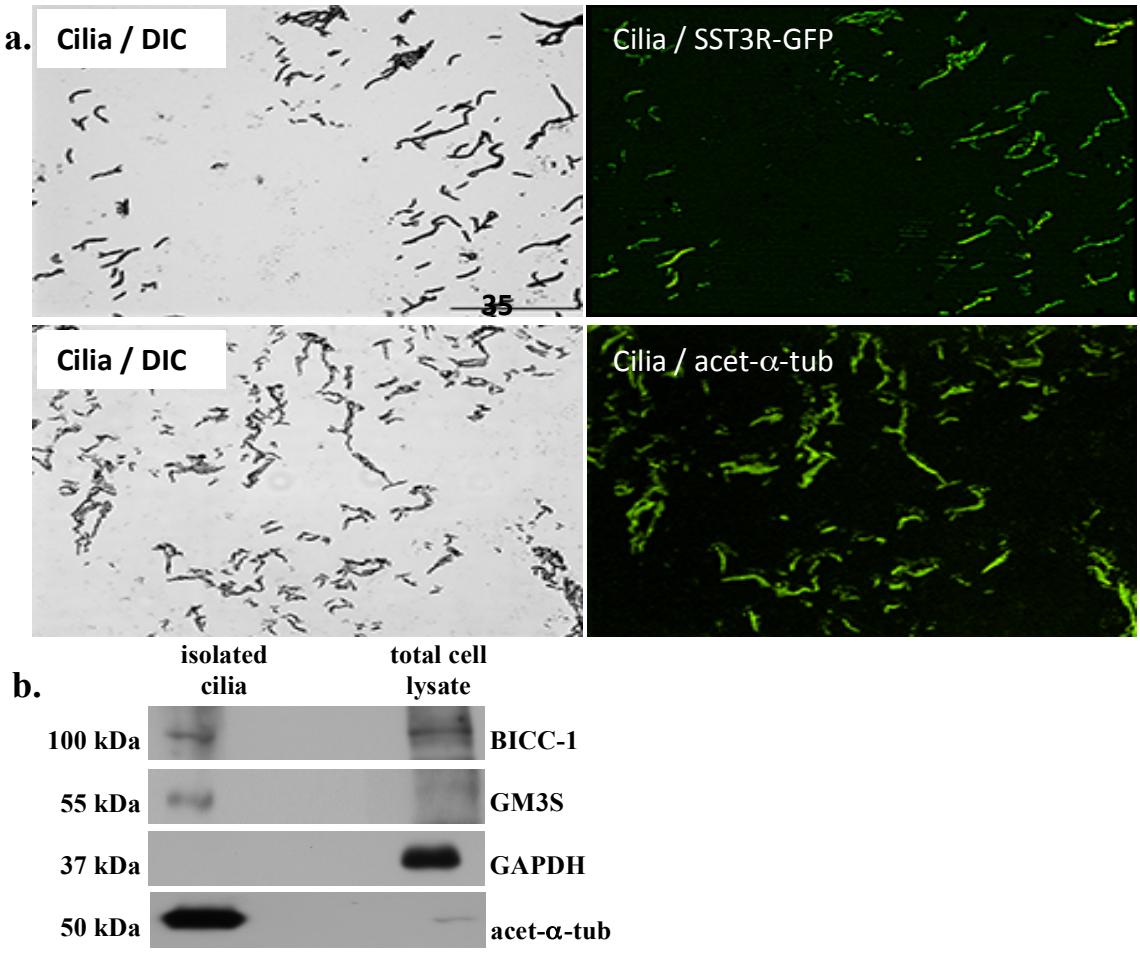

Figure 2.5. GM3S and BICC-1 were detected in isolated primary ciliay.

Stably transfected LLCPK cells with SST3R-GFP were used as confirmation for the primary cilia isolation (**a; upper panels**). Isolated cilia from LLCK cells were immunostained with ciliary marker, acetylated-a-tubulin (acet-a-tub; **lower panels**). The DIC and green fluorescence images demonstrate the purity of primary cilia isolation. The isolated primary cilia were immunoblotted to further confirm the presents of GM3S and BICC-1 in the primary cilia (**b**). GAPDH was used as a negative control while acetylated-a-tubulin was used as a positive control for ciliary marker.

While PC2 has been shown to localize to the entire cilia, some studies have shown a more distinct pattern (Pazour et al., 2002; Yoder et al., 2002). Our result showed that PC2 was localized more specifically to the ciliary bulb rather than the ciliary shaft (**Figure 2.4c**). PC2 has been shown to be modulated by many proteins, but its expression

is specifically regulated by Bicc-1 (Tran et al 2010). Indeed, Bicc-1 was also specifically localized to the ciliary bulb (**Figure 2.4d**).

To our knowledge, we were the first to show that the bulb was glycosylated, possibly by GM3S and that Bicc-1 was localized to the cilia. To verify our finding, we next confirmed if GM3S and Bicc-1 could be detected in cilia using cilia isolation and Western Blot analyses. Using stably transfected-SST3R in LLCPK cells to help visualize isolated cilia, we were able to isolate cilia by shearing the cilia off the cell surface (**Figure 2.5a**) (Mitchell, 2013). This was confirmed using non-transfected cells, where isolated cilia were immunostained with ciliary marker acetylated-a-tubulin. In the Western Blot analyses, we compared lysates from the isolated cilia and the cell body (**Figure 2.5b**). GAPDH as a marker for cell body and acetylated-a-tubulin as a ciliary marker demonstrated the purity of our cilia isolation. Moreover, GM3S was mainly localized in cilia of fully differentiated cells, while that Bicc-1 was detected in both cilia and cell body. This confirmed that GM3s and Bicc1 were localized on the primary cilia.

2.2.4. Shear-induced bulb formation was partly modulated by GM3S, but not Bicc-1 or PC2.

To identify if formation of ciliary bulb was regulated by GM3S, Bicc-1 and/or PC2, we generated knockdown cell lines for each gene (*St3gal5*, *Bicc-1* and *Pkd2*). We tested knockdown efficiencies of these genes using four different knockdown sequences (**Figure 2.6a**). In the case of *Bicc-1*, we used both chemical siRNA transfection and shRNA viral infection approaches. All stably knockdown cell lines were verified for

their corresponding protein expression, and *Bicc-1* #B, *St3gal5* #D, and *Pkd2* #D shRNA knockdown cell lines were selected for further studies.

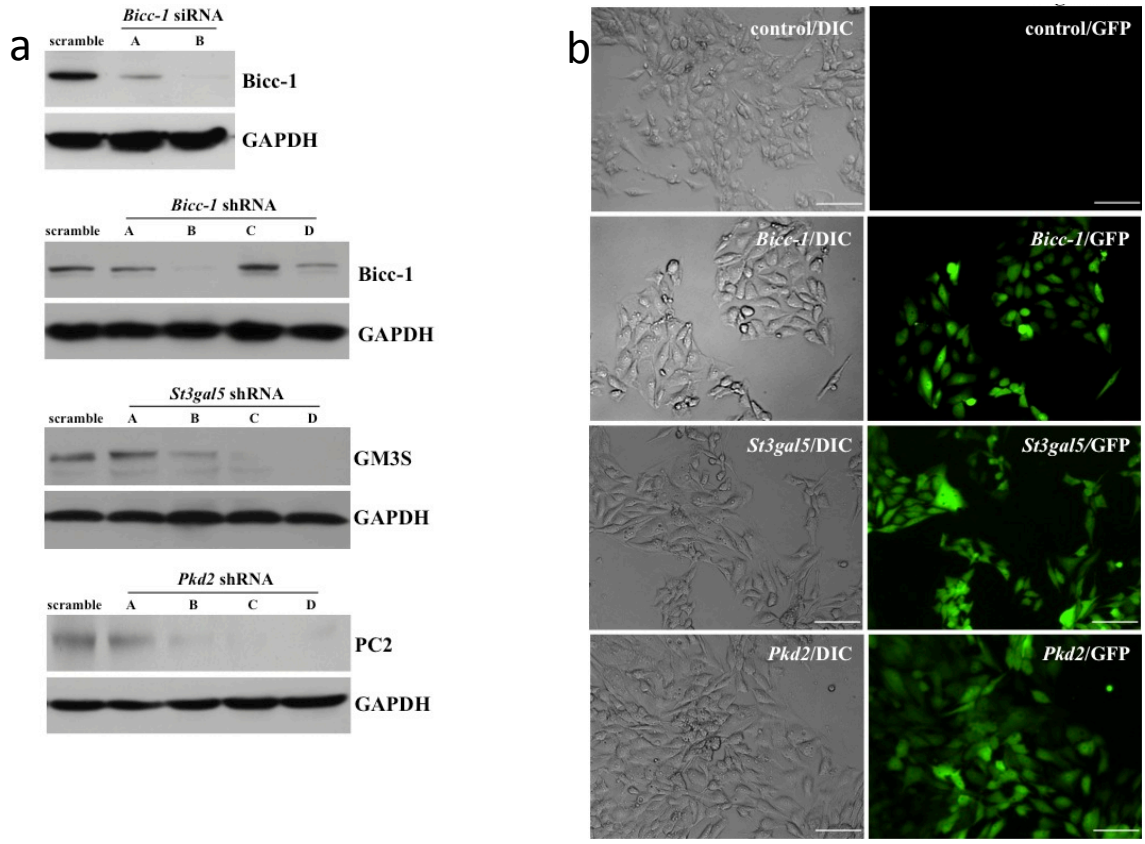

Figure 2.6. Stable *Bicc-1, St3gal5* and *Pkd2* knockdown cell lines were generated.

Knockdown efficiency was first examined with silencing different regions of each gene, and siRNA was also tested as an earlier approach (**a**). Total cell lysate from scramble (control) and various siRNAs or shRNA-GFP lentivirus sequences (A, B, C, D) of each gene were analyzed. Once the shRNA-GFP knockdown efficiency was selected, infection efficiency among cell population was visualized with DIC and fluorescence microscopy (**b**). Stable knockdown cells were further verified with flow cytometer to show high efficiency knockdown.

Because the shRNA expression was tagged with fluorescence GFP, we confirmed the stability of the shRNA integration in these knockdown cell lines after several passages by immunofluoresce microscopy (**Figure 2.6b**) and flow-cytometry (**Figure 2.6c**). To test the hypothesis that GM3S, Bicc-1 and/or PC2 were involved in bulb formation, we studied the bulb formation in *St3gal5*, *Bicc-1* and *Pkd2* knockdown cells. The presence of bulb was apparent in *St3gal5* knockdown cells (**Figure 2.7a**). As expected, GM3S was not observed in the ciliary bulb in *St3gal5* knockdown cells. Surprisingly, Bicc-1 was also not detected in ciliary bulb, whereas PC2 was still present. Bulb formation was detected in *Bicc-1* knockdown cells (**Figure 2.7b**).

As expected, Bicc-1 was not observed in the ciliary bulb in *Bicc-1* knockdown cells. Interestingly, GM3S was also not detected in ciliary bulb, whereas PC2 was still present. As seen in *St3gal5* and *Bicc-1* knockdown cells, bulb formation was detected in *Pkd2* cells (**Figure 2.7c**). As expected, PC2 was not observed in the ciliary bulb in *Pkd2* knockdown cells. Surprisingly, GM3S was also not detected in ciliary bulb, whereas Bicc-1 was still present. Our studies indicated that localization of GM3S to ciliary bulb, in part, was regulated by Bicc-1 and PC2. More importantly, our results demonstrated that GM3S, Bicc-1 and/or PC2 were not involved in bulb formation. To further investigate if flow-induced bulb formation was altered in these cells, we challenged the cells with fluid-shear stress and quantified formation of the bulb in each of these cells (**Figure 2.7d**). Our results showed that unlike for PC2 and Bicc-1, GM3S was in part required for flow-induced bulb formation.

a. *St3gal5* knockdown

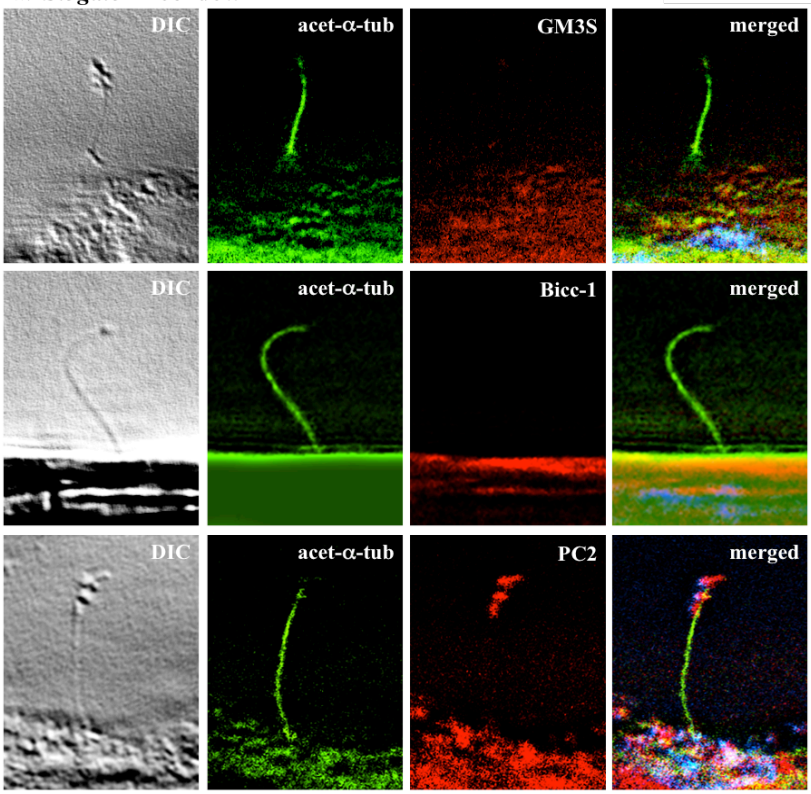

b. *Bicc-1* knockdown

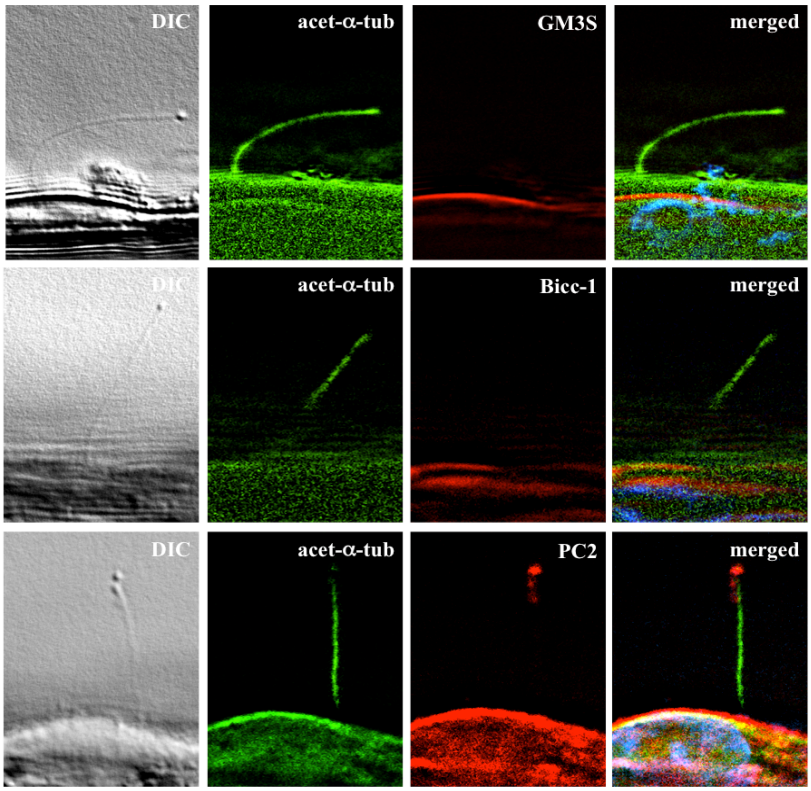

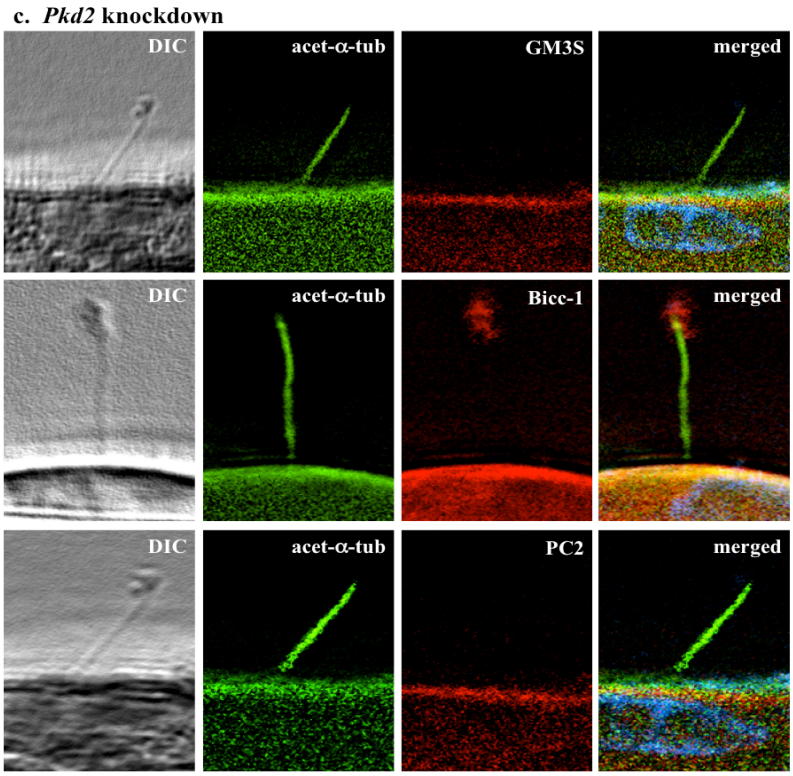

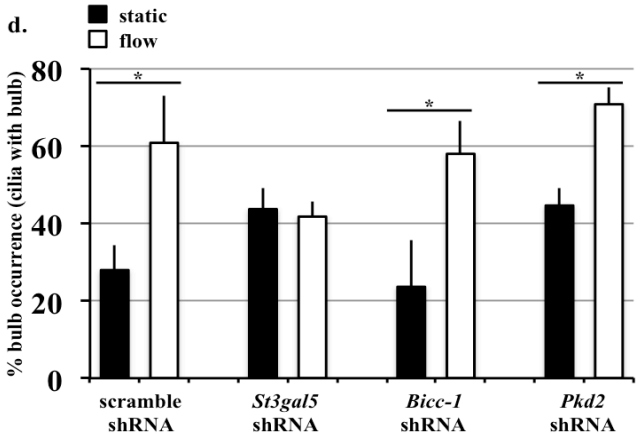

Figure 7. Flow-induced bulb formation was modulated by GM3S.

GM3S, Bicc-1 or PC2 expression (red) in ciliary bulb was examined in *St3gal5* (**a**), *Bicc-1* (**b**) and *Pkd2* (**c**) knockdown cell lines. Acetylated-a-tubulin (acet- a -tub; green) and DAPI (blue) were used as ciliary and nuclear markers, respectively. High resolution differential interference contrast (DIC) images are shown to visualize and confirm the presence of ciliary bulbs. All

knockdown cells had primary cilia and bulb formation. However, only *St3gal5* knockdown cells lost bulb formation in response to fluid-shear stress (**d**). Asterisks denote significant difference between groups ($p<0.05$; n=65-242 for each group).

2.2.5. Global expressions of miRNA17, Bicc-1, GM3S and PC2 were interrelated at the cellular level.

To understand the global effect of the knockdown genes at the cell level, we performed immunoblotted studies to understand the interrelationship between the ciliary and cytoplasmic proteins. In particular, Bicc-1 (Tran et al., 2010), GM3S (Berselli et al., 2006; Harduin-Lepers et al., 2005) and PC2 (Koulen et al., 2002) have been detected at the cell body. miRNA-17 (Mir-17) was included in this experiment, because Mir-17 has been known to modulate PC2 and Bicc-1 (Tran et al., 2010). Our studies indicated while knockdown of *Mir-17* induced Bicc-1 expression level, knockdown of *Bicc-1*, *St3gal5*, or *Pkd2* could have an effect on the global expression of each other (**Figure 2.8**).

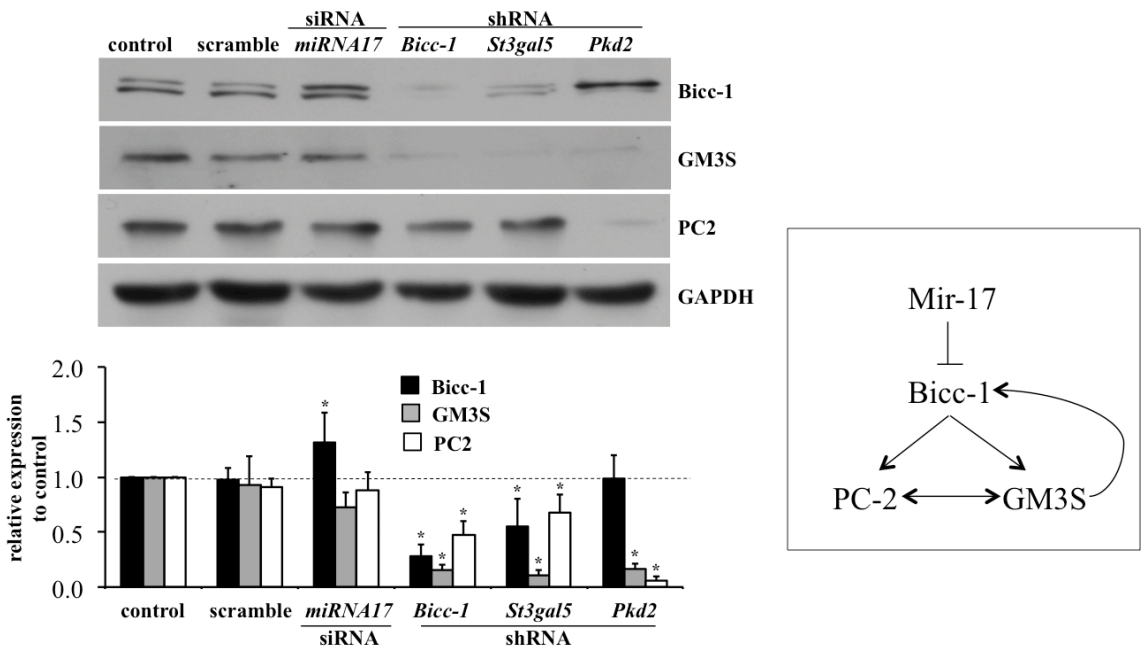

Figure 2.8. Relative gene expression was analyzed in the whole cell lysate.

To examine if there is any interrelationship between the ciliary bulb proteins at the cell level, protein expressions from the total cell lysate were analyzed in wild-type (control), scramble, *miRNA17*, *st3gal5*, *Bicc-1* and *Pkd2* knockdown cells. Asterisks denote significant difference between groups ($p<0.05$; $n=3$).

2.3. Discussion

Previous studies have shown the presence of the ciliary bulb along the ciliary shaft in both primary and secondary cilia of vertebrates (Albrecht-Buehler and Bushnell, 1980; Dalen, 1981; Elofsson et al., 1984; Su et al., 2013), as well as invertebrates (Dilly, 1977a; Dilly, 1977b; Matera and Davis, 1982). The presence of the ciliary bulb on these studies was observed in the proximal tip and at the middle of the ciliary shaft. Some have suggested that these ciliary bulbs are the resultant of chemical fixation artifacts (Ehlers and Ehlers, 1978). Along this assumption, another study has suggested that the ciliary bulb represents circumscribed regions of the ciliary membrane that are sensitive to osmotic pressure (Dalen, 1981). In addition, ciliary bulb has also been observed *in vivo* (Roth et al., 1988),which further supports that the bulb is not an artifact.

Observing the entire cilium from the side-view allowed us to visualize and study the dynamics of ciliary bulb for the very first time in a single living cell. Proximal tubular epithelial LLCPK cells were used among other cells types, because of their long cilia, which enabled us to image and differentiate ciliary bulb from the cell body. Based on our results, the ciliary bulb was neither a result of chemical fixation artifacts nor caused by osmotic pressure. Our time-lapsed imaging studies **(Figure 2.1; Movie B.6)** confirmed that ciliary bulb was observed in LLCPK cells without any presence of chemical reagents. Furthermore, ciliary bulb was also observed to move dynamically along the ciliary shaft without the presence of fluid-shear stress.

This indicated that ciliary bulb movement along the ciliary shaft could occur (1) without the bending of the cilia and (2) without the osmotic pressure. It has also been suggested that the formation of ciliary bulb is only observed in the ciliary tip of growing cilia due to differences in the growth rates between the ciliary membrane and the axonemal microtubules (Jensen et al., 1987). Another suggestion is that intraflagellar-transport (IFT) molecules within the cilia are the main modulator of the ciliary bulb formation, and IFT forms the bulb-like structure during the absence of elongating axonemal microtubules (Dilly, 1977b; Jensen et al., 1979). Our current results further indicated that ciliary bulbs were dynamically observed in the ciliary tip only during fluid-shear stress, but during static condition, ciliary bulbs were mostly observed along the ciliary shaft **(Figure 2.2)**. Noteworthy, our analyses were performed in fully differentiated LLCKP cells with optimal length of cilia.

Based on our studies, a cilium can have multiple bulbs along its ciliary shaft **(Figure 2.1; Movie B.7)**. Interestingly, the multiple ciliary bulbs could come very close to each other. In some cases, the bulbs may have arrived from a split of an existing bulb. However, we did not directly capture such an event. One of the most obvious examples was seen from a cilium that did not initially have a bulb **(Figure 2.1; Movie B.8)**. In this case, bulb appearance was induced by fluid-flow and was observed from the middle of ciliary shaft. Interestingly, when a new bulb was induced by fluid-flow, it always traveled to the proximal tip of cilia. This phenomenon was also confirmed in our immunefluorescence studies **(Figures 2.4 and 2.7)**, where most of the bulbs were observed on the tip of the cilia. Of note is that immunostaining method required frequent washing steps, before and

after fixation, which would generate fluid-flow on the top of the cells. This fluid-flow helped the ciliary bulb to move to the tip of the cilia, which further supported our live-imaging studies and our hypothesis that ciliary bulb was a sensitive structure responsive to the surrounding microenvironment.

Although the presence of ciliary bulb has been reported (Dilly, 1977b; Roth et al., 1988), the ultrastructure of a bulb had not been previously identified. Our studies now indicate that ciliary bulb shared an intact structure along with the ciliary shaft, and there is no indication that ciliary bulb was attached to the outer ciliary membrane **(Figure 2.3)**. This was observed with not only SEM but also FFTM, which gave us the ability to visualize the ciliary bulb without the use of any chemical fixation. Furthermore, the FFTM images showed particle indentions along the ciliary membrane, including the ciliary bulb. This finding suggested that ciliary bulb and the cilia itself contained integral and/or matrix proteins and that the bulb bilayer was part of the cilia bilayer.

The GM3 ganglioside is one of the members of the glycosphingolipid family (Seyfried et al., 1978). Previous study has shown that GM3 is co-localized with acetylated-a-tubulin to the cilium in MDCK cells (Janich and Corbeil, 2007). The study showed that GM3 is enriched in the cilium and found at the base up to the tip of the cilium. Together with our FFTM study, GM3 was a good candidate to investigate in the ciliary bulb. To our surprise, we found that GM3 specifically localized on the ciliary bulb of a cilium **(Figure 2.4)**. To further investigate about the GM3 ganglioside, we looked at the GM3S, which synthesizes GM3 in the Golgi (Berselli et al., 2006). Like GM3, GM3S was also localized to the ciliary bulb. To our knowledge, this was the first time that GM3S had

been shown to localize to the primary cilia, specifically on the ciliary bulb. These findings further confirmed that ciliary bulb had a distinct protein moiety on its surface, consistence with our FFTM result.

PC2 has also been shown to contain N-glycosylation sites where it can be N-glycosylated (Cai et al., 1999; Hidaka et al., 2004). In addition, N-liked sugar moiety can be removed by endoglycosidase from PC2. Thus, PC2 might potentially co-localize with GM3 and/or GM3S. Because PC2 is also known as a mechanosensory protein and because shear-stress could induce bulb formation, we asked if PC2 could be localized to the ciliary bulb. In agreement with our assumption, we found that PC2 localized to ciliary bulb **(Figure 2.4)**. This might suggest that glycosylated proteins (1) direct PC2 to the bulb, (2) maintain ciliary bulb structure (*st3gal5*), (3) and therefore play an important role in PC2 and *Bicc-1* signaling pathway. Worth mentioning, PC2 has been known to localize to the primary cilia. However, we have found that PC2 was expressed and localized more specifically in the ciliary bulb than in the ciliary shaft, at least in LLCPK cells.

Many proteins can modulate PC2, but the RNA-binding protein Bicc-1 specifically regulates PC2 expression through antagonizing the repressive activity of the microRNA-17 (miR-17) on the 3′UTR of *Pkd2* mRNA (Tran et al., 2010). In addition, Bicc1 mouse mutant died prenatally and developed severe polycystic kidney disease. We thus asked if Bicc-1 could also be localized to the ciliary bulb. Our immunofluorescence studies suggested that Bicc-1was specifically localized to the ciliary bulb, and Bicc-1 localization to cilia was also confirmed with western blot analyses (**Figure 2.5**).

Our data unfortunately did not indicate any of these proteins were directly involved in the ciliary bulb formation. Knockdown of any of these proteins showed that ciliary bulb formation remained unaffected (**Figure 2.7**). When stably knockdown cells for each gene and challenged with fluid-shear stress, only stable cell line with *st3gal5* knockdown showed a decrease in bulb formation in response to fluid-shear. This indicated that mutation in *st3gal5* gene could be responsible for the modulating ciliary bulb formation during fluid-shear stress.

Interestingly, only PC2 expression was observed on the ciliary bulb in either *st3gal5* or *Bicc-1* cells. This might also indicate that there was a cross talk between GM3S and Bicc-1. Noteworthy, Bicc-1 has been shown to regulate mRNA stability and translation via modulation of mRNA polyadenylation in Drosophila and C. elegans (Mahone et al., 1995; Saffman et al., 1998; Wang et al., 2002). In addition, Mir-17 regulated by Bicc1 has been shown to regulate PC2 expression (Tran et al., 2010). However, due to the cross talk between GM3S and Bicc1, it was not known whether Mir-17 was involved in the expression of GM3S. As a result, we included siRNA Mir-17 transfected cells to see its effects on GM3S, Bicc-1 and PC2 **(Figure 2.8)**. Our studies indicated that while knockdown of *Mir-17* induced an increase in Bicc-1 expression level, knockdown of *Bicc-1*, *St3gal5*, or *Pkd2* could have an effect on the expression of each other at the cell level.

Overall, our studies demonstrated for the first time that ciliary bulb was a dynamic structure and that its dynamic movement could be regulated by fluid-shear stress. Furthermore, the bulb was glycosylated, possibly by GM3S, and we showed that Bicc-1, GM3S and PC2 were localized to the ciliary bulb. Together, our findings provide an opportunity to future studies on the structural complexity of the primary cilia, which will lead to better understanding of cilia-related diseases.

Acknowledgements

This work partially fulfills the requirements of a PhD degree in Medicinal and Biological chemistry for Ashraf M. Mohieldin. This work was supported by the National Institute of Health, R01DK080640 (SMN), R01DK080745 (OW) and F31DK096870 (AMM).

2.4. **Methods and Materials**

2.4.1 Cell culture

The porcine kidney epithelial cells (LLC-PK1) were used in this study and cultured in Dulbecco's Modified Eagle Medium (DMEM) (*Corning Cellgro*), 10% fetal bovine serum (FBS) (*HyClone, Inc*.) and 1% penicillin/streptomycin (*Corning Cellgro*) at 37°C in 5% CO_2 incubator. Prior to experiments, cells were serum starved 24 hours for differentiation.

2.4.2. Formvar technique

We have adopted a new technique to visualize cilium from the side (Jin et al., 2014). Briefly, a special flexible substratum (Formvar; *Electron Microscopy Science*) was dissolved in ethylene dichloride to make a 2-4% Formvar solution. A 18x18 glass slide was then coated with the fomvar solution, and the glass slide was placed in a six-well plate until dry, followed with 50 μg/ml collagen coating on the top of the Formvar layer. The six-well plate was then placed under ultraviolet light for 30 minutes for sterilization. After sterilization, the Fomvar cover slide was briefly washed with phosphate buffer saline (PBS, pH 7.4). Cells were then grown on this collagen-coated formvar flexible substratum (FFS). A pair of sharp forceps was used to peel the FFS and gently folded to form a triangle shape where cilia were oriented upward for visualization. After folding, the FFS was placed on a special made glass-bottom plate and held with a cover glass slide.

2.4.3. Live imaging

The FFS was put on a Nikon TiU stage. A special thin pipette tip (*Fisher scientific, Inc.*) was connected with inlet and outlet clear plastic PVC tubes with a 0.031 inch inside diameter (*Nalgene, Inc.*). The tubes were inserted into the in-flow and out-flow pumps (*InsTech P720*) and the pipette tips were inserted between the bottom glass plate and the glass cover slide to generate shear stress of 0.78 dyne/cm^2 as described previously (Jin et al., 2014).

2.4.4. Immunostaining

LLCPK cells were immunostained using a standard protocol (AbouAlaiwi et al., 2011). Briefly, cells were preferred to be at 80-90 % confluence before immunostaining. Cells were rinsed with sodium cacodylate buffer, fixed with 3 % glutaraldehyde in 0.2 M sodium cacodylate buffer for 10 minutes and permeabilized with 1% Triton-X in sodium cacodylate for 5 minutes. All primary antibodies were diluted in 10% FBS solution; acetylated-a-tubulin (1:10,000; *Sigma, Inc*.), BICC-1 (1:500; *ABGENT, Inc.*), GM3 (1:200; *Seikagaku Biobusiness, Inc*) GM3S (1:800; *LSCBIO, Inc*.), and PC2 (1:50; *Santa Cruz, Inc.*). All secondary antibody was also diluted in 10% FBS to decrease background florescence; FITC fluorescence secondary antibody (1:500; *Pierce, Inc*.) and TexasRed fluorescence secondary antibody (1:500; *Pierce, Inc*.). Cells were then washed twice with cacodylate buffer and mounted with DAPI (*Vector laboratories, Inc.*). Images were taken with Nikon TE2000 using Metamorph software.

2.4.5. RNAi Knockdown

To generate stable knockdown cell lines, HEK-293T cells were transfected with shRNA lentiviral vectors specific to *St3gal5*, *Bicc1* or *Pkd2* (Origene; pGFP-C-shLenti). Viral particles were collected after 48 hours, centrifuged at 4000 rpm, and passed through a 0.45 μm filter. Cells were then centrifuged at 2,500 rpm for 30 minutes at 30°C with viral particles containing 8 μg/ml polybrene and then cultured for up to 72 hours. Gene silencing was further confirmed by Western blot, and only the shRNA lentivirus with higher knockdown efficiency was selected. Stable knockdown cell lines were obtained through cell sorting (*BD Bioscience, Inc.*) and puromycin dihydrochloride (*Santa Cruz, Inc.*). The shRNA sequences used in this study are listed below.

Table 2.1. Sequence of the shRNA used

Descriptions		**Sequences**
Scrambled		5′-TGA CCA CCC TGA CCT ACG GCG TGC AGT GC-3′
St3gal5	A	5′-CAA GAT GGT CCT GAG TGT CCT CAC TTC GT-3′
	B	5′-CAT AAT GCA CTG CTC GCG CTG TTG TAT CC-3′
	C	5′-GAG CTGT AGG CGT TGT GTG GTC ATC GGA A-3′
	D	5′-TCT TGC GGT GAT CGG AAC AGA CAA GTT CT-3′
Bicc1	A	5′-CGA ATG TAT GGT GCT ACT GTGA TAG TTC G-3′
	B	5′-ATG GAA CAG CTC GAT GTC TTC ATC AGT AT -3′
	C	5′-GAA CTC GCT CCT GAA TGC TCT CAA TAG CT-3′
	D	5′-AGA TCG ACC TTC AGA CAT TCC TCA CTC TC-3′
Pkd2	A	5′-TTG TGC ATC TTG ACC TAC GGC ATG ATG AG-3′
	B	5′-TAC GGC ATG ATG AGC TCC AAT GTG TAC TA-3′
	C	5′-TTT GAT TTC TTC CTG GCA GCC TGT GAG AT-3′
	D	5′-GTC TGG ATT AAG CTC TTC AAA TTC ATC AA-3′

2.4.6. siRNA Transfection

Cells were plated so that they reached 60-80% confluence upon the time of transfection as previously described (AbouAlaiwi et al., 2011). Diluted lipofectamine reagent and siRNA were used according to the manufacturer guideline (*Invitrogen, Inc.*). Cells were transfected for 48-72 hours, and the siRNA sequences used in this study are listed below.

Table 2.2. List of the siRNA sequences

Descriptions	**Sequences**
Scrambled	5′-ACG UGA CAC GUU CGG AGA ATT-3′
Bicc1(A)	5′-UUA AAG GAC ACA GAA ACG C-3′
Bicc1(B)	5′-CCA ACC ACG UAU CCU AUA A-3′
Bicc1(C)	5′- GGA AGC AAU GGC UGU AAC CUG AAC A-3′
Mir-17	5′-CUC AAA GUG CUU ACA GUG CAG GUA GUU-3′

2.4.7. Flow cytometer

All stable cell line *St3gal5-GFP*, *Bicc1-GFP* and *Pkd2-GFP* were further analyzed for GFP expression efficiency. Prior to analysis, cells were rinsed with 1X PBS, detached with trypsin, pelleted at 4000 rpm, resuspended in PBS and analyzed using C6 Flow Cytometer (*Accuri Cytometers*, MI, USA).

2.4.8. Immunoblotting

Cell lysate was prepared using a standard technique as previously described (AbouAlaiwi et al., 2011). Briefly, cells were rinsed with PBS, added fresh radioimmunoprecipitation

assay (Ripa) buffer containing protease inhibitor, placed on ice, gently shaken for 30 minutes, scraped from the culture dish, transferred to microcentrifuge tube, and spun for 15 minutes at 10,000 *g (accuSpin Micro 17, Fisher scientific, Inc.)*. Total cell lysate was transferred into another microcentrifuge tube and stored in -20°C and analyzed using a standard 6-10% gradient sodium dodecyl sulfate–polyacrylamide gel electrophoresis. Antibody against GM3S (*LSCBIO*, Inc.), bicaudal C (*ABGENT, Inc.*), polycystin-2 (*Santa Cruz, Inc.*), GAPDH (*cell signaling, Inc.)* and acetylated-a-tubulin (*Sigma, Inc*.) were used at dilutions of 1:800, 1:1000, 1:200, 1:1000 and 1:1000 respectively.

2.4.9. Scanning electron microscopy (SEM)

SEM was carried out as previously describe (Abdul-Majeed et al., 2012). Briefly, cells were fixed with 2.5% of glutaraldehyde in 0.085 M cacodylate buffer for 1 hour and then washed with cacodylate buffer for 5 minutes. A 1% of osmium tetroxide in 0.085 M cacodylate buffer was used for 10 minutes and dehydrated the samples through a graded series of ethanol. The sample was then infiltrated with hexamethyldisilazane and left air dry overnight. The sample was then coated with gold particles and examined (*Hitachi* S-4800).

2.4.10. Freeze Fracture Transmission Electron Microscopy (FFTEM)

Sample was prepared on replica specimens prepared by combining high pressure freezing and freeze fracture. LLCPK cells were grown directly inside gold-plated FF carriers, and they were then cryo-fixed with the original culture media in a Leica EM Pact 2 high-pressure freezer. To optimize sample preparation, we also replaced the culture media in

some of the carriers with 20% dextran solution (40K Mr) right before the freezing, which did not result in noticeable difference. After high pressure freezing, the carriers were quickly transferred into a freeze-fracture vacuum chamber (*BalTec BAF060*) and fractured at -165°C. The topography of the fractured surface was then replicated by the deposition of a thin (~4 nm) Pt/C layer at 45° followed by a continuous carbon film (~20 nm) deposited normally to the surface. The replicas were collected by holey lacey carbon grids after dissolving all the culture media with water, and investigated in a FEI Tecnai F20 TEM operated at 200 KV.

2.4.11. Isolation of primary cilia

The LLCPK primary cilia were isolated by shear force (Mitchell, 2013). First, LLCPK cells were grown in 150 mm culture dish in 10% DMEM and 1% penicillin/streptomycin in a humidified incubator at 37°C in 5% CO2. Cells were grown for maximum 8 days and were starved for differentiation before the shaking. Cells were rinsed with PBS briefly and gently, added 10 ml of PBS. The dish was then placed on a rotary shaker and shook for 4 minutes at 350 rpm *(Orbital shaker, Cole-Parmer, Inc.)*. Carefully, the 10 ml media was transferred to a 50 ml centrifuge tube and spun for 30 minutes at 3,000 *g* at 4°C (*Eppendrof 5810R*). The supernatant was then transferred to a polyallomer tube and spun for 1 hour at 70,000 *g* at 4°C in an ultracentrifuge (*Beckman optima L-60*). Primary cilia (pellet) were then resuspended in either Ripa buffer or resuspension buffer.

2.4.12. Visualization of isolated primary cilia

A nitrogen smearing technique was used to visualize and verify the efficiency of isolated primary cilia. Right after the isolation process, isolated primary cilia were fixed in 10 uL of 2 % paraformaldehyde, transferred and spread equally on a glass slide. The coverslip was then placed on top of the glass slide. The whole glass slide was then placed in liquid nitrogen for about 1-2 minutes. The coverslip was then peeled off with a razor blade from the glass slide, and was washed with PBS three times for 5 minutes each. The glass slide was then let to air dry and stored in -80°C. Images were taking using Nikon TE2000.

2.4.13. Statistics

All quantifiable experimental values are expressed as mean ± SEM, and values of $p < 0.05$ are considered significant. All comparisons between two groups were performed with Student's *t* test. Comparisons of three or more groups were done using ANOVA, followed with Tukey's posttest. Data analysis was performed using SigmaPlot software version 11.

Reference

Abdul-Majeed, S., Moloney, B. C. and Nauli, S. M. (2012). Mechanisms regulating cilia growth and cilia function in endothelial cells. *Cell Mol Life Sci* **69**, 165-73.

AbouAlaiwi, W. A., Ratnam, S., Booth, R. L., Shah, J. V. and Nauli, S. M. (2011). Endothelial cells from humans and mice with polycystic kidney disease are characterized by polyploidy and chromosome segregation defects through survivin down-regulation. *Hum Mol Genet* **20**, 354-67.

AbouAlaiwi, W. A., Takahashi, M., Mell, B. R., Jones, T. J., Ratnam, S., Kolb, R. J. and Nauli, S. M. (2009). Ciliary polycystin-2 is a mechanosensitive calcium channel involved in nitric oxide signaling cascades. *Circ Res* **104**, 860-9.

Albrecht-Buehler, G. and Bushnell, A. (1980). The ultrastructure of primary cilia in quiescent 3T3 cells. *Exp Cell Res* **126**, 427-37.

Berselli, P., Zava, S., Sottocornola, E., Milani, S., Berra, B. and Colombo, I. (2006). Human GM3 synthase: a new mRNA variant encodes an NH2-terminal extended form of the protein. *Biochim Biophys Acta* **1759**, 348-58.

Cai, Y., Maeda, Y., Cedzich, A., Torres, V. E., Wu, G., Hayashi, T., Mochizuki, T., Park, J. H., Witzgall, R. and Somlo, S. (1999). Identification and characterization of polycystin-2, the PKD2 gene product. *J Biol Chem* **274**, 28557-65.

Cano, D. A., Murcia, N. S., Pazour, G. J. and Hebrok, M. (2004). Orpk mouse model of polycystic kidney disease reveals essential role of primary cilia in pancreatic tissue organization. *Development* **131**, 3457-67.

Cano, D. A., Sekine, S. and Hebrok, M. (2006). Primary cilia deletion in pancreatic epithelial cells results in cyst formation and pancreatitis. *Gastroenterology* **131**, 1856-69.

Dalen, H. (1981). An ultrastructural study of primary cilia, abnormal cilia and ciliary knobs from the ciliated cells of the guinea-pig trachea. *Cell Tissue Res* **220**, 685-97.

Delaine-Smith, R. M., Sittichokechaiwut, A. and Reilly, G. C. (2014). Primary cilia respond to fluid shear stress and mediate flow-induced calcium deposition in osteoblasts. *FASEB J* **28**, 430-9.

Dilly, P. N. (1977a). Further observations of transport within paddle cilia. *Cell Tissue Res* **185**, 105-13.

Dilly, P. N. (1977b). Material transport within specialised ciliary shafts on Rhabdopleura zooids. *Cell Tissue Res* **180**, 367-81.

Ehlers, U. and Ehlers, B. (1978). Paddle cilia and discocilia - genuine structures? Observations on cilia of sensory cells in marine turbellaria. *Cell Tissue Res* **192**, 489-501.

Elofsson, R., Andersson, A., Falck, B. and Sjoborg, S. (1984). The ciliated human keratinocyte. *J Ultrastruct Res* **87**, 212-20.

Gilula, N. B. and Satir, P. (1972). The ciliary necklace. A ciliary membrane specialization. *J Cell Biol* **53**, 494-509.

Harduin-Lepers, A., Mollicone, R., Delannoy, P. and Oriol, R. (2005). The animal sialyltransferases and sialyltransferase-related genes: a phylogenetic approach. *Glycobiology* **15**, 805-17.

Hidaka, S., Konecke, V., Osten, L. and Witzgall, R. (2004). PIGEA-14, a novel coiled-coil protein affecting the intracellular distribution of polycystin-2. *J Biol Chem* **279**, 35009-16.

Ishii, A., Ohta, M., Watanabe, Y., Matsuda, K., Ishiyama, K., Sakoe, K., Nakamura, M., Inokuchi, J., Sanai, Y. and Saito, M. (1998). Expression cloning and functional characterization of human cDNA for ganglioside GM3 synthase. *J Biol Chem* **273**, 31652-5.

Janich, P. and Corbeil, D. (2007). GM1 and GM3 gangliosides highlight distinct lipid microdomains within the apical domain of epithelial cells. *FEBS Lett* **581**, 1783-7.

Jensen, C. G., Davison, E. A., Bowser, S. S. and Rieder, C. L. (1987). Primary cilia cycle in PtK1 cells: effects of colcemid and taxol on cilia formation and resorption. *Cell Motil Cytoskeleton* **7**, 187-97.

Jensen, C. G., Jensen, L. C. and Rieder, C. L. (1979). The occurrence and structure of primary cilia in a subline of Potorous tridactylus. *Exp Cell Res* **123**, 444-9.

Jin, X., Mohieldin, A. M., Muntean, B. S., Green, J. A., Shah, J. V., Mykytyn, K. and Nauli, S. M. (2014). Cilioplasm is a cellular compartment for calcium signaling in response to mechanical and chemical stimuli. *Cell Mol Life Sci* **71**, 2165-78.

Koulen, P., Cai, Y., Geng, L., Maeda, Y., Nishimura, S., Witzgall, R., Ehrlich, B. E. and Somlo, S. (2002). Polycystin-2 is an intracellular calcium release channel. *Nat Cell Biol* **4**, 191-7.

Liu, W., Murcia, N. S., Duan, Y., Weinbaum, S., Yoder, B. K., Schwiebert, E. and Satlin, L. M. (2005). Mechanoregulation of intracellular Ca2+ concentration is attenuated in collecting duct of monocilium-impaired orpk mice. *Am J Physiol Renal Physiol* **289**, F978-88.

Mahone, M., Saffman, E. E. and Lasko, P. F. (1995). Localized Bicaudal-C RNA encodes a protein containing a KH domain, the RNA binding motif of FMR1. *EMBO J* **14**, 2043-55.

Masyuk, A. I., Masyuk, T. V., Splinter, P. L., Huang, B. Q., Stroope, A. J. and LaRusso, N. F. (2006). Cholangiocyte cilia detect changes in luminal fluid flow and transmit them into intracellular Ca2+ and cAMP signaling. *Gastroenterology* **131**, 911-20.

Matera, E. M. and Davis, W. J. (1982). Paddle cilia (discocilia) in chemosensitive structures of the gastropod mollusk Pleurobranchaea californica. *Cell Tissue Res* **222**, 25-40.

McGrath, J., Somlo, S., Makova, S., Tian, X. and Brueckner, M. (2003). Two populations of node monocilia initiate left-right asymmetry in the mouse. *Cell* **114**, 61-73.

Mitchell, K. A. (2013). Isolation of primary cilia by shear force. *Curr Protoc Cell Biol* **Chapter 3**, Unit 3 42 1-9.

Nauli, S. M., Alenghat, F. J., Luo, Y., Williams, E., Vassilev, P., Li, X., Elia, A. E., Lu, W., Brown, E. M., Quinn, S. J. et al. (2003). Polycystins 1 and 2 mediate mechanosensation in the primary cilium of kidney cells. *Nat Genet* **33**, 129-37.

Nauli, S. M., Kawanabe, Y., Kaminski, J. J., Pearce, W. J., Ingber, D. E. and Zhou, J. (2008). Endothelial cilia are fluid shear sensors that regulate calcium signaling and nitric oxide production through polycystin-1. *Circulation* **117**, 1161-71.

Nauli, S. M., Rossetti, S., Kolb, R. J., Alenghat, F. J., Consugar, M. B., Harris, P. C., Ingber, D. E., Loghman-Adham, M. and Zhou, J. (2006). Loss of polycystin-1 in human cyst-lining epithelia leads to ciliary dysfunction. *J Am Soc Nephrol* **17**, 1015-25.

Pazour, G. J., San Agustin, J. T., Follit, J. A., Rosenbaum, J. L. and Witman, G. B. (2002). Polycystin-2 localizes to kidney cilia and the ciliary level is elevated in orpk mice with polycystic kidney disease. *Curr Biol* **12**, R378-80.

Praetorius, H. A. and Spring, K. R. (2001). Bending the MDCK cell primary cilium increases intracellular calcium. *J Membr Biol* **184**, 71-9.

Qiu, N., Xiao, Z., Cao, L., Buechel, M. M., David, V., Roan, E. and Quarles, L. D. (2012). Disruption of Kif3a in osteoblasts results in defective bone formation and osteopenia. *J Cell Sci* **125**, 1945-57.

Roth, K. E., Rieder, C. L. and Bowser, S. S. (1988). Flexible-substratum technique for viewing cells from the side: some in vivo properties of primary (9+0) cilia in cultured kidney epithelia. *J Cell Sci* **89 (Pt 4)**, 457-66.

Rydholm, S., Zwartz, G., Kowalewski, J. M., Kamali-Zare, P., Frisk, T. and Brismar, H. (2010). Mechanical properties of primary cilia regulate the response to fluid flow. *Am J Physiol Renal Physiol* **298**, F1096-102.

Saffman, E. E., Styhler, S., Rother, K., Li, W., Richard, S. and Lasko, P. (1998). Premature translation of oskar in oocytes lacking the RNA-binding protein bicaudal-C. *Mol Cell Biol* **18**, 4855-62.

Seyfried, T. N., Ando, S. and Yu, R. K. (1978). Isolation and characterization of human liver hematoside. *J Lipid Res* **19**, 538-43.

Siroky, B. J., Ferguson, W. B., Fuson, A. L., Xie, Y., Fintha, A., Komlosi, P., Yoder, B. K., Schwiebert, E. M., Guay-Woodford, L. M. and Bell, P. D. (2006). Loss of primary cilia results in deregulated and unabated apical calcium entry in ARPKD collecting duct cells. *Am J Physiol Renal Physiol* **290**, F1320-8.

Su, S., Phua, S. C., DeRose, R., Chiba, S., Narita, K., Kalugin, P. N., Katada, T., Kontani, K., Takeda, S. and Inoue, T. (2013). Genetically encoded calcium indicator illuminates calcium dynamics in primary cilia. *Nat Methods* **10**, 1105-7.

Tobin, J. L. and Beales, P. L. (2009). The nonmotile ciliopathies. *Genet Med* **11**, 386-402.

Tran, U., Zakin, L., Schweickert, A., Agrawal, R., Doger, R., Blum, M., De Robertis, E. M. and Wessely, O. (2010). The RNA-binding protein bicaudal C regulates polycystin 2 in the kidney by antagonizing miR-17 activity. *Development* **137**, 1107-16.

Wang, L., Eckmann, C. R., Kadyk, L. C., Wickens, M. and Kimble, J. (2002). A regulatory cytoplasmic poly(A) polymerase in Caenorhabditis elegans. *Nature* **419**, 312-6.

Xu, C., Rossetti, S., Jiang, L., Harris, P. C., Brown-Glaberman, U., Wandinger-Ness, A., Bacallao, R. and Alper, S. L. (2007). Human ADPKD primary cyst epithelial cells with a novel, single codon deletion in the PKD1 gene exhibit defective ciliary polycystin localization and loss of flow-induced Ca2+ signaling. *Am J Physiol Renal Physiol* **292**, F930-45.

Yoder, B. K., Hou, X. and Guay-Woodford, L. M. (2002). The polycystic kidney disease proteins, polycystin-1, polycystin-2, polaris, and cystin, are co-localized in renal cilia. *J Am Soc Nephrol* **13**, 2508-16.

Yoshiba, S., Shiratori, H., Kuo, I. Y., Kawasumi, A., Shinohara, K., Nonaka, S., Asai, Y., Sasaki, G., Belo, J. A., Sasaki, H. et al. (2012). Cilia at the node of mouse embryos sense fluid flow for left-right determination via Pkd2. *Science* **338**, 226-31.

Chapter 3

Abstract Single-cell Imaging Technique to Study Cilia Dynamics From the Side

Ashraf M. Mohieldin [1,2], Hanan S. Haymour [2], Shao T. Lo [3], Jin Xingjian [4], Ali Zarban [3], Surya M. Nauli [5] & Wissam A. AbouAlaiwi [3].

[1] Department of Medicinal & Biological Chemistry, University of Toledo Health Science Campus. Toledo, OH (USA). Email: Ashraf.Mohieldin@rockets.utoledo.edu. [2] Department of Chemistry, Purdue University. West Lafayette, IN (USA). Email: hhaymour@purdue.edu. [3] Department of Pharmacology, University of Toledo, Toledo, OH (USA). Email: Shao.Lo@rockets.utoledo.edu. [4] Department of Medicine, Renal Division, Washington University. Saint Louis, MO (USA). Email: Xingjian.Jin@rockets.utoledo.edu. [5] Department of Biomedical & Pharmaceutical Sciences, Chapman University Rinker Health Science campus. Irvine, CA (USA). Email: Nauli@chapman.edu.

Corresponding author
AbouAlaiwi Wissam, Ph.D.
Department of Pharmacology; MS 1015
The University of Toledo,
College of Pharmacy and Pharmaceutical Sciences
Health Education building; Room 282E
3000 Arlington Ave
Toledo, OH 43614
Phone: 419-383-1949
Fax: 419-383-1909
Email: Wissam.Abou-Alaiwi@UToledo.Edu

Abstract

Signaling within the cilioplasm has never been visualized and recorded in live cells due to the tiny diameter of primary cilia. The dynamics of some ciliary components, like ciliary bulb, cilioplasm calcium signals and protein localizations within certain ciliary compartments can only be examined accurately when visualized from the side. We have developed a new differential side-view imaging technique called "The formvar-folding technique" which uses renal epithelial *LLC-PK* cells grown on a formvar-collagen substratum. This substratum is later folded into a triangular shape, embedded into a glass-bottom plate and covered with a glass cover-slide. Imaging the cells grown at the folded edge of the formvar allows observing and studying the dynamics of ciliary molecules, such as ciliary bulbs, along the length of the primary cilium before, during and after fluid shear stress application. It also allows recording and measuring cilioplasm calcium signals and performing ciliary protein localization and immunofluorescence studies.

3.1. INTRODUCTION

Studies focusing on the structure and function of primary cilia have caught the attention of researchers in the past decade due to the involvement of cilia in a group of pathogeneses collectively known as ciliopathies. These include: Oral-facial-digital syndrome, Nephronophthisis, Bardet-Biedl syndrome, Meckel syndrome, Joubert syndrome, Polycystic kidney diseases, Mental retardation, Obesity and others [1]. Primary cilia are hair-like structures that are supported by circumferentially arranged microtubules "9+0" and enclosed by the ciliary membrane. Structurally, the primary cilium is composed of five main compartments: the axoneme, the ciliary membrane, the cilioplasm, the basal body and the transition zone [2-5]. The primary cilium is about 1–5 μm in length and 0.2 μm in width, but the width decreases as it progresses to the distal tip [6]. This makes this unique organelle very hard to observe directly under the microscope.

The non-motile primary cilium is a sensory organelle that senses mechanical signals on the apical membrane of the cells [7-10]. Mechanical signals that produce enough force on the surface of cells will bend and activate sensory cilia. These biomechanical properties play a very important role in visceral organs that support bodily fluid perfusion, including the kidney, the liver and the heart. In addition, the primary cilium has many mechano- and chemosensory functions where it can sense and activate a range signaling pathways in response to mechanical and chemical stimuli [11-14]. Mechanosensory cilia function is demonstrated through the observation that primary cilia bending in response to fluid shear stress results in cytosolic calcium release [15]. Moreover, many studies have demonstrated that fluid flow and many pharmacological agents are able to stimulate primary cilia and activate primary signaling pathways such as

calcium/calmodulin, sonic hedgehog, Wnt, mTOR, JAK/STAT, and MAPK. These pathways play a key role in various vital cellular processes like development, differentiation, cell cycle, chromosomal segregation, apoptosis, tissue homeostasis and planar cell polarity [14, 16, 17].

Primary cilia are visualized as dots above the dorsal cell surface when monolayers of kidney epithelial cells are observed through focus from above [2]. In 1988, Roth *et al.* first projected the special flexible-substratum technique [2]. The main idea is to overcome the issues related to optical distortion associated with traditional two-dimensional live-cell imaging techniques. To our knowledge, there has never been a direct visualization of any dynamic movement or signaling within the primary cilium of mammalian cells. This is primarily due to the size of primary cilia with a diameter of ~200 nm. Of note is that most primary cilia are oriented perpendicular to the cell surface, which makes visualizing ciliary signaling in live cells extremely challenging, in addition to the tiny diameter of primary cilia. Despite the important role of primary cilia and its involvement in many inherited diseases and as the list of ciliary proteins/molecules that are involved in inherited diseases continues to grow, there is an urgent need for a reliable and physiologically relevant technique to visualize the cilia from the side with high precision.

3.2. Development of the protocol

For more than a decade, our research team has focused on mechanisms involved in cilia signaling within the renal and vascular systems. The development of this novel technique presents an opportunity to understand ciliary signaling at a level that has not been possible until now. The overall goal of this technique is to provide the first model to

understand signaling within the cilioplasm of a living cell. Using a single-cell imaging technology that facilitates imaging the cell from the side will allow us for example to differentiate calcium influx between primary cilium and the cytosol.

We have developed a differential side-view single-cell imaging technique by growing porcine kidney epithelial cells derived from the proximal tubules (*LLC-PK*) on a flexible substratum, formvar. This project is directed through a series of setups that must be carried out vigilantly step by step. The first challenging step was to design an approach to grow the cells on a flexible substratum to have the cilia protruding from the side for clear observation. Thus, formvar was chosen; it is a synthetic film insulation containing polyvinyl acetal and phenolic resins. The 2% concentration of formvar powder dissolved in ethylene dichloride was found to be optimal. Of note is that formvar powder is a very hydrophobic compound that doesn't dissolve easily in ethylene dichloride. Therefore stirring the solution for long enough to enable complete dissolving of the solution was required. The solution can alternatively be placed in a water bath at 37° C to dissolve faster. Too thick a layer of formvar can affect the growing of the cells as well as the folding process and too thin a layer of formvar can be ripped easily when folding. When growing *LLC-PK* cells on formvar, cells have to be dispersed well, in order to avoid mountain-like growth, as the cells can grow on top of each other. This can prevent optimal follow when applying the fluid shear stress to the cilia and ease the detachment of cells from the substratum layer. In addition, a hydrophilic collagen solution is then used on top of the hydrophobic formvar to facilitate the process of cell attachment to the formvar layer. The detachment of the cell can cause other problems when observing the cilia under the microscope, especially during fluid perfusion. The cells are grown on the

formvar substratum until they are 70-80 % confluent, after which the cells are allowed to differentiate for a period of 2-3 days by growing in a medium devoid of serum. The formvar grown cells are subsequently transferred into a glass-bottom culture plate after folding the formvar into a triangular shape. Folding the formvar into a triangular shape allows visualizing the cells growing on the folded edge of the formvar and consequently imaging the cells from the side (**Fig. 3.1a**). The cells are then covered with a glass cover slide to hold the formvar in place and facilitate imaging of the cells (**Fig. 3.1b**). Overall, this technique is amenable to different applications on primary cilia, such as live ciliary signaling, ciliary protein co-localizations, overexpression and knockdown, and ciliary molecular dynamic movements in response to fluid shear stress.

3.3. Applications of the method

Our present work integrates three technologies to allow direct measurement of ciliary signaling in an individual living cell. These technologies include formvar folding, immunofluorescence staining and modified microscopy system. This integrated single-cell analysis offers the possibility to study protein colocalization within the ciliary body independent of extracellular factors, the first evidence of calcium signaling in the primary cilium of a living renal epithelium and the first evidence to study the dynamics of ciliary molecules such as ciliary bulbs along the length of the primary cilium.

3.4. High resolution live imaging

Our group previously demonstrated that primary cilia behave as cellular communication organelles simply by housing an array of mechano- as well as chemo-sensory molecules or proteins [18]-[22]. These sensory molecules could be present alone or organized with other interacting molecules within a dynamic bulged structure in the ciliary body called

the ciliary bulb. The movement of the ciliary bulb along the cilia length could in turn be regulated by intracellular or extracellular factors such as fluid shear stress [19]. Observing the entire cilium from the side allows us to visualize and study the dynamics of ciliary bulb for the very first time in a single living cell. Proximal tubular epithelial *LLC-PK* cells are used among other cells types, because of its long cilia, which enabled us to image and differentiate ciliary bulb from artifacts. Live cell imaging experiments are performed using high-resolution differential interference contrast (DIC) microscopy. To facilitate live cell imaging and to avoid condensation on the objective lens, our microscopy system is enclosed within an environmental chamber to regulate humidity, temperature, and CO_2. Due to the dynamic behaviors of cell movements, the microscope also has automatic XY and Z directional modules. Cells grown on the formvar are embedded in a glass bottom plate and covered with glass cover slip. Fluid flow is applied from one edge of the glass cover slip through a tubing system connected to a fluid flow pump and removed from the other edge of the coverglass (**Fig. 1c**). Cilia in upright position (under static conditions/no fluid flow) and cilia bending (after fluid flow) can be imaged from the side and the movement of ciliary bulb along the length of primary cilium can be recorded with high precision under both static and fluid flow conditions (**Movie B.1**). Both cilia function and structure in response to fluid shear stress can be studied by acquiring time-lapse DIC images before, during and following application of fluid flow to the surface of the cells (**Fig. 3.2a**). Of note is that we are able to image the cells under live conditions for two weeks using our modified microscopy system. Moreover, this technique allows observation of transfected *LLC-PK* cell with Sstr3-GFP

plasmid during *in vitro* culture to confirm the time-lapse live DIC imaging observation of the cilia (**Fig. 3.2b)**.

3.5. Immunofluorescence analysis

Because primary cilia are involved in a number of clinical pathologies, it is extremely crucial to determine the involvement of ciliary molecules in these pathologies by studying cilia-specific signaling. One application is to study by immunofluorescence analysis the localization of ciliary proteins in order to determine their involvement in ciliary bulb formation. We use primary antibodies that are considered structural and functional markers of primary cilia such as acetylated α-tubulin and polycystin-2, respectively. Other antibodies used include CaV1.2 (Alomone Lab, Inc.), dopamine receptor-type 5 (Calbiochem, Inc.), thrombin receptor (Santa Cruz, Inc.), the ganglioside GM3, GM3 synthase (GM3S) [20], and the RNA-binding protein bicaudal-c1 (Bicc-1) (Mohieldin et al). All immunostaining experiments can be done in a 6-well plate containing cells grown on formvar-covered glass-coverslide. Following fixation, permeabilization and incubation with primary antibodies, the cells are then incubated with secondary antibodies such as fluorescein anti-mouse IgG, fluorescein anti-rabbit IgG, texas-red anti-mouse IgG or texas-red anti-rabbit IgG. The nucleus or DNA is counterstained with 4,6-diamidino-2-phenylindol, DAPI (**Fig. 3.2c**). Fluorescence imaging is performed using a TiU Nikon microscope equipped with a Coolsnap EZ CCD monochrome digital camera and a filter wheel which accommodates up to six filter sets. Acquisition of images is controlled by Metamorph software. Cells transfected with siRNA to knock down the expression of certain ciliary proteins can also be stained using this procedure.

3.6. Differential visualization of cilioplasm calcium

Early studies by Nauli *et al*. and others revealed for the first time that primary cilia of kidney epithelial cells bending in response to fluid shear stress or other mechanical applications resulted in the activation of intracellular signaling such as an increase in intracellular calcium concentration [21],[15]. Similar findings were later confirmed in other cell types such as vascular endothelial, liver, bone, nodal and pancreatic cells[14, 22],[23], [24],[25]. However, it was extremely challenging to reveal or visualize any intra-ciliary calcium signaling within the cilioplasm. This is mainly due to the small size of cilia as well as to the absence of model systems to study this phenomenon. The development of this protocol allows the differential visualization between the cilioplasm and the cytoplasm and thus facilitates the study of signaling-specificity within the cilioplasm vs. the cytoplasm. Briefly, cells grown, as described above, on formvar are transfected with a custom designed CTS-G-CaMP3 construct containing the gene encoding for the intracellular C-tail of fibrocystin (*Pkhd1*) fused to the N-terminus of the calcium indicator, G-CaMP3. The cells grown on top of the formvar are then moved to a custom-designed perfusion chamber and live imaging of both ciliary and cytosolic calcium recordings are performed at the excitation and emission wavelengths of 495 and 515 nm, respectively [5]. Our technique is performed in renal epithelial *LLC-PK* cells treated with fenoldopam to induce cilium-specific calcium or with dopamine to induce non-specific calcium influx. Although our studies are done in renal epithelial cells, this technique can be adopted to other cell types. Our group demonstrated that fluid shear stress and dopamine receptor type 5 (DR5) agonist generate cilioplasm-specific calcium signals through distinct ciliary calcium channels, polycystin-2 and CaV1.2, respectively.

These cilioplasm-specific calcium signals can be easily differentiated from cytosolic calcium signals induced by other treatments [5] (**Fig. 3.4 or 3.3b**).

3.7. Comparison with other methods

Our group has recently adopted a modification to this method by growing the cells on a precision micro-wire instead of formvar. This micro-wire is specially made from Tungsten wire with a purity of greater than 99.9 % and a standardized diameter of 100 μm. Renal epithelial cells have been successfully grown and imaged from the side on this micro-wire when the wire is coated with collagen for similar applications to the ones mentioned in our protocol. A drawback of these tungsten micro-wires is that they cannot be reused and are not cost effective. On the other hand, another method was developed, which involves the use of spheroids of mouse inner medullary collecting duct (mIMCD) cells as a 3-D cell culture model to represent the static environment within the of kidney tubules lumen [26]. Although this 3D culture model was designed to mimic the *in vivo* architectural and biochemical properties, it is only amenable to certain applications such as siRNA knockdown and immunofluorescence. A very critical limitation of this model is the inability to study dynamic fluid and ciliary movements inside the spheroid lumen. This is specifically important when studying the mechanism of pathogenesis of a ciliopathy disorder such as Polycystic Kidney Disease with respect to fluid flow. Another limitation to the spheroid technique and as mentioned by the authors is the selectivity towards a certain population of cells of forming spheroids, which should be carefully addressed especially when considering siRNA transfection analysis.

3.8. Experimental design

The formvar substratum is selected due to its optimal chemical as well as optical properties. It can be polymerized into a thin layer of plastic- or gel- like material, which allows observing the entire cilium length from the side. The formvar substratum is prepared under sterile conditions by first dissolving in ethylene chloride. The formvar solution is then allowed to harden on top of a glass cover slide suitable for high resolution imaging. The cells are seeded on top of the cover slide following coating the glass cover slide with rat collagen type I. This step ensures the attachment of the cells to the flexible substratum and reduces the chances of cellular toxicities. We have tried several types and concentrations of substrata with different collagen concentrations and found that 2% formvar combined with 50 μM collagen to be an optimal combination for our specific cell types. The cell types tested for our application include porcine kidney epithelial cell lines (*LLC-PK*), mouse embryonic aortic endothelial lines and others. *LLC-PK* cells represent an ideal and physiologically relevant culture model simply due to the presence of relatively long cilia in addition to their apical-basal polarity. These characteristics make *LLC-PK* cells an appropriate model to study cilia-related disease while facilitating high-resolution imaging of the cilia from the side.

The advantage of this model over other existing *in vitro* cellular models is its feasibility for several applications. One example is the ability to study the effect of fluid shear stress on cilia function. It is well known that cilia bending in response to fluid shear stress triggers the activation of both ciliary and intracellular signaling cascades both *in vitro* and *in vivo* systems [14]. To our knowledge, until the development of this technique, it has not been possible to study this physiologically important phenomenon neither *in vitro* nor *in vivo* using other methods including the recently developed cellular spheroids model

system [26]. This is simply due to the fact that although the cells grown using the spheroid system develop a lumen similar in a way to the kidney tubular lumen; however, this lumen is closed and not accessible to fluid flow as is the case of the kidney tubular flow. In our model, this criterion of kidney epithelial or other cell type accessibility to the extracellular environment, specifically fluid flow makes it an ideal model to study this phenomenon. Of note is that our technique has been successfully used for *in vitro* siRNA knockdown approach.

3.9. Limitations

One of the few minor limitations to our technique is the possible detachment of the cells from the formvar-collagen platform. Detachment of the cells sometimes occurs if the cells are overconfluent or if they are subjected to vigorous fluid flow conditions. In order for renal epithelial *LLC-PK* cells to generate long cilia, it is recommended that the cells are fully confluent and differentiated. This is usually attained by seeding the cells in media without fetal bovine serum (FBS) for the last 48-72 hrs before the experiment. These culture conditions sometimes might affect the attachment of the cells to the collagen-formvar substrate and consequently alter their viability. These limitations can be overcome by continuously monitoring the growth of the cells so as to avoid overconfluency and by precisely calibrating the fluid shear stress rates so as to apply the minimum physiologically relevant rates that produce a physiological ciliary signal. Another limitation is related to photo-bleaching or photo toxicity associated with the use of fluorescent dyes during live imaging. This limitation can be overcome by the use of minimum exposure rates to fluorescent light during image recording. When transfecting the cells with constructs encoding ciliary proteins fused to GFP, it is critical to

standardize the transfection procedure to obtain maximum transfection efficiencies; hence, the generation of stably transfected cell lines is a more reliable alternative approach to transient transfection.

3.10. Materials

3.10.1 REAGENTS

- DMEM (Mediatech, Inc., cat. no. 10-013-CV).
- Fetal bovine serum (FBS) (HyClone, cat. no. SH30088-03).
- Penicillin-streptomycin solution, 100x (Corning Life Sciences, cat.no. 30-002-CI).
- PBS 1x, pH 7.4, (Thermo Scientific, cat. no. SH30256-0).
- Trypsin-EDTA, 0.05% (1x), (Thermo Scientific, cat. no. SH30236.01).
- Glutaraldehyde, 3% (vol./vol), (Thermo Scientific, cat. no. BP2547-1).

  ▲**CAUTION** Handle it with care in a chemical fume hood.
- Na-Cacodylate, (Electron Microscopy Sciences, cat. no. 11652).
- Triton X-100, (Fisher Scientific, cat. no. BP151-500).

  ▲**CAUTION** Handle it with care.
- Monoclonal anti-acetylated tubulin antibody, mouse (Sigma-Aldrich, cat. no. T6793).
- Sucrose, 2%, (Sigma-Aldrich, cat. no. 35H03583).
- 1, 2-Dichloroethane (Fisher Scientific. Cat.no. E190-4).

  ▲ **CAUTION** Use only under chemical fume hood.
- FORMAR RESIN, 15/95 (Electron Microscopy Science, cat. no. 15800).

- Collagen solution, (Corning Life Sciences, cat. no. 354236).
- DAPI, (Vector Lab., cat. no. H-1500).

  ▲ **CAUTION** Handle it with care and protect it from light.
- G-CaMP3 (ADDGENE, cat. no. 22692).
- SSTR3-GFP plasmid, (SSTR3-GFP was a gift).
- X-tremeGENE HP DNA Transfection Reagent, (Roche, cat. no. 06366244001).
- Fluorescein anti-mouse (Vector Lab, cat. no. FI-2000).

  ▲ **CRITICAL** Store secondary antibody in the dark.
- 4',6-diamidino-2-phenylindole (DAPI), (Vector labs, cat. no. H-1500).
- Microscope immersion oil, (Nikon 50 Type A, cat. no. MXA20234).
- One-minute Epoxy Instant Mix Glue (LOCTITE).

3.10.2. EQUIPMENT

- Six-well plate (Thermo Fisher Scientific, cat. no. 130184).
- Microscope cover glass 18x18 # 1.5 (VWR, cat. no. 16004-326).
- Water bath (Fisher scientific, cat. no. 15-462-10).
- Micro-perfusion pumps (INSTECH, cat. no. P720).
- PCR (Eppendorf, serial; 6325YO203217).
- Corning Costar 60-mm culture plate (Thermo scientific, cat. no. 130181).
- Corning 100-mm culture plate (Thermo scientific, cat. no. 130182).
- Cell culture microscope (Nikon, cat. no. TS100).
- Inverted fluorescence microscope (Nikon, cat. no. TE2000-U).

- Microscope glass slides (Fisher Scientific, cat. no. 12-549).
- Cell culture incubator (at 37 °C and 5% CO_2), (Thermo Scientific, cat. no. 15-462-10).
- Biological Safety Cabinet.
- Aspirator.
- Pipette tips (Fisher scientific, Inc. cat. no. 05-408-152).
- Pasteur capillary pipettes, glass (Fisher Scientific, cat. no. 10209381).
- Automatic pipette.
- Serological pipettes.
- Tubing (Nalgene, Inc. cat. no. WU-06407-70).
- Electronic balance.
- 15-ml centrifuge tubes, sterile (Corning Life Sciences, cat. no. 430791).
- Clear Scotch tape.
- Forceps (VWR, cat.no. 82027-384).
- Scissors.

3.10.3. REAGENT SETUP

Formvar solution: The optimal amount of formvar solution was prepared by dissolving 0.9 g of formvar powder in 45 mL of ethylene dichloride, which is about 2% w/v of formvar concentration. Other concentrations of formvar can be used, but should not exceed 4% w/v, to obtain the optimal flexibility of the formvar folding. To dissolve completely, formvar solution can be placed in 37 °C water bath till solution is clear. Although fresh formvar solution is preferred, solution can be stored at room temperature and reused for up to two weeks.

Collagen solution: The collagen solution was prepared by dissolving 578.40 µl of collagen in 45 mL of cold PBS solution. The optimal final concentration of collagen solution was found to be 50 µM. Solution is stored in 4^{o}C and can be reused for up to one month.

Permeabilization buffer: To make 10 ml of permeabilization buffer, add 0.1 ml of Triton X-100 to 9.9 ml of 1XPBS and mix the solution very well by vortexing to completely dissolve the Triton-X.

Primary antibody solution: Anti-Acetylated α-tubulin is prepared at a dilution of 1:5,000 in 10% FBS in 1XPBS.

Secondary antibody solution: Fluorescein anti-mouse IgG is prepared at a dilution of 1:500 in 10% FBS in 1XPBS solution.

Fixation buffer: Prepare a 3% v/v solution of glutaraldehyde in 0.4M Na-cacodylate to fix the cell. It is preferred to warm the solution in 37 °C water bath before use, to avoid any deformation of the primary cilia structure morphology. Always prepare fresh solution of fixation buffer.

3.10.4. EQUIPMENT SETUP

Description of the microscope

Live cell imaging experiments are performed using high-resolution differential interference contrast (DIC) Nikon TiU microscope. The microscope is used for fixed-tissue and live-imaging studies. It is equipped with an environmental chamber to regulate humidity, temperature, and CO_2 to avoid condensation on the objective lens. Due to the dynamic behaviors of cells movement, the microscope also has automatic XY and Z directional modules. The Coolsnap EZ CCD Monochrome Digital Camera delivers a

1392 x 1040 imaging array and 6.45 x 6.45-µm pixels. It also delivers fast, high-resolution imaging for low-light life sciences applications. This moderately cooled CCD camera provides 12-bit digitization at 20 MHz. It has the capability of acquiring up to 5,820 frames/sec at binning 8x8 and 2512 frames/sec at binning 1x1 for capturing the highest resolution images. Hardware control and acquisition of images are controlled by Metamorph software. The filter wheel can accommodate up to six filter sets. Microscope is attached with Prior Proscan stage controller with Joy stick.

3.11. PROCEDURE

3.11.1. Preparing *LLC-PK* cells TIMING 24-48 h

1| Grow cells in Dulbecco's Modified Eagle's Medium (DMEM) containing 10-15% fetal bovine serum (FBS) and 1% penicillin/streptomycin at 37 °C in the presence of 95%/5% O_2/CO_2 in a cell culture incubator, until they reach 70-80% confluency.

3.11.2. Preparing formvar solution TIMING 40 min

2| Prepare a 2% formvar solution by dissolving 0.9 g of formvar powder in 45 ml of ethylene dichloride. **CAUTION** ethylene dichloride is a hazardous material used only under a chemical fume hood.

3| Using a forceps, dip 18x18 no. 1.5 glass cover slides into the formvar solution and place as quickly as possible inside a six-well plate and allow to dry.

4| Wash two times with 1XPBS solution and place under UV light inside the biological safety cabinet for 30 min for sterilization.

5| All these steps following the preparation of the 2% formvar solution must be done under sterile conditions. **CRITICAL STEP** avoids bubble of air between the slide and the bottom of the well plate as this makes observation of the cell growth under the microscope difficult.

3.11.4. Preparing collagen solution TIMING 40 min

6| Prepare a 50 µM collagen solution by dissolving 578.40 µl of collagen in 45 ml ice-cold 1XPBS solution.

7| Add collagen solution into the wells of a six-well plate containing the formvar substratum and incubate for 1 hr at room temperature.

8| Remove any unsolidified collagen and wash two times with 1XPBS and place under UV light for 30 min.

3.11.5. Growing cells on top of the collagen formvar substratum TIMING 48-72 h

9| Grow *LLC-PK* cells in collagen containing-plate until they reach 70-80% confluence.

10| Differentiate the cells by growing in DMEM containing 1% penicillin/streptomycin without any FBS for 24-48 hr.

3.11.6. Folding technique TIMING 35 min

11| Observe the cells under the microscope to make sure cells are healthy and confluent, and then remove the media from the well plate.

12| Wash the cells gently two times with pre-warmed (37 °C) 1XPBS.

13| Add 2 ml of warmed 1XPBS to the well plate.

14| Scrape each corner, using a sharp forceps, to help detach the formvar from the 18x18 glass cover slide and then lift each corner slightly to loosen it further.

15| Gently lift the formvar from the opposite corners and allow it to fold down on itself, forming a triangle shape to allow for the maximum surface area to be observed, as shown in **Figure 3.1a**.

16| Place the folded triangle shape formvar in a glass-bottom plate containing 1XPBS solution with or without 10 % FBS, as shown in **Figure 3.1b**.

3.11.7. Flow shear-stress technique TIMING 35 min

17| Use fluid flow micro-perfusion pumps to apply fluid shear stress to the cilia on the cell surface from one side and to remove extra fluid perfusate from the other side of the glass cover slide.

18| Place a thin flat pipette tip between the glass-bottom plate and the glass cover slide, as shown in **Figure 3.1c**.

19| Use warm 1XPBS solution with or without 10 % FBS to apply the shear stress.

20| Place the solution in a water bath at 37° C, during perfusion (optional).

21| Turn the inflow pump on prior to the experiment to prevent air bubbles or any other solution that might be in the tube prior to perfusion.

22| When ready, place the plate under the microscope for observation, as shown in **Figure 3.2**.

23| Adjust the rate of fluid flow between10.3 µL/min (low flow) and 35.3 µL/min (high flow). **CRITICAL STEP** The pipette tip should be placed gently, as it can break the covering glass or damage the triangle-shaped formvar.

3.11.8. Calcium imaging technique **TIMING 24-72 h**

24| Grow cells on formvar as mentioned in step 9 to observe cells from the side.

25| For live-cell imaging, transfect the cells grown on the formvar with the CTS-GCaMP3 construct using Xtreme6 tansfection system.

26| Move the formvar-containing cells to a custom-designed perfusion chamber made of a standard 6-cm culture plate. The plate would allow a tight seal of the microscope coverslip, upon which the formvar is mounted.

27| Stream live images of CTS-G-CaMP3 at the excitation and emission wavelengths of 495 and 515 nm, respectively. Ciliary and cytosolic calcium will be recorded in wild-type LLCPK cells as recently published [5].

3.11.9. Immunofluorescence technique **TIMING ~ 27 h**

28| Fix the cells with phosphate buffer saline solution containing 3% glutaraldehyde for 10 min at room temperature [27].

29| Wash the cells three times with 1XPBS for 5 min each.

30| Incubate the cells with a solution of 0.1% Triton-X in 1XPBS for 5 min then rinse three times with 1XPBS for 5 min each.

31| Incubate the cells with mouse primary antibody, anti-acetylated α-tubulin used at a dilution of 1:5,000 in 10% FBS in 1XPBS for one hour at RT or overnight at 4°C.

32| Wash the cells three times with 1XPBS for 5 min each.

33| Incubate the cells in secondary antibody, fluorescein anti-mouse IgG at a dilution of 1:500 in 10% FBS in 1XPBS solution for 1 hr at RT.

34| Wash the cells three times with 1XPBS for 5 min each.

35| Before observing under a TiU fluorescent microscope, counterstain the cells with DAPI for 5 min to stain the nucleus (or DNA) [27].

3.11.10. Acquiring live images TIMING 1-3 h

36| Place the glass-bottom plate on the microscope stage. The microscope enclosed chamber environment is adjusted to 37 °C supplied with 95%/5% O_2/CO_2 content.

37| Collect the cilia images at 60X magnification using 60X objective Nikon Plan Apo 60X/1.4 numerical aperture oil immersion lens.

38| Place an oil drop on the 60X objective lens and focus the cells with regular DIC transmitted light by touching the coverslip-bottom of the plate.

39| Choose an area containing healthy cells with cilia using the DIC filter. Once the cilia are found, adjust the light and focus to obtain a satisfactory picture.

40| Set the live imaging parameters according to your purpose using Metamorph software. In our demonstration, twenty four-bit images are acquired with the

camera binning set to 1x1 combined with 60X objective and 5-10 millisecond exposure time.

41| Collect the DIC images.

42| Examine the structure and behavior of primary cilia and the ciliary bulb before, during and after fluid shear stress application (**Movie B.1 and Fig. 3.2a**).

? TROUBLESHOOTING

Troubleshooting advice can be found in **Table 3.1.**

TABLE 3.1 | Troubleshooting table.

Step	Problem	Possible reason	Solution
3, placing the formvar covering glass slide on the plate	Air bubble obstructing the visibility of cell growth	Placing the glass slide quickly and directly on the bottom plate	The glass cover slide should be placed at an angle until the glass slide reaches the bottom of the well plate.
14, scrapping the formvar from the glass slide	Ripping the formvar layer	Using too much force to peel the formvar from the glass slide	Be as careful and gentile as possible. Peel the formvar from each corner to the center of the glass slide and return back to loosen the whole formvar layer away from the glass slide.
18, placing the pipette tip for shear-stress	Breaking the cover glass slide; not enough flow, detachment of the cells	Not placing the pipette tip correctly	First option: Make sure to place the pipette tip gently between the cover glass slide and the bottom plate. Make sure not to place the pipette tip on the fomrvar. It should be placed couple of cm away from the formvar. Second option: Mount the pipette tip with glue on the plate before starting the experiment.
21, using the pump to generate the shear-stress	Bubbles, contamination, impurities during flow	Tubes used to generate flow are not sterile; Air bubbles are present in the tube before starting the flow experiment	Clean the tube with 70% v/v alcohol for about 2-4 min and clean the tube with 1XPBS for about 5 min.

• TIMING

STEP 1, preparing LLCPK cells: 24-48 h

STEP 2-5, preparing formvar solution: 40 min

STEP 6-8, preparing collagen: 40 min

STEP 9-10, growing cells on top of the collagen formvar substratum: 48-72 h

STEP 11-16, folding technique: 35 h

STEP 17-23, flow shear-stress technique: 35 min

STEP 24-28, calcium imaging technique: 24-72 h

STEP 29-36, immunofluorescence technique: 27 h

STEP 37-43, acquiring live images: 24-48 h

3.12. ANTICIPATED RESULTS

Live imaging of a single cilium from *LLC-PK* cell can be recorded from the side. To image the cilium, the cells are grown on the formvar substratum as illustrated in **Fig. 3.1a**. The figure shows a step by step folding of the formvar into a triangular shape for optimal observation of cilia (Steps 1- 4). Following this step, it can be demonstrated how growing the cells on the formvar substratum can be successfully utilized to observe and record cilia function and structure before, during and after fluid shear stress application. To observe cilia function and structure in response to fluid shear stress, the cells grown on the formvar are placed in a glass-bottom plate and covered with glass cover slip (**Fig. 3.1b**). Fluid flow can be applied to the surface of the cell from one edge through a tubing system connected to a fluid flow pump and removed from the other edge of the cover-glass (**Fig. 3.1c**). The time-lapse DIC imaging observations of the cilia bending from the side are demonstrated in **Movie B.1** with representative DIC images of primary cilia with or without ciliary bulb at different locations along the ciliary shaft in **Fig. 3.2a**. Transfection of *LLC-PK* cell with SSTR3-GFP plasmid during *in vitro* culture is further carried to study ciliary structure in live cells imaged from the side (**Fig. 3.2b)**. Furthermore, immunofluorescence analysis can be successfully implemented using the formvar technique to perform ciliary protein localization studies using anti-acetylated-α-tubulin as ciliary marker (**Fig. 3.2c**).

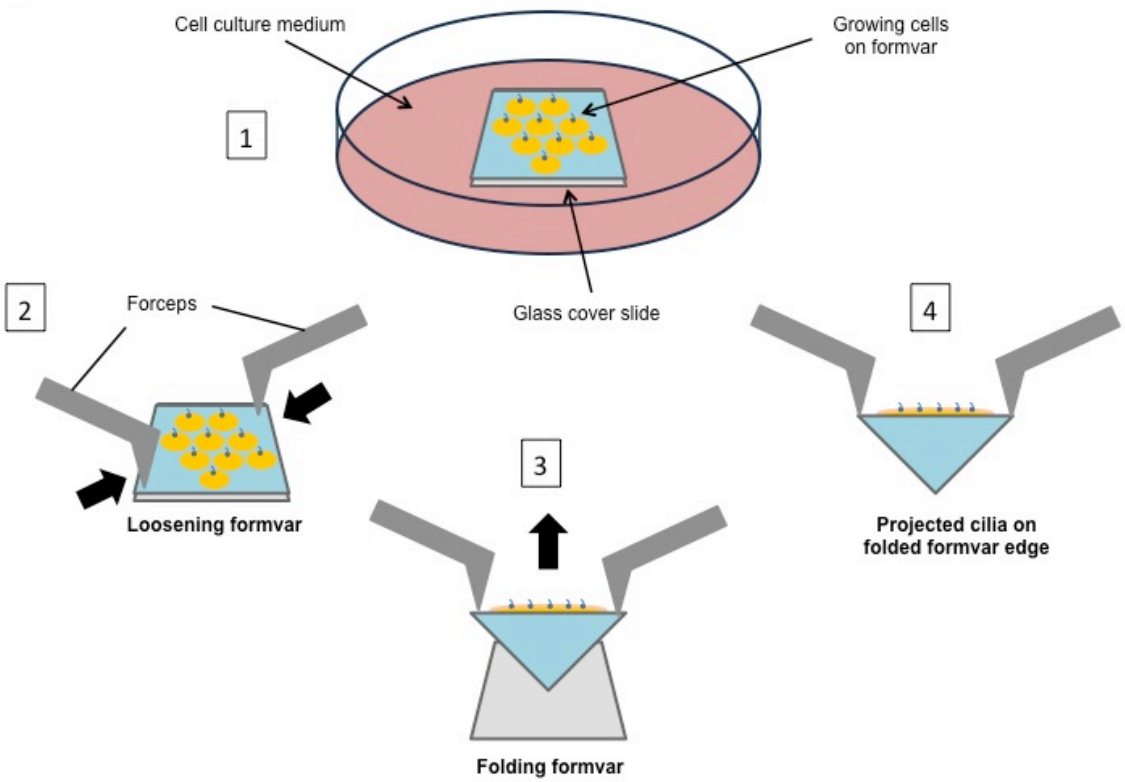
Cell culture medium
Growing cells on formvar
1
Glass cover slide
2
Forceps
Loosening formvar
3
Folding formvar
4
Projected cilia on folded formvar edge

5

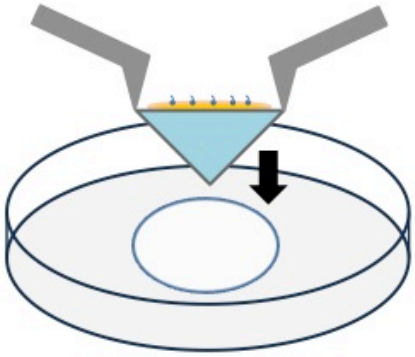

Placing folded formvar
In glass-bottom plate

6

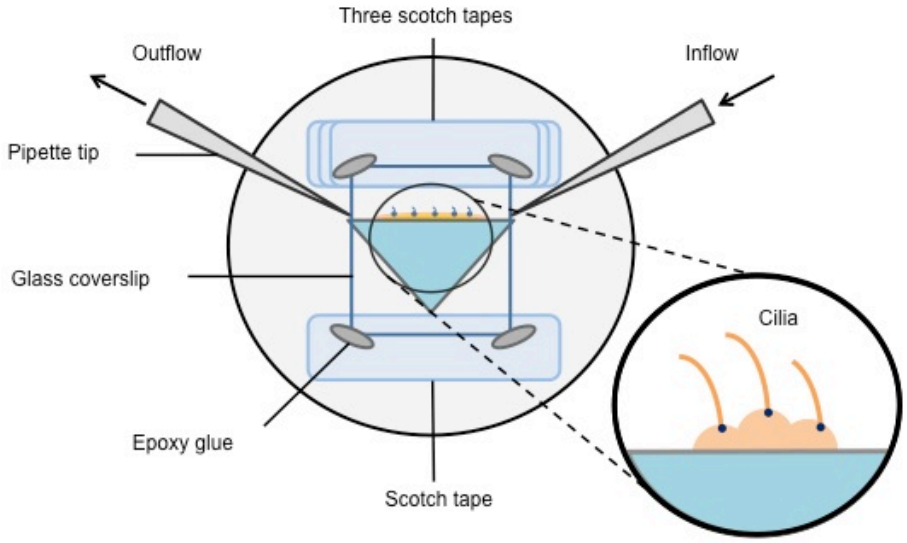

Setup for fluid flow analysis

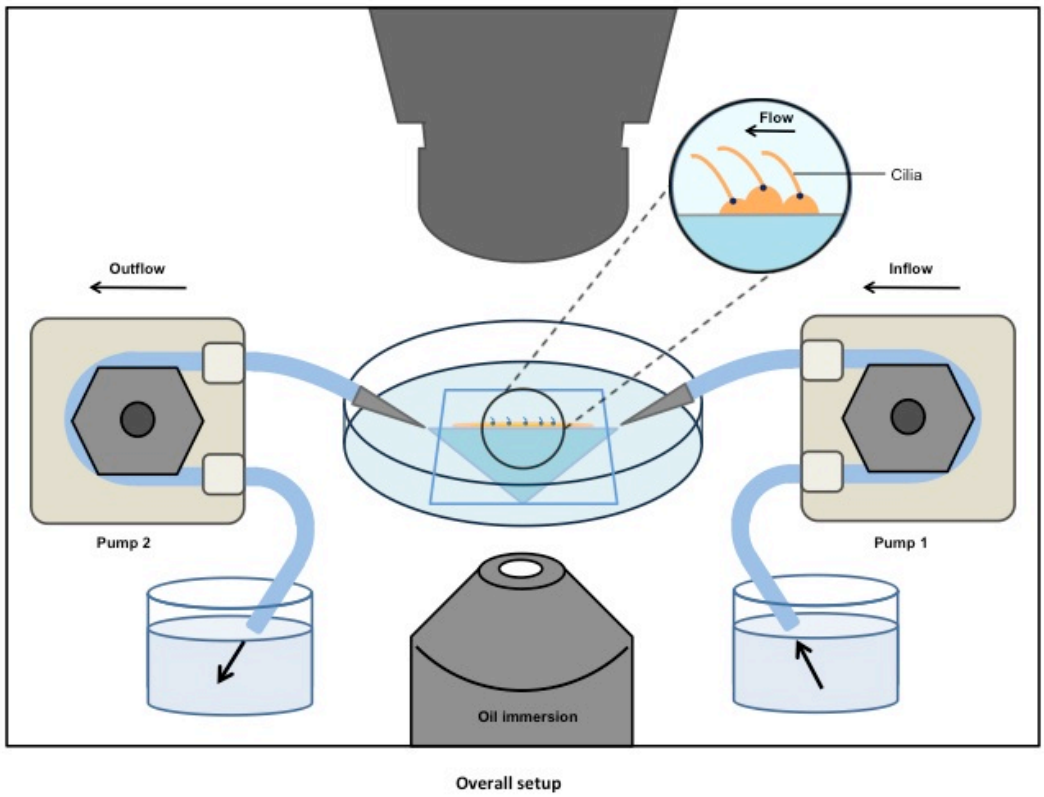

Figure 3.1| Illustration of the formvar technique setup. (**a**) The diagram shows a step by step folding of the formvar into a triangle shape for optimal observation of cilia (Steps 1- 4). The cells are grown on top of the formvar-coated cover slide (step 1). Each corner of the formvar is then scraped by sharp forceps to help detach the formvar from the 18x18 glass cover slide (step 2), and then each corner is lifted slightly to loosen it further. The formvar is gently lifted from the opposite corners to allow folding down on itself (step 3), forming a triangle shape to allow imaging of the cells grown on the folded edge of the formvar (step 4). (**b**) In order to prepare for the fluid flow setup, the triangle-shaped formvar is placed in the center of a glass-bottom cell-culture plate (step 5). Epoxy glue is used to glue an 18x18 glass cover slide to sandwich the formvar to facilitate high-resolution imaging. Scotch tape is also used to support the cover slide and help create a small space between the cover glass and the cells for optimal fluid flow. A pipette tip connected to a tubing system is then placed between the edges of the scotch tape and the folded formvar, as shown in this diagram (step 6). (**c**) A schematic illustration of the overall set-up. The plate is mounted on the microscope stage and the cells are imaged using 60X oil immersion lens as shown in the diagram. This culture plate supports the inlet and outlet of fluid perfusion through two micro-perfusion pumps with adjustable flow rate connected to fluid reservoirs.

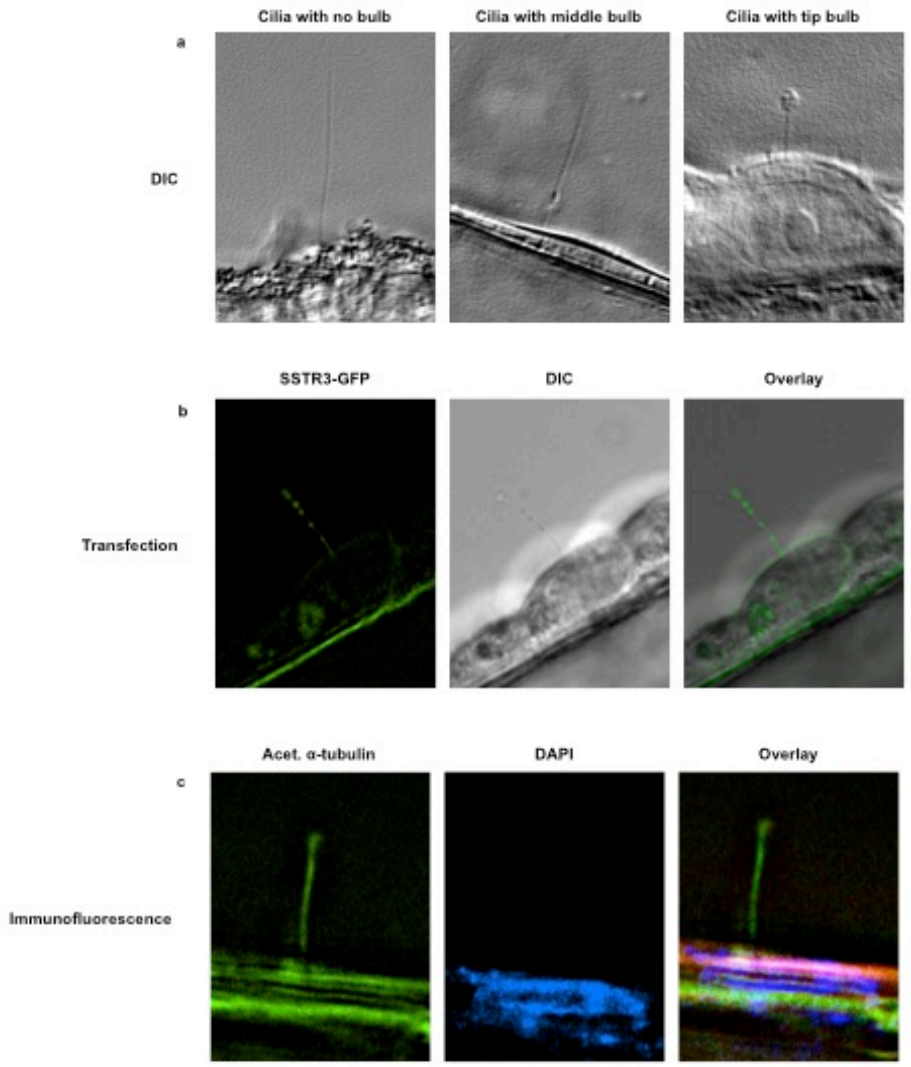

Figure 3.2| Live imaging of the whole primary cilium from the side. (**a**) Representative DIC images of primary cilium on the surface of *LLC-PK* cells using the formvar folding technique. Shown here are DIC images of the cilia from the side without ciliary bulb. Also shown are cilia with ciliary bulb at different locations along the ciliary shaft. (**b**) An *LLC-PK* cell transfected with SSTR3-GFP (a ciliary marker) is shown under both DIC and fluorescent microscopy. (**c**) The *LLC-PK* cells were stained with anti-acetylated-α-tubulin, a ciliary marker [5], and counterstained with DAPI, a nuclear/DNA marker (blue). An overlay image is shown.

To visualize calcium signaling within the cilium by live-cell imaging, a differential side-view imaging platform using formvar technique can be adopted. Ciliary and cytosolic calcium will be studied in wild-type *LLC-PK* cells treated with fenoldopam to induce cilium-specific calcium or with dopamine to induce non-specific calcium influx as we have just recently published [5]. The nature of this subcellular localization allows us to measure both ciliary and cytosolic calcium levels differentially and simultaneously. Result not shown. Of note and as mentioned earlier, the modification to this technique can be adopted by growing cells on a tungsten micro-wire coated with collagen as an alternative to formvar. This will allow for more flexible rotation of the wire to adjust for dynamic movements of the cells.

To determine whether bending of cilia results in increased ciliary calcium, we applied fluid-shear stress of 0.7 dyne/cm^2, which has been previously shown to activate cilium-dependent intracellular calcium signaling [21, 28]. This magnitude of shear stress also allows optimal physical bending of a cilium. In the presence of fluid shear, the bending of the cilium induces an increase in ciliary calcium levels. The increase in ciliary calcium is then followed by an increase in cytosolic calcium.

ACKNOWLEDGEMENTS

Authors would like to thank Maki Takahashi for her technical support. A. Mohieldin's work partially fulfilled the requirements for a PhD degree in Medicinal and Biological Chemistry. This work was supported by the National Institute of Health, R01DK080640 to S.M.N and F31DK096870 to A.M.M.

AUTHOR CONTRIBUTIONS

S.M.N and W.A.A designed the protocol. A.M.M, H.S.H, S.T.L and J.X validated the protocol. W.A.A, A.M.M. and Z.A drafted the manuscript.

COMPETING FINANCIAL INTERESTS

The authors declare that they have no competing financial interests.

References

1. Tobin, J.L. and P.L. Beales, *The nonmotile ciliopathies.* Genetics in Medicine, 2009. **11**(6): p. 386-402.

2. Roth, K.E., C.L. Rieder, and S.S. Bowser, *Flexible-substratum technique for viewing cells from the side: some in vivo properties of primary (9+0) cilia in cultured kidney epithelia.* J Cell Sci, 1988. **89 (Pt 4)**: p. 457-66.

3. Garcia-Gonzalo, F.R. and J.F. Reiter, *Scoring a backstage pass: mechanisms of ciliogenesis and ciliary access.* J Cell Biol, 2012. **197**(6): p. 697-709.

4. Gilula, N.B. and P. Satir, *The ciliary necklace. A ciliary membrane specialization.* J Cell Biol, 1972. **53**(2): p. 494-509.

5. Jin, X., et al., *Cilioplasm is a cellular compartment for calcium signaling in response to mechanical and chemical stimuli.* Cell Mol Life Sci, 2014. **71**(11): p. 2165-78.

6. Scherft, J.P. and W.T. Daems, *Single cilia in chondrocytes.* J Ultrastruct Res, 1967. **19**(5): p. 546-55.

7. AbouAlaiwi, W.A., A.M. Nauli, and S.M. Nauli, *Deciphering mechanosensory function of primary cilia in cardiovascular system.* Transworld Research Network Publisher, 2010. **Chapter 2**: p. 25-37.

8. Muntean, B.S., X. Jin, and S.M. Nauli, *Primary cilia are mechanosensory organelles with chemosensory roles.* Springer Publisher, 2012. **Chapter 9**: p. 201-22.

9. Nauli, S.M., *Primary cilia are mechanosensory organelles in vascular tissues.* Proceedings of the 15th World Congress on Heart Disease, 2011: p. 23-6.

10. Nauli, S.M., et al., *Primary Cilia are Mechanosensory Organelles in Vestibular Tissues.* Springer Publisher, 2010. **Chapter 14**: p. 317-50.

11. Nauli, S.M., X. Jin, and B.P. Hierck, *The mechanosensory role of primary cilia in vascular hypertension.* Int J Vasc Med, 2011. **2011**: p. 376281.

12. Abdul-Majeed, S. and S.M. Nauli, *Calcium-mediated mechanisms of cystic expansion.* Biochim Biophys Acta, 2011. **1812**(10): p. 1281-90.

13. Nauli, S.M. and J. Zhou, *Polycystins and mechanosensation in renal and nodal cilia.* Bioessays, 2004. **26**(8): p. 844-56.

14. AbouAlaiwi, W.A., et al., *Ciliary polycystin-2 is a mechanosensitive calcium channel involved in nitric oxide signaling cascades.* Circ Res, 2009. **104**(7): p. 860-9.

15. Praetorius, H.A. and K.R. Spring, *Bending the MDCK cell primary cilium increases intracellular calcium.* J Membr Biol, 2001. **184**(1): p. 71-9.

16. Satir, P., L.B. Pedersen, and S.T. Christensen, *The primary cilium at a glance.* J Cell Sci, 2010. **123**(Pt 4): p. 499-503.

17. AbouAlaiwi, W.A., et al., *Endothelial cells from humans and mice with polycystic kidney disease are characterized by polyploidy and chromosome segregation defects through survivin down-regulation.* Hum Mol Genet, 2011. **20**(2): p. 354-67.

18. AbouAlaiwi, W.A., et al., *Ciliary Polycystin-2 Is a Mechanosensitive Calcium Channel Involved in Nitric Oxide Signaling Cascades.* Circulation Research, 2009. **104**(7): p. 860-869.

19. Mohieldin, A.M., et al., *Protein composition and movements of membrane swellings associated with primary cilia.* Cell Mol Life Sci, 2015. **72**(12): p. 2415-29.

20. Berselli, P., et al., *Human GM3 synthase: a new mRNA variant encodes an NH2-terminal extended form of the protein.* Biochim Biophys Acta, 2006. **1759**(7): p. 348-58.

21. Nauli, S.M., et al., *Polycystins 1 and 2 mediate mechanosensation in the primary cilium of kidney cells.* Nat Genet, 2003. **33**(2): p. 129-37.

22. Masyuk, A.I., et al., *Cholangiocyte cilia detect changes in luminal fluid flow and transmit them into intracellular Ca2+ and cAMP signaling.* Gastroenterology, 2006. **131**(3): p. 911-20.

23. Delaine-Smith, R.M., A. Sittichokechaiwut, and G.C. Reilly, *Primary cilia respond to fluid shear stress and mediate flow-induced calcium deposition in osteoblasts.* FASEB J, 2014. **28**(1): p. 430-9.

24. McGrath, J., et al., *Two populations of node monocilia initiate left-right asymmetry in the mouse.* Cell, 2003. **114**(1): p. 61-73.

25. Cano, D.A., et al., *Orpk mouse model of polycystic kidney disease reveals essential role of primary cilia in pancreatic tissue organization.* Development, 2004. **131**(14): p. 3457-67.

26. Giles, R.H., H. Ajzenberg, and P.K. Jackson, *3D spheroid model of mIMCD3 cells for studying ciliopathies and renal epithelial disorders.* Nat Protoc, 2014. **9**(12): p. 2725-31.

27. Aboualaiwi, W.A., et al., *Survivin-induced abnormal ploidy contributes to cystic kidney and aneurysm formation.* Circulation, 2014. **129**(6): p. 660-72.

28. Nauli, S.M., et al., *Loss of polycystin-1 in human cyst-lining epithelia leads to ciliary dysfunction.* J Am Soc Nephrol, 2006. **17**(4): p. 1015-25.

Chapter 4

Chemical-Free Technique to Study Ultrastructure of Primary Cilium

Ashraf M. Mohieldin[1], Min Gao[2], Surya M. Nauli[3]

[1]Department of Medicinal & Biological Chemistry, University of Toledo School of Pharmacy, Toledo, OH 43614. [2]Liquid Crystal Institute, Kent State University, Kent, OH 44242. Department of Biomedical & Pharmaceutical Sciences. [3]Chapman University School of Pharmacy, Irvine, CA 92618. Department of Urology, University of California at Irvine Medical Campus, Orange, CA 92868.

Corresponding:
Surya M. Nauli
Chapman University, School of Pharmacy
University of California at Irvine, Urology
9401 Jeronimo Road
Irvine, CA 92618-1908

Tel: 714-516-5485
Fax: 714-516-5481

Email: nauli@chapman.edu
Email: snauli@uci.edu

Min Gao
Kent State University
1425 University Esplanade
Kent, Ohio 44242

Tel: 330-672-7999

Email: mgao@kent.edu

Abstract

A primary cilium is a hair-like structure with a width of about 200 nm. Over the past decades, the main challenge to study the ultrastructure of a cilium is particularly due to the high sensitivity of cilium to chemical fixation, required by many imaging techniques. In this paper, we report a combined freeze fracture transmission electron microscopy (FFTEM) and high pressure freezing (HPF) techniques to examine the ultrastructure of a cilium. Our main objective is to develop an optimal high resolution imaging approach, which reserves cilia structure in its best natural form without chemical interference that can change cilia morphology. Our result showed that a cilium can have a swelling-like structure (termed bulb), and the ciliary bulb is part of an integral structure within the ciliary membrane. In addition, the intramembrane particles observed via FFTEM/HPF indicated the presence of integral membrane proteins and soluble matrix proteins along the ciliary bulb and that the bulb bilayer was part of the cilia bilayer. We propose that FFTEM/HPF is an important chemical-free method to study the ultrastructure of primary cilium that is sensitive to chemical fixation.

4.1. INTRODUCTION

Primary cilia have been intensively studied over the last few years, because they are relevant to a group of diseases, called ciliopathies. Ultrastructurally, primary cilia have hair-like structures supported by microtubules and enclosed by the ciliary membrane. These microtubules are arranged circumferentially, without a central pair "9+0" unlike the one that is seen in motile cilia. The basal body and centriole join together to form a centrosome, which serves as the cell's main microtubule organization. The ciliary necklace, which is made up by a distinct set of membrane proteins at the transition zone, helps differentiate the ciliary membrane from the cell's plasma membrane and cilia membrane [1]. Various receptors, ion channels, transporters and sensory proteins that serve different functions reside on the ciliary membrane. Furthermore, the cilioplasm of a primary cilium is enriched with many signaling intermediates, including calcium signaling [2].

Primary cilium has a bulging structure, known as bulb, which was initially observed in 1977 [3]. It was proposed that ciliary bulb contained substances to be transported within the cilium. The ciliary bulb or swelling is associated with the ciliary shaft and may represent a circumscribed region of the ciliary membrane which was once thought to be sensitive to environmental osmatic pressure [4]. To our knowledge, however, the ultrastructure of a non-motile primary cilium had never been studied with transmission electron microscopy (TEM) to analyze its nanoscale structural detail.

4.2. Development of the protocol

The ciliary structure exhibits high sensitivity to chemical fixation. It has been known since 1990s that chemical fixation during sample preparations for cilia analysis will result in fixation artifact [5,6]. Thus, a successful technique to study cilia requires the sample to be fixed in their living state very rapidly and without the involvements of chemicals and lengthy process. However, such a requirement makes it difficult for some of the widely used imaging techniques to get reliable results correlated to the native structure.

To overcome this challenge in our most recent study on ultrastructure of primary cilium [7], we have since established freeze-fracture transmission electron microscopy (FFTEM) technique to examine the morphology of the cilia fixed by abrupt high-pressure freezing (HPF). In our present technique, we grow the cells directly in the HPF carriers, which will minimize the structural change before and after the fixation. The FFTEM/HPF technique is substantially different form other techniques that require chemical fixations. The FFTEM/HPF technique is chemical-independent technique that uses rapid freezing and solution-free sample preparation.

4.3. Applications of the method

The freeze-fracture technique was first discovered in the 1950s for the preparation of samples for electron microscopy [8,9]. Hall and Meryman started the sublimation of ice to reveal surface structures by using the combination of freezing and etching techniques. Over the years, the technique started to have more impact in studying biological ultrastructure [10]. The effectiveness of this technique was further demonstrated when the

freeze fractured was performed in the yeast cells to reveal the three-dimensional ultrastructural of the specimen [11,12]. Since then, the freeze-fracture technique has been a very useful tool in studying the ultrastructure of lipid structures, fats and oils, membrane lipids, non-lipid lamellae, dry lipids thermotropic states, lyotropic states, lateral phase separation in lipid bilayers and biological membranes, non-lamellar lipid structures, single micelles, aggregates of micelles, bicontinuous cubic phases of type II, biological membrane and surface views or membrane splitting [10].

The FFTEM/HPF technique is certainly appropriate for all these studies. Furthermore, we believe that the FFTEM/HPF technique is particularly suitable for studies associated with cell cytoskeletal-based structures, such as microvilli, kinocilia, photoreceptor cilia, motile and non-motile cilia, and various junctional proteins or receptors which structural activities depend on intermediate filaments.

4.4. Comparison with other methods

A wide range of variations of FFTEM-related techniques has been developed over the past half century and is still widely used for biological materials and some other soft-matter materials, such as liquid crystals. FFTEM is often considered to be a traditional or even "old" technique compared to some of the new developments, such as cryo-EM of vitreous sections (CEMOVIS) and freeze substitution. However, some of the advantages that FFTEM can provide are often found to be irreplaceable for some special systems. For example, its unique surface sensitivity was found to be extremely useful in the studies of complex liquid crystal systems [13]. For biological materials, one of the

strengths of FFTEM is that the frozen membranes may tend to fracture along the central hydrophobic core, which makes FFTEM a valuable tool for cilia study. On the other hand, CEMOVIS and freeze substitution are both ultramicrotomy-based techniques. It is generally difficult to obtain similar information without going for an extra effort, such as serial sectioning and 3D reconstruction.

Of note is that many of other FFTEM techniques require various chemicals and cyroprotectants that can deteriorate the biological samples easily. On the other hand, other cryo-TEM techniques use plunge-frozen thin solution films and require blotting of the excessive solution with filter papers. In addition to a shorter sample-processing time, FFTEM/HPF technique is thus superior by avoiding the use of cryo-TEM and chemical fixation throughout the process.

4.5. Limitations

Like other imaging techniques, a high level of expertise is needed to implement the FFTEM/HPF protocol. It is advisable that the implement of protocol should be initiated by a qualified TEM specialist within the TEM core facility. However, the FFTEM/HPF protocol is simple enough that if trained properly, a graduate student (Ashraf M. Mohieldin) should be able to perform the technique independently. There is also expected that a student needs to be supervised and trained by an electron microscopy specialist (Min Gao).

4.6. MATERIALS

4.6.1 Reagents

1. Porcine kidney epithelial cells (LLC-PK1), or any cultured cells
2. Phosphate buffer saline (PBS, pH 7.4; *Fisher, Inc*)
3. Modified Eagle Medium (DMEM) (*Corning*)
4. Fetal bovine serum (FBS) (*HyClone, Inc*)
5. Penicillin/streptomycin (*Corning Cellgro*)
6. Formvar (*Electron Microscopy Science*)
7. Tissue culture dish (35 mm; Biolite)
8. Ethylene dichloride (*VWR*)
9. Collagen (*Corning*)
10. Trypsin (*Fisher, Inc.*)
11. Ethanol (*Fisher, Inc.*)

4.6.2. Equipment

1. Cell Culture Incubator (*Sanyo* MCO-19AIC)
2. Freeze fracture ring for the freeze fracture carrier (*Leica* 16706867)
3. Freeze fracture carrier for Leica EM Patc2 high pressure freezer (*Leica* 16706866)
4. Freeze fracture bayonet pod to lock carrier and ring (*Leica* 16707829)
5. Freeze-fracture apparatus (*BalTec*; BAF060)
6. Transmission Electron Microscope (FEI Tecnai F20 operated at 200 KV)

4.7. PROCEDURE

Overall, the protocol for FFTEM/HPF procedure is straightforward and involved the following steps **(Figure 4.1)**.

4.7.1. Solution preparations

A. Preparing Fomvar solution

i. Prepare 2% Formvar solution by dissolving 0.9 g of Formvar powder in 45 mL of ethylene dichloride

ii. Incubate solution in 37 C water bath

iii. Shake solution vigorously if not dissolved

B. Preparing collagen solution

i. Prepare 50 μM collagen solution by dissolving 578.40 μl of collagen in 45 mL of cold PBS solution

ii. Collagen should dissolve easily

iii. Check and adjust pH to 7.4 if not dissolved.

C. These solutions are for cell culture use only. No additional solution is needed for FFTEM/HPF sample preparation and processing.

4.7.2. PAUSE POINT:

A. Formvar and collagen solutions can be stored for one week

B. Formvar solution can be stored at room temperature

C. Collagen solution should be stored at 4 °C

D. Do not freeze formvar and collagen solutions

4.7.3. Preparing the gold-plated flat carriers for cell growth (60 minutes)

A. Immerse the gold-plated flat carriers in 75% ethanol for 5 minutes

B. Wash the gold-plated flat carriers with sterile PBS three times under the cell culture hood

C. Carriers can be further sterilized under ultraviolet light for 30 minutes

D. Immerse the gold-plated flat carriers in 2 % formvar solution for 3-5 seconds

E. Place the gold-plated flat carriers in small petri dish and let it dry for 10 minutes

F. Add 50 μM collagen directly into the gold-plated flat carriers and let it dry for 10 minutes

G. Wash the petri dish containing the gold-plated flat carriers with sterile PBS two times to wash out excess collagen solution

H. Place the petri dish containing the gold-plated flat carriers under ultraviolet light for 30 minutes to sterilize the carriers

I. Use sterile technique from here on

4.7.4. PAUSE POINT: The carriers can be kept for 2-4 days at 4 °C.

4.7.5. Growing the LLCPK cells on the gold-plated flat carriers (15 minutes)

A. Wash grown 60-70 % confluent LLCPK cells with PBS two times and add appropriate amount of trypsin

B. Incubate cells in incubator for about 3 minutes

C. Collect cells and remove trypsin by briefly centrifuge the cells down in a test tube.

D. Add DMEM media containing 10% FBS and 1% penicillin/streptomycin

E. Gently disperse cells

F. Add about a million cells directly on each of the gold-plated flat carriers

G. Incubate cells at 37°C in 5% CO_2 incubator for 24 hours

H. At this stage, cells should reach about 70-80% confluent

4.7.6. CRITICAL STEP

A. A long well developed cilium is easier to image and analyze

B. Cilia growth can be induced through cell differentiation

First Option:

i. Use DMEM containing 2% FBS

ii. Recommend 2% FBS to prevent cell death

iii. Recommend to withdraw penicillin/streptomycin to accelerate cell differentiation

iv. Grow cells for additional 24-48 hours

Second Option:

i. Use cell-cell contact inhibition to promote cell differentiation

ii. Grow cells for additional 48-72 hours

C. Note that cells on the gold-plated flat carriers can only be observed using upright or surgical microscope

4.7.7. Preparing cells for FFTEM/HPF

A. With live cells grown inside gold-plated flat carriers (*Leica* 16706866), carefully remove once carrier from the petri dish

B. Place a ring (*Leica* 16706867) on top of the carrier.

C. Load the carrier-ring assembly into a bayonet pod (*Leica* 16707829)

D. Tighten the diamond locking screw of the bayonet pod (on the side of the ring) so that the carrier assembly is securely sealed together

E. Quickly transfer the bayonet pot into the Leica EM Pact2 high-pressure freezer for the rapid cryo-fixation

F. Apply a high pressure (~2,000 bar) to the sample

G. CRITICAL STEP: use 2,000 bar pressure to significantly slow down the crystallization of water. This will prevent a sudden imploding of cell membrane.

H. During the pressurized process, inject liquid nitrogen rapidly onto the sealed assembly for the vitreous freezing

I. After successful freezing, quickly transfer the assembly into a BalTec BAF060 freeze-fracture apparatus

J. A successful freezing can be determined based on the relative changes of both measured pressure and temperature

K. Set the sample stage to -165 °C inside the vacuum chamber

L. Employ a built-in microtome to knock off the ring to fracture the frozen sample inside the carrier

M. Perform the fracture immediately by the replication of the surface topography, which is performed by depositing a thin (~4 nm) Pt/C layer at 45° and a continuous carbon film (~20 nm) at 90°

N. Take the sample to the airlock and then move outside

O. Put the carrier into distilled water to dissolve the culture media

P. Collect the suspended pieces of the replica by holey lacey carbon coated TEM grids.

Q. Observe sample using a Tecnai TF20 field emission TEM operated at 200 KV

R. Look for a typical fracture configuration for a cilium (**Figure 4.2**)

4.8. Results

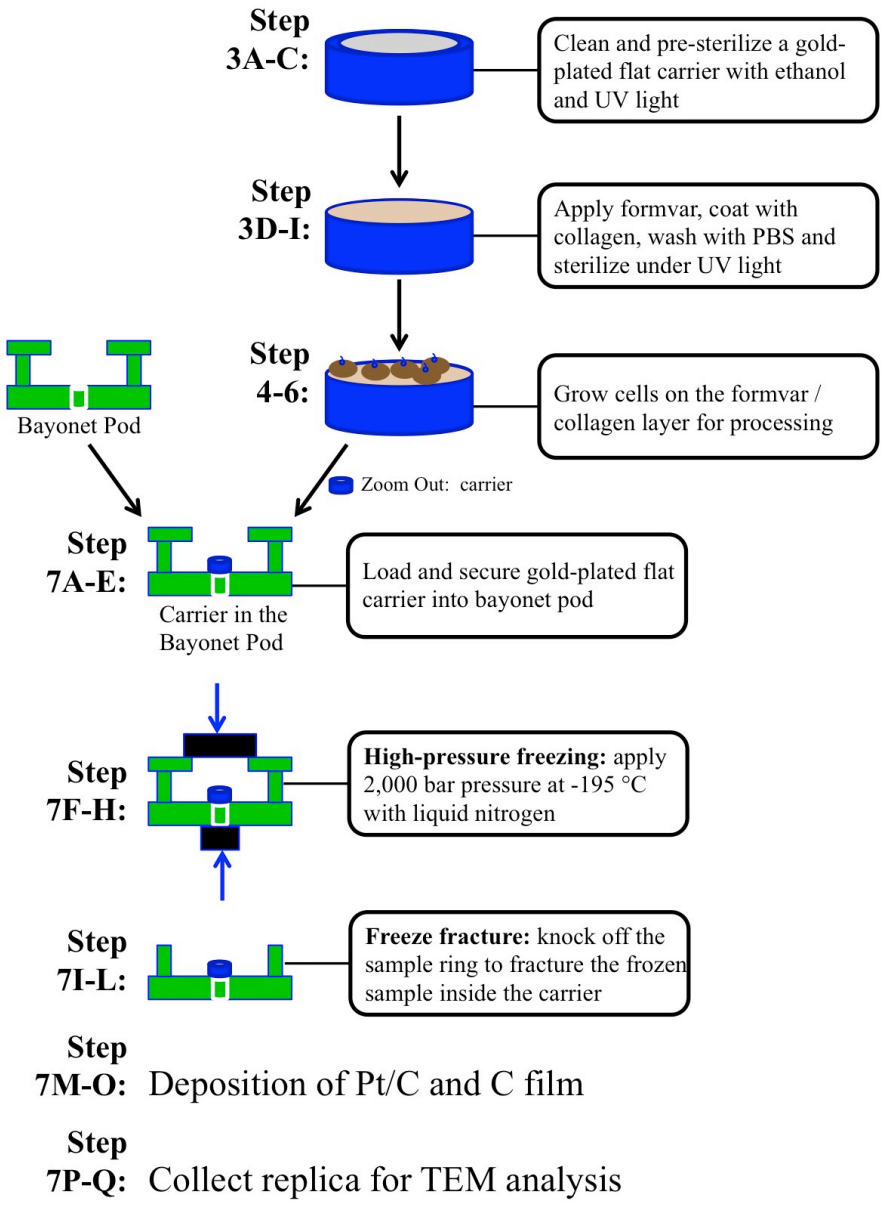

Figure 4.1. Schematic of experimental procedure

Schematic diagram depicts FFTEM/HPF procedure used in our study. Each of the steps illustrates the key procedural steps and is described in more detail in the *Procedure* section of the manuscript.

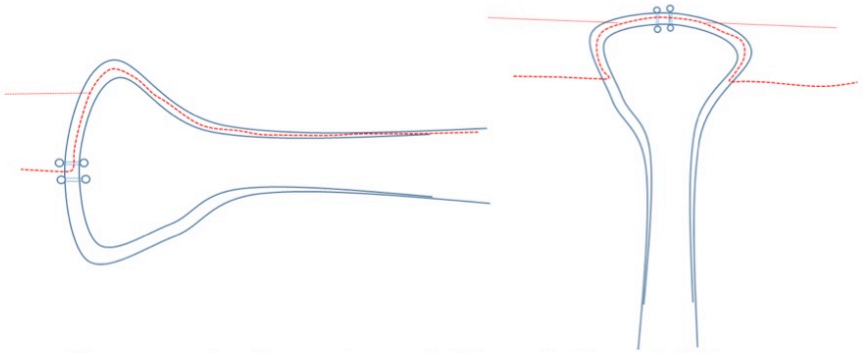

Figure 4.2. Schematic of fracture configurations

Schematic diagram illustrates configurations for analysis of ciliary bulb and cilium. For a quick screen to check the quality of the fracture and replica, these configurations should be observed under the field emission TEM. The fracture configurations could then be further zoomed-in or magnified for greater image quality and analysis.

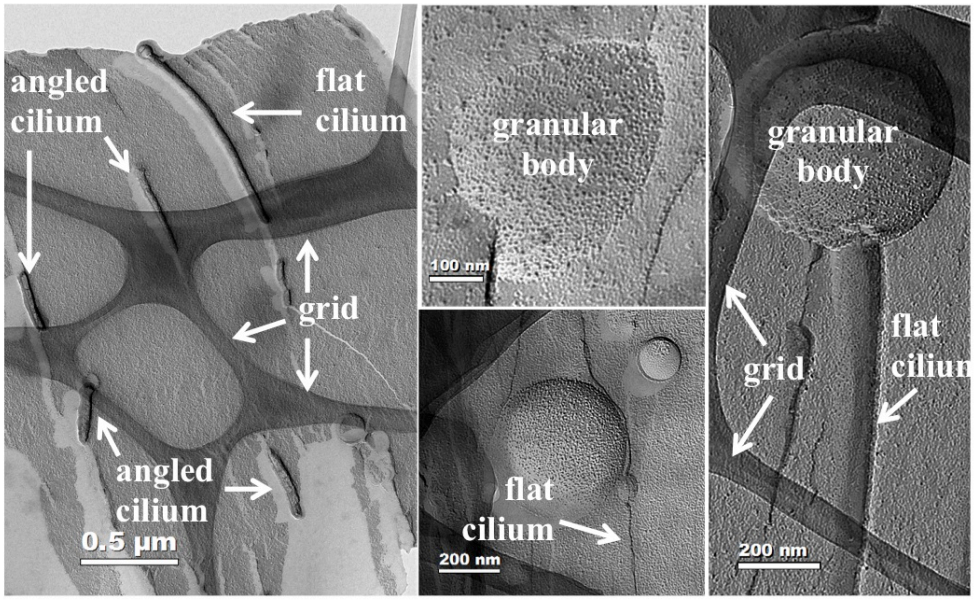

Figure 4.3. Typical FFTEM/HPF for cilia analysis

Shown here are some examples of FFTEM/HPF images; some preparations are cleaner that others. Clean preparations for cilia study are those with less granular body. The grid of sample support mesh can also be seen. Incomplete replica image of cilium (angled cilium) can be due to the less optimal angle or position of cilium during fracture or imprint. A cilium laying flat on the surface during fracture and imprint would generate a more complete length of cilium, which termed flat cilium.

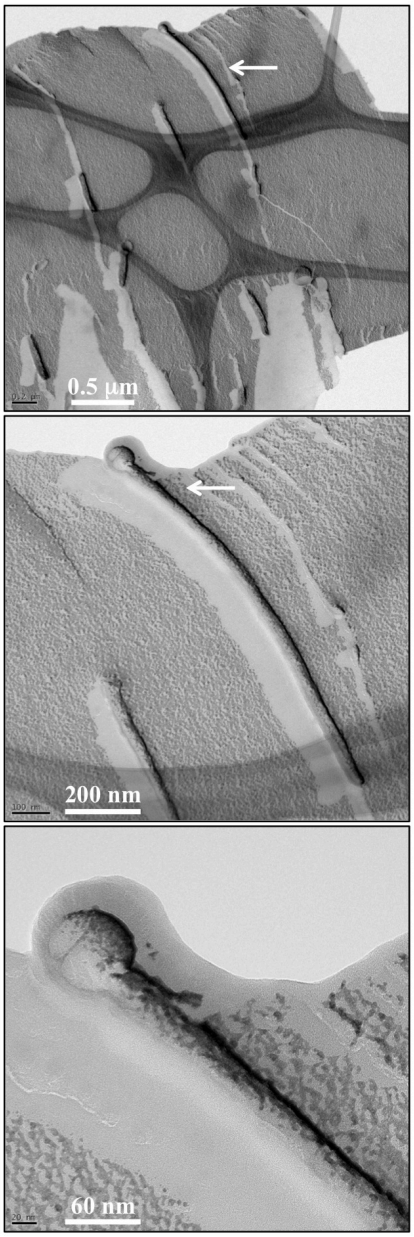

Figure 4.4. Examining renal epithelial cilia with FFTEM/HPF

Once a suitable structure configuration is selected (**top panel**), a higher magnification can be used for analysis (**middle panel**). To further understand the ultrastructure of ciliary bulb, we could increase the magnification and image visibility (**lower panel**). Shown here is a typical ciliary bulb, which indicate that bulb membrane is continuous from cilia bilayer and that particle indentions are observed in the ciliary membrane and bulb.

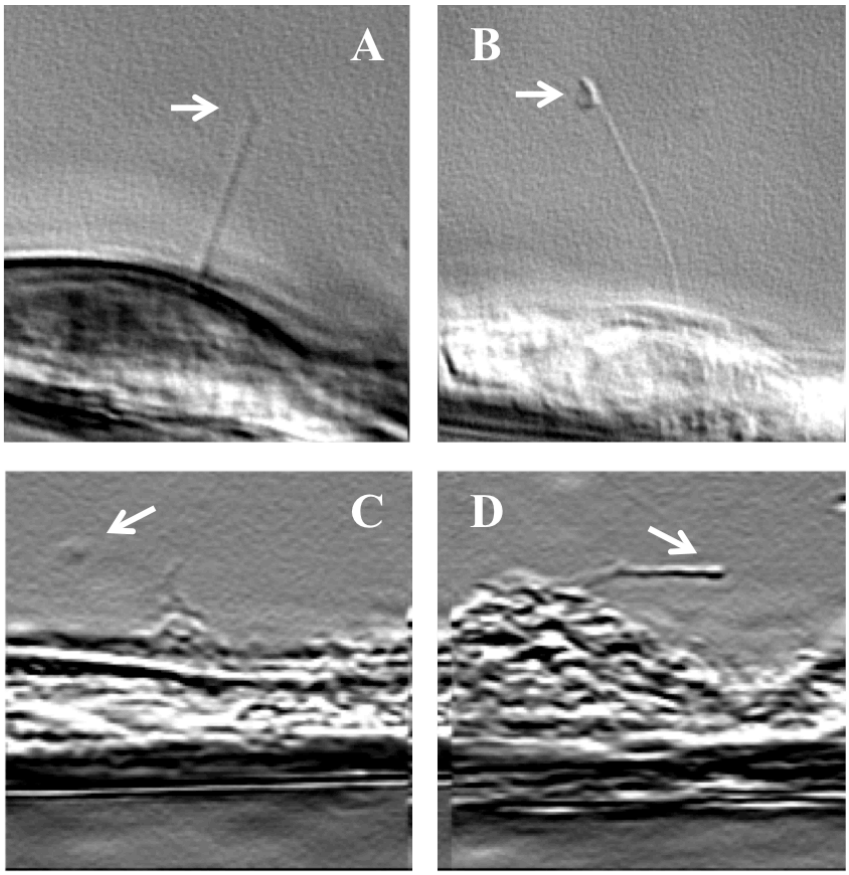

Figure 4.5. Effect of chemical fixation on ciliary structure

Shown here are live images of renal primary cilia in control (**a, b**) and formaldehyde treated cell (**c, d**). A nice smooth elongated cilium was observed in control, whereas treatment with formaldehyde for 5 minutes grossly damages the structure integrity of the cilium.

4.9. **ANTICIPATED RESULTS**

During the fracture of the cells, many fracture configurations are possible (**Figure 4.3**). Some of the primary cilium is more obvious in one preparation than others. In most cases, however, a greater magnification is required to confirm the structure of a cilium. The position of the cilium also dictates the clarity of the image. For example, the grid of sample support mesh and/or the replica image of granular cell body could potentially hinder capturing and analyzing the entire cilium. In a different case, the cilium may not have been replicated throughout the entire ciliary shaft. We term this as "angled cilium", in which only a short replica image of cilium is observed. An optimal imaging of a cilium can be obtained when the cilium lays flat on the replica plate, and we call this "flat cilium".

Many flat-cilia have bulging structures (**Figure 4.4**). These bulging structures or bulbs can have spherical or irregular shapes. The size of the replicated bulbs can range from 80 nm to about 1 mm. The biological functions of these bulbs have just been recently studied [2]. The significance of the bulb size, however, is still not clear. Technically speaking, the small ones might be due to the shallow fracture. However, various sizes of the bulb have also been observed in the live-cell imaging, indicating that a cell may have the mean to regulate the size and appearance of the bulb [2].

Our results indicated that ciliary bulb shares an intact structure along with the ciliary shaft, and there was no indication that ciliary bulb is attached separately to the outer

ciliary membrane. It is apparent that the bulb bilayer is part of the cilia bilayer. Furthermore, the FFTEM/HPF images show particle indentions along the ciliary membrane, including the ciliary bulb. In all replica of any cell membrane, scattered particles are often visible indicating the existence of integral membrane proteins. This finding therefore suggests that ciliary bulb and cilium itself contained integral and/or matrix proteins.

Our approach by growing cells directly on the HPF carrier for FFTEM analysis has yielded the first insight of the ciliary bulb structure. To our knowledge, we believe that our study was the first to provide TEM image on mammalian non-motile cilium [2]. The main challenge with other TEM approaches is the detrimental effect of fixation chemicals toward cilia structure. Many fixatives, including 4% paraformaldehyde, could dramatically alter ciliary morphology (**Figure 4.5**). In general, shorter and unbalanced cilia are observed when chemically fixed. The grossly damage structure of the cilium makes it extremely hard to obtain a nicely flat-cilium for imaging purposes. We therefore believe that the challenge with many TEM approaches is the inability to obtain cilia with excellent structure integrity.

We propose that the ultrastructure of the mammalian primary cilium is best studied with no fixative chemical. The use of FFTEM/HPF approach offers various advantages to study the ultrastructure of a cilium. Technically, the same cryo-fixation procedure can also be used for other TEM techniques, namely CEMOVIS (or cryo-TEM on thin specimens prepared by focused ion beam) and freeze substitution. Compared to the latter

two, the FFTEM/HPF technique provides a much simpler process and is more focused on the membrane structure and ultrastructure of primary cilia. FFTEM/HPF also involves an inexpensive procedure to reveal the ultrastructure of the ciliary bulb without the use of any chemical fixation and to maintain the cilia morphology in its best natural form. This technique is therefore an indispensible tool to study the etiology of cilia-related diseases by offering high-resolution of the ultrastructure image of primary cilia.

Author contributions statements

AMM performed the study and drafted the manuscript; MG facilitated in revising manuscript, improving the protocol and technical troubleshooting; SMN wrote the manuscript and provided technical advice to overcome challenges in cilia imaging.

Acknowledgement

The TEM data were obtained at the Cryo-TEM facility at the Liquid Crystal Institute, Kent State University, supported by the Ohio Research Scholars Program Research Cluster on Surfaces in Advanced Materials. This work was supported by the National Institute of Health (R01DK080640 to SMN and F31DK096870 to AMM) and Department of Defense (CDMRP PR130153 to SMN).

Competing financial interests

none

REFERENCES

1. Gilula, N.B. & Satir, P. The ciliary necklace. A ciliary membrane specialization. *J Cell Biol* **53**, 494-509 (1972).

2. Jin, X. *et al.* Cilioplasm is a cellular compartment for calcium signaling in response to mechanical and chemical stimuli. *Cell Mol Life Sci* **71**, 2165-78 (2014).

3. Dilly, P.N. Material transport within specialised ciliary shafts on Rhabdopleura zooids. *Cell Tissue Res* **180**, 367-81 (1977).

4. Roth, K.E., Rieder, C.L. & Bowser, S.S. Flexible-substratum technique for viewing cells from the side: some in vivo properties of primary (9+0) cilia in cultured kidney epithelia. *J Cell Sci* **89 (Pt 4)**, 457-66 (1988).

5. Beninger, P.G., Potter, T.M. & Stjean, S.D. Paddle cilia fixation artifacts in pallial organs of adult Mytilus edulis and Placopecten magennanicus. *Canadian J Zool* **73**, 610-14 (1995).

6. Short, G. & Tamm, S.L. On the nature of paddle cilia and discocilia. *Biol Bull* **180**, 466-74 (1991).

7. Mohieldin, A.M. *et al.* Protein composition and movements of membrane swellings associated with primary cilia. *Cell Mol Life Sci* (2015).

8. Meryman, H.T. Replication of frozen liquids by vacuum evaporation. *Journal of Applied Physics (abstr.)* **21**, 68 (1950).

9. Hall, C.E. A low temperature replica method for electron micro-scopy. *Journal of Applied Physics* **21**, 61-2 (1950).

10. Meyer, H.W. & Richter, W. Freeze-fracture studies on lipids and membranes. *Micron* **32**, 615-44 (2001).

11. Moor, H. Endoplasmic reticulum as the initiator of bud formation in yeast (S. cerevisiae). *Arch Mikrobiol* **57**, 135-46 (1967).

12. Moor, H. & Muhlethaler, K. Fine Structure in Frozen-Etched Yeast Cells. *J Cell Biol* **17**, 609-28 (1963).

13. Gao, M. *et al.* Direct observation of liquid crystals using cryo-TEM: specimen preparation and low-dose imaging. *Microsc Res Tech* **77**, 754-72 (2014).

Chapter 5

Proteomic Analysis of *LL-CPK-1* Isolated Cilia

Ashraf M. Mohieldin[1], John R. Yates[2], Surya M. Nauli [3,4]

[1]Department of Medicinal & Biological Chemistry, University of Toledo School of Pharmacy, Toledo, OH 43614 [2]Department of Chemical Physiology and Cell Biology, The Scripps Research Institute, La Jolla, California 92037 [3]Department of Biomedical & Pharmaceutical Sciences, Chapman University School of Pharmacy, Irvine, CA 92618 [4]Department of Urology, University of California at Irvine Medical Campus, Orange, CA 92868

Corresponding:
Surya M. Nauli
Chapman University, School of Pharmacy
University of California at Irvine, Urology
9401 Jeronimo Road
Irvine, CA 92618-1908

Tel: 714-516-5485
Fax: 714-516-5481

Email: nauli@chapman.edu
Email: snauli@uci.edu

Abstract

The primary cilia have been intensively studied over the last years, due to the fact that they are relevant to a group of diseases, called ciliopathies. To fully understand the primary cilia functions and its molecular mechanisms that underlying ciliopathies, it is very crucial to generate a catalog of ciliary proteins. Even though many of ciliary proteins have been linked to many important biochemical processes, many other are yet to be identified. In previous studies we have identified key proteins that localized particularly on the ciliary swelling, using immunofluorescence and immuneblotting techniques. Here we report 19 new ciliary proteins, through a proteomic study, using a sensitive multidimensional protein identification technology (MudPIT) method. Overall, our studies provided an important step toward understanding the cilia function and structure.

5.1. Introduction

Primary cilia exist on almost all mammalian cell types, including renal epithelia. They were shown to act as mechanosensory organelles by sensing and responding to urinary flow in the nephron [1] [2]. In addition, the ciliary membrane houses many receptors, ion channels, transporters and other sensory proteins where each one has a definitive and distinctive function. In addition, the cilioplasm part of the cilia is enriched with many signaling proteins. Both signaling, transport and mechanosensing proteins are required to coordinate a key role in cilia assembly and function. Moreover, mechanosensory proteins receptors along the ciliray shaft, including Polycystin-1 and -2, have an important role in sensing the overpassing fluid [3-5]. In complementary, the non-ciliated cells, when they are genetically manipulated or chemically treated, were found to be mechano-insensitive to fluid flow [6, 7]. However, many other ciliary membrane proteins are not yet been established. This can partially be due the fact that some of these protein receptors are localized to the ciliary membrane only at a certain time, to perform a defined function, and then translocated out of the cilia.

The use of method to identify these proteins is very important, on generating a comprehensive ciliary protein data, than using single protein detection technique by immunofluorescences and/or immunoblotting. The mass spectrometer (MS) is one of the useful methods directed to address this requirement. For this reason, many studies have comprehensively determined ciliary proteins, using many different mass spectrometers techniques. In a previous study, the ciliary genomics and proteomics data sets estimated that the vertebrate cilium function might involve about 1000 different polypeptides, using

RPS-BLAST method [8]. However, due to the large complex scale of the ciliary protein, a sensitive MS technique must be considered. The multidimensional protein identification technology (MudPIT) is one of the sensitive techniques that were designed to study large complex samples, without prior electrophoretic separation [9]. With femtomolar sensitivity, and based on the high capacity of strong cation-exchange (SCX) resin, the high resolution of SCX and reverse phase resins (RP), the MudPIT can identify over 2500 proteins [10]. As a result, we selected MudPIT technique to study mammalian ciliary membrane proteins.

5.2. Methods and Materials

Cell culture

The porcine kidney epithelial cells (LLCPK) were cultured in Dulbecco's Modified Eagle Medium (DMEM) (*Corning Cellgro*), 10% fetal bovine serum (FBS) (*HyClone, Inc*.) and 1% penicillin/streptomycin (*Corning Cellgro*) at 37°C in 5% CO_2 incubator. The cells were differentiated by serum starvation for 24 hours prior to experiment.

Isolating primary cilia:

The isolation of the primary cilia was induced by shear stress force [11]. Cells were grown in 150 mm culture dish and/or 100 mm culture dish in 10% DMEM and 1% penicillin/streptomycin in a humidified incubator at 37°C in 5% CO2. 8 days were the maximum for cells growth and were cells was starved for differentiation before shaking. Cells were rinsed with 10 ml of PBS briefly and gently. The dish was placed on a rotary shaker and shook for 4 minutes at 350 rpm *(Orbital shaker, Cole-Parmer, Inc.).* Carefully, the media containing isolated cilia was transferred into a 50 ml centrifuge tube and spun for 30 minutes at 3,000 *g* at 4°C (*Eppendrof 5810R*). The supernatant , which containing the isolated cilia, was then transferred to a polyallomer tube and spun for 1 hour at 70,000 *g* at 4°C in an ultracentrifuge (*Beckman optima L-60*). Isolated primary cilia (pellet) were then resuspended in a Ripa buffer for BSA protein quantification and then proteomic analysis.

MudPIT analysis

To test for the purity fraction of the isolated primary cilia, cilia lysate were immunoblotted and GAPDH was used as a negative control while acetylated-a-tubulin was used as a positive

control for ciliary marker [12]. MudPIT method was used to analysis the cilia lysate, in which complex mixtures of proteins were analyzed without prior to electrophoretic separation [13]. MudPIT analysis of cilia lysate detected a total of 4,768 proteins in total, which included known ciliary membrane proteins and ciliary immunoproteins, as well as known non-ciliary proteins (Table 5.1 and 5.2).

5.3. Results

The isolated primary cilia were compared to the non-isolated cells. The following tables indicate the percentage of the found proteins. Table 5.1 and 5.2 list the ciliary proteins in immunoproteins and ciliary membrane receptor proteins respectively. In addition, each found protein was classified to either new or already known ciliary proteins. Further, the function of each newly identified ciliary protein was illustrated in table 5.3.

Table 5.1 Ciliary immunoproteins:

Accession	% Control	% Cilia	Description	Classification
tr|A7XP20_PIG	0	14.20%	B-cell CLL/lymphoma	New
sp|P15982_PIG	0	8.80%	SLA class II histocompatibility antigen, DQ haplotype C beta chain	New
sp|Q07717_PIG	10.20%	45.80%	Beta-2-microglobulin	New
sp|Q3ZDR4_PIG	7.40%	17.90%	CD70 antigen	New
tr|K7GMI9_PIG	0	30.40%	CD9 antigen	Known [14]
sp|P80928_PIG	35.70%	36.50%	Macrophage migration inhibitory factor	Known [15]
tr|Q31072_PIG	4.10%	14.30%	MHC class II antigen	New
tr|A2SW51_PIG	0	8.30%	Monocyte differentiation antigen CD14	Known [16]
tr|F1SL37_PIG	0	12.50%	Leukocyte surface antigen CD47	New
tr|B6EUU6_PIG	0	4.50%	Toll-like receptor 3 short-type	New
tr|K7GKQ2_PIG	0	37.90%	Tumor necrosis factor receptor superfamily member 5	New
sp|O77736_PIG	0	4.20%	Tumor necrosis factor receptor superfamily member 6	New

Table 5.2 Ciliary membrane receptor proteins:

Accession	% Control	% Cilia	Description	Classification
sp|Q8HZV3_PIG	0	2.70%	Transferrin receptor protein 1	New
sp|Q1RPR6_PIG	0	5.10%	Integrin beta-6	New
tr|F1S8A4_PIG	0	3.30%	Receptor-type tyrosine-protein phosphatase	New
tr|A2TEQ2_PIG	0	9.60%	Poliovirus receptor related 2	New
tr|A9LM01_PIG	0	15.20%	Progesterone receptor membrane component 2	New
tr|K7GKV2_PIG	0	3.00%	Prolactin receptor	Known [17]
tr|F1SI16_PIG	0	4.30%	Bone morphogenetic protein type II receptor	New
tr|D3K5K6_PIG	0	2.70%	EPH receptor B3	New
tr|B2ZI35_PIG	0	20.80%	F11 receptor	New
sp|B2ZHY2_PIG	0	2.00%	G-protein coupled receptor 39	New
tr|B6E241_PIG	4.10%	9.70%	Growth factor receptor bound protein 2	Known [18]
sp|Q29000_PIG	8.90%	31.60%	Insulin-like growth factor 1 receptor	Known [19, 20]
tr|K7GSJ4_PIG	19.30%	33.60%	Membrane-associated progesterone receptor component 1	Known [21, 22]
tr|B3TFD9_PIG	0	17.10%	Poliovirus receptor-related 2 transcript variant delta	New
tr|K7GSX5_PIG	2.40%	18.90%	Tyrosine-protein kinase receptor	Known [23]
sp|P32307_PIG	0	9.20%	Vasopressin V2 receptor	Known [24, 25]

Table 5.3 Newly identified ciliary proteins and their functions:

Accession	Protein	Function	Reference
tr|A7XP20_PIG	BCL10	Immune system	[26]
sp|P15982_PIG	SLA-DQB1	Immune system	[27]
sp|Q07717_PIG	B2M	Involved in the presentation of peptide antigens to the immune system	[28]
sp|Q3ZDR4_PIG	CD70	Plays a role in T-cell activation	[29]
tr|Q31072_PIG		Process and present antigen	[30]
tr|F1SL37_PIG	CD47	Involved in the increase in intracellular calcium concentration that occurs upon cell adhesion to extracellular matrix	[31]
tr|B6EUU6_PIG	TLR3	Innate immune response	[32]
tr|K7GKQ2_PIG	CD40	Immune and inflammatory response	[33]
sp|O77736_PIG	FAS	Programmed cell death	[34]
sp|Q8HZV3_PIG	TFRC	Uptake cellular iron	[35]
sp|Q1RPR6_PIG	ITGB6	Type of adhesion receptors that function in signaling from the extracellular matrix to the cell	[36]
tr|F1S8A4_PIG	PTPRS	Many cell processes, cell growth, differentiation and mitotic cycle	[37]
tr|A2TEQ2_PIG	prr2	Cell-Cell spreading of virus	[38]
tr|A9LM01_PIG	PGRMC2	Regulated ciliary beat frequency	[39]
tr|F1SI16_PIG	BMPR2	Regulate pulmonary arterial hypertension, right ventricle systolic pressure, vasoconstriction.	[40]
tr|D3K5K6_PIG	EPHB3	Involved in both central and peripheral nervous system	[41]
tr|B2ZI35_PIG	F11R	Promotes proliferation and inhibit apoptosis of gastric cancer	[42]
sp|B2ZHY2_PIG	GPR39	Expressed in kidney, heart and aorta. Improves energy balance, modulate autonerves system, directly act on mycardiocytes .	[43, 44]
tr|B3TFD9_PIG	PRR2	Regulate adhesion and adherence involved in directional motility, proliferation, survival and ocular development.	[45]

5.4. Discussions

To fully understand the function of primary cilia, many studies have used MS technique to identify ciliary proteins [46-48]. Since MudPIT technique is one of the sensitive techniques, Wallace et al first used it on generic mammalian isolated primary cilia for proteomic analysis [49]. In their study, Wallace et al isolated mouse IMCD3 cell line cilia, derived from kidney collecting ducts, by using a modified calcium shock method. They were able to identify 195 potential primary cilia proteins. However, the study failed to detect many known ciliary membrane proteins.

Due to the important of ciliary membrane proteins in many intercellular and extracellular processes, and their association with many ciliopathies disorders, we tested the ability of screening these proteins on isolated LLCPK cell line cilia, by using shear stress method and MudPIT technique. In the study, we identified 19 ciliary proteins, in which 9 of them were ciliary immunoprotiens and 10 of them were ciliary membrane protein receptors, as indicated in table 5.1 and 5.2.

Not surprisingly, some of the newly identified ciliary membrane receptor proteins have effect on cilia function like PGRMC2, PRR2 and BMPR2 proteins. In addition, the newly identified ciliary immunoproteins were also very close in function to the already known localized ciliary immnunoproteins, as shown table 5.3. This further supports our list of ciliary protein findings. All together, our newly identified ciliary proteins can be a useful source for further studies to better understand the importance of these proteins and how they play a role in ciliopathies disorders.

5.5. Limitations

Even though that we were successfully able to test the purity of the isolated cilia lysate, some samples can still have some cytosolic proteins. This can be due the anchored cilia to the cell body, when it is pulled by shear stress force, as it can pull some of the cytosolic protein with it. To over come this issue, isolated cilia pellet was spun two to three time, for 1 hour at 70,000 *g* at 4°C in an ultracentrifuge, each time was resuspended in a PBS buffer. Additional immunoblotting tests were performed to test for impurities. After several MudPIT analyses we were able to limit the interference of the cytosolic proteins in cilia lysate samples.

Acknowledgement

The MudPIT data were obtained in John Yates' laboratory at the Scripps Research Institute, La Jolla, California. This work was supported by the National Institute of Health (R01DK080640 to SMN and F31DK096870 to AMM) and Department of Defense (CDMRP PR130153 to SMN).

Competing financial interests

none

References

1. Dilly, P.N., Further observations of transport within paddle cilia. Cell Tissue Res, 1977. 185(1): p. 105-13.

2. Dilly, P.N., Material transport within specialised ciliary shafts on Rhabdopleura zooids. Cell Tissue Res, 1977. 180(3): p. 367-81.

3. Nauli, S.M., et al., Loss of polycystin-1 in human cyst-lining epithelia leads to ciliary dysfunction. J Am Soc Nephrol, 2006. 17(4): p. 1015-25.

4. Nauli, S.M., et al., Polycystins 1 and 2 mediate mechanosensation in the primary cilium of kidney cells. Nat Genet, 2003. 33(2): p. 129-37.

5. AbouAlaiwi, W.A., et al., Ciliary polycystin-2 is a mechanosensitive calcium channel involved in nitric oxide signaling cascades. Circ Res, 2009. 104(7): p. 860-9.

6. Satir, P., L.B. Pedersen, and S.T. Christensen, The primary cilium at a glance. J Cell Sci, 2010. 123(Pt 4): p. 499-503.

7. Praetorius, H.A. and K.R. Spring, Removal of the MDCK cell primary cilium abolishes flow sensing. J Membr Biol, 2003. 191(1): p. 69-76.

8. Gherman, A., E.E. Davis, and N. Katsanis, The ciliary proteome database: an integrated community resource for the genetic and functional dissection of cilia. Nat Genet, 2006. 38(9): p. 961-2.

9. Francis, S.S., et al., A hierarchy of signals regulates entry of membrane proteins into the ciliary membrane domain in epithelial cells. J Cell Biol, 2011. 193(1): p. 219-33.

10. Yates, J.R., C.I. Ruse, and A. Nakorchevsky, Proteomics by mass spectrometry: approaches, advances, and applications. Annu Rev Biomed Eng, 2009. 11: p. 49-79.

11. Mitchell, K.A., Isolation of primary cilia by shear force. Curr Protoc Cell Biol, 2013. Chapter 3: p. Unit 3 42 1-9.

12. Mohieldin, A.M., et al., Protein composition and movements of membrane swellings associated with primary cilia. Cell Mol Life Sci, 2015.

13. Washburn, M.P., D. Wolters, and J.R. Yates, 3rd, Large-scale analysis of the yeast proteome by multidimensional protein identification technology. Nat Biotechnol, 2001. 19(3): p. 242-7.

14. Martin-Alonso, J.M., et al., Molecular cloning of the bovine CD9 antigen from ocular ciliary epithelial cells. J Biochem, 1992. 112(1): p. 63-7.
15. Matsuda, A., et al., Detection and immunolocalization of macrophage migration inhibitory factor in rat iris and ciliary epithelium. Immunol Lett, 1996. 53(1): p. 1-5.

16. Jersmann, H.P., Time to abandon dogma: CD14 is expressed by non-myeloid lineage cells. Immunol Cell Biol, 2005. 83(5): p. 462-7.

17. Iwanaga, T., Y. Hozumi, and H. Takahashi-Iwanaga, Immunohistochemical demonstration of dopamine receptor D2R in the primary cilia of the mouse pituitary gland. Biomed Res, 2011. 32(3): p. 225-35.

18. Christopher, G.K. and C.A. Sundermann, Isolation and partial characterization of the insulin binding sites of Tetrahymena pyriformis. Biochem Biophys Res Commun, 1995. 212(2): p. 515-23.

19. Al-Jamal, R.T. and T. Kivela, Prognostic associations of insulin-like growth factor-1 receptor in primary uveal melanoma. Can J Ophthalmol, 2011. 46(6): p. 471-6.

20. Yeh, C., et al., IGF-1 activates a cilium-localized noncanonical Gbetagamma signaling pathway that regulates cell-cycle progression. Dev Cell, 2013. 26(4): p. 358-68.

21. Gerdes, D., et al., Cloning and tissue expression of two putative steroid membrane receptors. Biol Chem, 1998. 379(7): p. 907-11.

22. Nutu, M., et al., Distribution and hormonal regulation of membrane progesterone receptors beta and gamma in ciliated epithelial cells of mouse and human fallopian tubes. Reprod Biol Endocrinol, 2009. 7: p. 89.

23. Teilmann, S.C. and S.T. Christensen, Localization of the angiopoietin receptors Tie-1 and Tie-2 on the primary cilia in the female reproductive organs. Cell Biol Int, 2005. 29(5): p. 340-6.

24. Bouley, R., et al., Bypassing vasopressin receptor signaling pathways in nephrogenic diabetes insipidus. Semin Nephrol, 2008. 28(3): p. 266-78.

25. Raychowdhury, M.K., et al., Vasopressin receptor-mediated functional signaling pathway in primary cilia of renal epithelial cells. Am J Physiol Renal Physiol, 2009. 296(1): p. F87-97.

26. Huang, J., et al., BCL10 as a new candidate gene for immune response in pigs: cloning, expression and association analysis. Int J Immunogenet, 2010. 37(2): p. 103-10.

27. Chardon, P., C. Renard, and M. Vaiman, The major histocompatibility complex in swine. Immunol Rev, 1999. 167: p. 179-92.

28. Yamada, Y., et al., [Studies on the concentration of surgical stress-related cytokines in exudate from operative wound or cavity: preliminary report]. Nihon Geka Gakkai Zasshi, 1991. 92(6): p. 760.

29. Pahl, J.H., et al., Expression of the immune regulation antigen CD70 in osteosarcoma. Cancer Cell Int, 2015. 15: p. 31.

30. Gustafsson, K., et al., Structure of miniature swine class II DRB genes: conservation of hypervariable amino acid residues between distantly related mammalian species. Proc Natl Acad Sci U S A, 1990. 87(24): p. 9798-802.

31. Kaur, S., et al., CD47 signaling regulates the immunosuppressive activity of VEGF in T cells. J Immunol, 2014. 193(8): p. 3914-24.

32. Ley, B., K.K. Brown, and H.R. Collard, Molecular biomarkers in idiopathic pulmonary fibrosis. Am J Physiol Lung Cell Mol Physiol, 2014. 307(9): p. L681-91.

33. Zhao, W.Q., et al., CD40 mutant expression and its clinical significance to prognosis in gastric cancer patients. World J Surg Oncol, 2014. 12: p. 167.

34. Wajant, H., The Fas signaling pathway: more than a paradigm. Science, 2002. 296(5573): p. 1635-6.

35. Pham, D.H., et al., Enhanced expression of transferrin receptor 1 contributes to oncogenic signalling by sphingosine kinase 1. Oncogene, 2014. 33(48): p. 5559-68.

36. Wang, S.K., et al., ITGB6 loss-of-function mutations cause autosomal recessive amelogenesis imperfecta. Hum Mol Genet, 2014. 23(8): p. 2157-63.

37. Hobiger, K. and T. Friedrich, Voltage sensitive phosphatases: emerging kinship to protein tyrosine phosphatases from structure-function research. Front Pharmacol, 2015. 6: p. 20.

38. Chengle, H., D. Kaihong, and B. Fuzhi, Association analysis of the poliovirus receptor related-2 gene in patients with nonsyndromic cleft lip with or without cleft palate. DNA Cell Biol, 2010. 29(11): p. 681-5.

39. Wessel, T., U. Schuchter, and H. Walt, Ciliary motility in bovine oviducts for sensing rapid non-genomic reactions upon exposure to progesterone. Horm Metab Res, 2004. 36(3): p. 136-41.

40. West, J., et al., Rescuing the BMPR2 signaling axis in pulmonary arterial hypertension. Drug Discov Today, 2014. 19(8): p. 1241-5.

41. O'Leary, D.D. and D.G. Wilkinson, Eph receptors and ephrins in neural development. Curr Opin Neurobiol, 1999. 9(1): p. 65-73.

42. Ikeo, K., et al., Junctional adhesion molecule-A promotes proliferation and inhibits apoptosis of gastric cancer. Hepatogastroenterology, 2015. 62(138): p. 540-5.

43. Mori, K., et al., Kidney produces a novel acylated peptide, ghrelin. FEBS Lett, 2000. 486(3): p. 213-6.

44. Nagaya, N., et al., Chronic administration of ghrelin improves left ventricular dysfunction and attenuates development of cardiac cachexia in rats with heart failure. Circulation, 2001. 104(12): p. 1430-5.

45. Wang, L., et al., Molecular cloning, characterization and three-dimensional modeling of porcine nectin-2/CD112. Vet Immunol Immunopathol, 2009. 132(2-4): p. 257-63.

46. Mayer, U., et al., Proteomic analysis of a membrane preparation from rat olfactory sensory cilia. Chem Senses, 2008. 33(2): p. 145-62.

47. Liu, Q., et al., The proteome of the mouse photoreceptor sensory cilium complex. Mol Cell Proteomics, 2007. 6(8): p. 1299-317.

48. Mayer, U., et al., The proteome of rat olfactory sensory cilia. Proteomics, 2009. 9(2): p. 322-34.

49. Ishikawa, H., et al., Proteomic analysis of mammalian primary cilia. Curr Biol, 2012. 22(5): p. 414-9.

Chapter 6

Summary

In summary, we showed for the first time that ciliary bulb is actually part of the cilium structure and ciliary bulb can be induced by flow. We were also able to show that Bicc-1 and GM3S are ciliary proteins for the first time and that PC2, Bicc-1, GM3 and GM3S co-localize particularly on ciliary bulb. In addition, based on our protein expression study we proposed a new mechanistic signaling pathway involving PC2, Bicc-1 and GM3S. However, based on our proteomic study, we successfully isolated the primary cilia from LLCPK cell type to identify ciliary proteins, using MutPIT technique for screening. We have Identified 19 new ciliary proteins. Overall, our studies provided important steps to better understand the importance of primary cilia and how they play a role in ciliopathy disorders.

References

Chapter 1

1. P. D. Wilson, Polycystic kidney disease. *The New England journal of medicine* **350**, 151 (Jan 8, 2004).

2. W. E. Braun, Autosomal dominant polycystic kidney disease: emerging concepts of pathogenesis and new treatments. *Cleve Clin J Med* **76**, 97 (Feb, 2009).

3. US Renal Data System: USRDS 2008 Annual Data Report. *The National Institutes of Health, National Institute of Diabetes and Digestive and Kidney Disease* **Bethesda, MD**, (2008).

4. Polycystic kidney disease: the complete structure of the PKD1 gene and its protein. The International Polycystic Kidney Disease Consortium. *Cell* **81**, 289 (Apr 21, 1995).

5. The polycystic kidney disease 1 gene encodes a 14 kb transcript and lies within a duplicated region on chromosome 16. The European Polycystic Kidney Disease Consortium. *Cell* **77**, 881 (Jun 17, 1994).

6. T. Mochizuki *et al.*, PKD2, a gene for polycystic kidney disease that encodes an integral membrane protein. *Science* **272**, 1339 (May 31, 1996).

7. C. J. Ward *et al.*, The gene mutated in autosomal recessive polycystic kidney disease encodes a large, receptor-like protein. *Nature genetics* **30**, 259 (Mar, 2002).

8. V. E. Torres, P. C. Harris, Polycystic kidney disease in 2011: Connecting the dots toward a polycystic kidney disease therapy. *Nature reviews. Nephrology* **8**, 66 (Feb, 2012).

9. P. C. Harris, V. E. Torres, in *GeneReviews,* R. A. Pagon, T. D. Bird, C. R. Dolan, K. Stephens, M. P. Adam, Eds. (Seattle (WA), 1993).

10. P. C. Harris, V. E. Torres, Polycystic kidney disease. *Annual review of medicine* **60**, 321 (2009).
11. S. M. Nauli *et al.*, Loss of polycystin-1 in human cyst-lining epithelia leads to ciliary dysfunction. *Journal of the American Society of Nephrology : JASN* **17**, 1015 (Apr, 2006).

12. S. M. Nauli *et al.*, Polycystins 1 and 2 mediate mechanosensation in the primary cilium of kidney cells. *Nature genetics* **33**, 129 (Feb, 2003).

13. B. K. Yoder, X. Hou, L. M. Guay-Woodford, The polycystic kidney disease proteins, polycystin-1, polycystin-2, polaris, and cystin, are co-localized in renal cilia. *Journal of the American Society of Nephrology : JASN* **13**, 2508 (Oct, 2002).

14. R. Sandford *et al.*, Comparative analysis of the polycystic kidney disease 1 (PKD1) gene reveals an integral membrane glycoprotein with multiple evolutionary conserved domains. *Human molecular genetics* **6**, 1483 (Sep, 1997).

15. J. Hughes *et al.*, The polycystic kidney disease 1 (PKD1) gene encodes a novel protein with multiple cell recognition domains. *Nature genetics* **10**, 151 (Jun, 1995).

16. J. Van Adelsberg, S. Chamberlain, V. D'Agati, Polycystin expression is temporally and spatially regulated during renal development. *The American journal of physiology* **272**, F602 (May, 1997).

17. L. Geng *et al.*, Distribution and developmentally regulated expression of murine polycystin. *The American journal of physiology* **272**, F451 (Apr, 1997).

18. S. Gonzalez-Perrett *et al.*, Polycystin-2, the protein mutated in autosomal dominant polycystic kidney disease (ADPKD), is a Ca2+-permeable nonselective cation channel. *Proceedings of the National Academy of Sciences of the United States of America* **98**, 1182 (Jan 30, 2001).

19. P. Koulen *et al.*, Polycystin-2 is an intracellular calcium release channel. *Nature cell biology* **4**, 191 (Mar, 2002).

20. B. S. Muntean, S. Jin, S. M. Nauli, Primary Cilia are Mechanosensory Organelles with Chemosensory Roles. *Mechanical Stretch and Cytokines, Mechanosensitivity in Cells and Tissues* **5**, 201 (2012).

21. N. B. Gilula, P. Satir, The ciliary necklace. A ciliary membrane specialization. *The Journal of cell biology* **53**, 494 (May, 1972).

22. A. Molla-Herman *et al.*, The ciliary pocket: an endocytic membrane domain at the base of primary and motile cilia. *Journal of cell science* **123**, 1785 (May 15, 2010).

23. H. L. Kee *et al.*, A size-exclusion permeability barrier and nucleoporins characterize a ciliary pore complex that regulates transport into cilia. *Nature cell biology* **14**, 431 (Apr, 2012).

24. R. Rohatgi, W. J. Snell, The ciliary membrane. *Current opinion in cell biology* **22**, 541 (Aug, 2010).

25. S. Wang *et al.*, Fibrocystin/polyductin, found in the same protein complex with polycystin-2, regulates calcium responses in kidney epithelia. *Molecular and cellular biology* **27**, 3241 (Apr, 2007).

26. C. Xu *et al.*, Human ADPKD primary cyst epithelial cells with a novel, single codon deletion in the PKD1 gene exhibit defective ciliary polycystin localization and loss of flow-induced Ca2+ signaling. *American journal of physiology. Renal physiology* **292**, F930 (Mar, 2007).

27. S. H. Low *et al.*, Polycystin-1, STAT6, and P100 function in a pathway that transduces ciliary mechanosensation and is activated in polycystic kidney disease. *Developmental cell* **10**, 57 (Jan, 2006).

28. V. Chauvet *et al.*, Mechanical stimuli induce cleavage and nuclear translocation of the polycystin-1 C terminus. *The Journal of clinical investigation* **114**, 1433 (Nov, 2004).

29. E. Fischer *et al.*, Defective planar cell polarity in polycystic kidney disease. *Nature genetics* **38**, 21 (Jan, 2006).

30. V. Patel *et al.*, Acute kidney injury and aberrant planar cell polarity induce cyst formation in mice lacking renal cilia. *Human molecular genetics* **17**, 1578 (Jun 1, 2008).

31. W. A. AbouAlaiwi, S. Ratnam, R. L. Booth, J. V. Shah, S. M. Nauli, Endothelial cells from humans and mice with polycystic kidney disease are characterized by polyploidy and chromosome segregation defects through survivin down-regulation. *Human molecular genetics* **20**, 354 (Jan 15, 2011).

32. A. Masoumi, B. Reed-Gitomer, C. Kelleher, M. R. Bekheirnia, R. W. Schrier, Developments in the management of autosomal dominant polycystic kidney disease. *Therapeutics and clinical risk management* **4**, 393 (Apr, 2008).

33. K. T. Bae *et al.*, Magnetic resonance imaging evaluation of hepatic cysts in early autosomal-dominant polycystic kidney disease: the Consortium for Radiologic Imaging Studies of Polycystic Kidney Disease cohort. *Clinical journal of the American Society of Nephrology : CJASN* **1**, 64 (Jan, 2006).

34. V. E. Torres, P. C. Harris, Y. Pirson, Autosomal dominant polycystic kidney disease. *Lancet* **369**, 1287 (Apr 14, 2007).

35. S. Abdul-Majeed, S. M. Nauli, Polycystic diseases in visceral organs. *Obstetrics and gynecology international* **2011**, 609370 (2011).

36. J. H. Grendell, T. H. Ermak, Anatomy, histology, embryology, and developmental anomalies ofthe pancreas. *Sleisenger and Fordtran's Gastrointestinal and Liver Disease*, 761 (1998).

37. O. Basar *et al.*, Recurrent pancreatitis in a patient with autosomal-dominant polycystic kidney disease. *Pancreatology* **6**, 160 (2006).

38. R. Torra *et al.*, Ultrasonographic study of pancreatic cysts in autosomal dominant polycystic kidney disease. *Clinical nephrology* **47**, 19 (Jan, 1997).

39. D. A. Cano, N. S. Murcia, G. J. Pazour, M. Hebrok, Orpk mouse model of polycystic kidney disease reveals essential role of primary cilia in pancreatic tissue organization. *Development* **131**, 3457 (Jul, 2004).

40. J. H. Moyer *et al.*, Candidate gene associated with a mutation causing recessive polycystic kidney disease in mice. *Science* **264**, 1329 (May 27, 1994).

41. D. A. Cano, S. Sekine, M. Hebrok, Primary cilia deletion in pancreatic epithelial cells results in cyst formation and pancreatitis. *Gastroenterology* **131**, 1856 (Dec, 2006).

42. S. Y. Li *et al.*, Recurrent retroperitoneal abscess due to perforated colonic diverticulitis in a patient with polycystic kidney disease. *Journal of the Chinese Medical Association : JCMA* **72**, 153 (Mar, 2009).

43. E. D. Lederman, G. McCoy, D. J. Conti, E. C. Lee, Diverticulitis and polycystic kidney disease. *The American surgeon* **66**, 200 (Feb, 2000).

44. E. D. Lederman, D. J. Conti, N. Lempert, T. P. Singh, E. C. Lee, Complicated diverticulitis following renal transplantation. *Diseases of the colon and rectum* **41**, 613 (May, 1998).

45. Z. H. Bajwa, K. A. Sial, A. B. Malik, T. I. Steinman, Pain patterns in patients with polycystic kidney disease. *Kidney international* **66**, 1561 (Oct, 2004).

46. T. Ecder, R. W. Schrier, Cardiovascular abnormalities in autosomal-dominant polycystic kidney disease. *Nature reviews. Nephrology* **5**, 221 (Apr, 2009).

47. G. M. Fick, A. M. Johnson, W. S. Hammond, P. A. Gabow, Causes of death in autosomal dominant polycystic kidney disease. *Journal of the American Society of Nephrology : JASN* **5**, 2048 (Jun, 1995).

48. A. B. Chapman, R. W. Schrier, Pathogenesis of hypertension in autosomal dominant polycystic kidney disease. *Seminars in nephrology* **11**, 653 (Nov, 1991).

49. A. B. Chapman, K. Stepniakowski, F. Rahbari-Oskoui, Hypertension in autosomal dominant polycystic kidney disease. *Advances in chronic kidney disease* **17**, 153 (Mar, 2010).

50. C. L. Kelleher, K. K. McFann, A. M. Johnson, R. W. Schrier, Characteristics of hypertension in young adults with autosomal dominant polycystic kidney disease compared with the general U.S. population. *American journal of hypertension* **17**, 1029 (Nov, 2004).

51. R. W. Schrier, A. M. Johnson, K. McFann, A. B. Chapman, The role of parental hypertension in the frequency and age of diagnosis of hypertension in offspring with autosomal-dominant polycystic kidney disease. *Kidney international* **64**, 1792 (Nov, 2003).

52. S. M. Nauli, X. Jin, B. P. Hierck, The mechanosensory role of primary cilia in vascular hypertension. *International journal of vascular medicine* **2011**, 376281 (2011).

53. M. Y. Chang, A. C. Ong, Endothelin in polycystic kidney disease. *Contributions to nephrology* **172**, 200 (2011).

54. Y. Kawanabe *et al.*, Cilostazol prevents endothelin-induced smooth muscle constriction and proliferation. *PloS one* **7**, e44476 (2012).

55. Y. Kawanabe, S. M. Nauli, Endothelin. *Cellular and molecular life sciences : CMLS* **68**, 195 (Jan, 2011).

56. A. C. Ong *et al.*, An endothelin-1 mediated autocrine growth loop involved in human renal tubular regeneration. *Kidney international* **48**, 390 (Aug, 1995).

57. A. C. Ong *et al.*, Human tubular-derived endothelin in the paracrine regulation of renal interstitial fibroblast function. *Experimental nephrology* **2**, 134 (Mar-Apr, 1994).

58. M. Y. Chang *et al.*, Haploinsufficiency of Pkd2 is associated with increased tubular cell proliferation and interstitial fibrosis in two murine Pkd2 models. *Nephrology, dialysis, transplantation : official publication of the European Dialysis and Transplant Association - European Renal Association* **21**, 2078 (Aug, 2006).

59. B. Hocher *et al.*, Renal endothelin system in polycystic kidney disease. *Journal of the American Society of Nephrology : JASN* **9**, 1169 (Jul, 1998).

60. C. Munemura, J. Uemasu, H. Kawasaki, Epidermal growth factor and endothelin in cyst fluid from autosomal dominant polycystic kidney disease cases: possible evidence of heterogeneity in cystogenesis. *American journal of kidney diseases : the official journal of the National Kidney Foundation* **24**, 561 (Oct, 1994).

61. R. Giusti *et al.*, Plasma concentration of endothelin and arterial pressure in patients with ADPKD. *Contributions to nephrology* **115**, 118 (1995).

62. D. Wang, J. Iversen, S. Strandgaard, Endothelium-dependent relaxation of small resistance vessels is impaired in patients with autosomal dominant polycystic kidney disease. *Journal of the American Society of Nephrology : JASN* **11**, 1371 (Aug, 2000).

63. M. A. Al-Nimri *et al.*, Endothelial-derived vasoactive mediators in polycystic kidney disease. *Kidney international* **63**, 1776 (May, 2003).

64. Y. Ge, P. K. Stricklett, A. K. Hughes, M. Yanagisawa, D. E. Kohan, Collecting duct-specific knockout of the endothelin A receptor alters renal vasopressin responsiveness, but not sodium excretion or blood pressure. *American journal of physiology. Renal physiology* **289**, F692 (Oct, 2005).

65. Y. Ge *et al.*, Collecting duct-specific knockout of endothelin-1 alters vasopressin regulation of urine osmolality. *American journal of physiology. Renal physiology* **288**, F912 (May, 2005).

66. D. E. Kohan, The renal medullary endothelin system in control of sodium and water excretion and systemic blood pressure. *Current opinion in nephrology and hypertension* **15**, 34 (Jan, 2006).

67. V. E. Torres, P. C. Harris, Autosomal dominant polycystic kidney disease: the last 3 years. *Kidney international* **76**, 149 (Jul, 2009).

68. M. Y. Chang, E. Parker, M. El Nahas, J. L. Haylor, A. C. Ong, Endothelin B receptor blockade accelerates disease progression in a murine model of autosomal dominant polycystic kidney disease. *Journal of the American Society of Nephrology : JASN* **18**, 560 (Feb, 2007).

69. R. W. Schrier, Renal volume, renin-angiotensin-aldosterone system, hypertension, and left ventricular hypertrophy in patients with autosomal dominant polycystic kidney disease. *Journal of the American Society of Nephrology : JASN* **20**, 1888 (Sep, 2009).

70. S. Abdul-Majeed, S. M. Nauli, Dopamine receptor type 5 in the primary cilia has dual chemo- and mechano-sensory roles. *Hypertension* **58**, 325 (Aug, 2011).

71. S. Abdul-Majeed, B. C. Moloney, S. M. Nauli, Mechanisms regulating cilia growth and cilia function in endothelial cells. *Cellular and molecular life sciences : CMLS* **69**, 165 (Jan, 2012).

72. W. A. AbouAlaiwi *et al.*, Ciliary polycystin-2 is a mechanosensitive calcium channel involved in nitric oxide signaling cascades. *Circulation research* **104**, 860 (Apr 10, 2009).

73. S. M. Nauli *et al.*, Endothelial cilia are fluid shear sensors that regulate calcium signaling and nitric oxide production through polycystin-1. *Circulation* **117**, 1161 (Mar 4, 2008).

74. A. C. Ong *et al.*, Coordinate expression of the autosomal dominant polycystic kidney disease proteins, polycystin-2 and polycystin-1, in normal and cystic tissue. *The American journal of pathology* **154**, 1721 (Jun, 1999).

75. S. Abdul-Majeed, S. M. Nauli, Calcium-mediated mechanisms of cystic expansion. *Biochimica et biophysica acta* **1812**, 1281 (Oct, 2011).

76. N. Hateboer *et al.*, Location of mutations within the PKD2 gene influences clinical outcome. *Kidney international* **57**, 1444 (Apr, 2000).

77. N. Hateboer *et al.*, Comparison of phenotypes of polycystic kidney disease types 1 and 2. European PKD1-PKD2 Study Group. *Lancet* **353**, 103 (Jan 9, 1999).

78. S. Hassane *et al.*, Pathogenic sequence for dissecting aneurysm formation in a hypomorphic polycystic kidney disease 1 mouse model. *Arteriosclerosis, thrombosis, and vascular biology* **27**, 2177 (Oct, 2007).

79. Z. L. Brookes *et al.*, Pkd2 mesenteric vessels exhibit a primary defect in endothelium-dependent vasodilatation restored by rosiglitazone. *American journal of physiology. Heart and circulatory physiology* **304**, H33 (Jan 1, 2013).

80. P. A. Gabow *et al.*, Renal structure and hypertension in autosomal dominant polycystic kidney disease. *Kidney international* **38**, 1177 (Dec, 1990).

81. M. Loghman-Adham, C. E. Soto, T. Inagami, L. Cassis, The intrarenal renin-angiotensin system in autosomal dominant polycystic kidney disease. *American journal of physiology. Renal physiology* **287**, F775 (Oct, 2004).

82. A. B. Chapman, P. A. Gabow, Hypertension in autosomal dominant polycystic kidney disease. *Kidney international. Supplement* **61**, S71 (Oct, 1997).

83. E. A. McPherson *et al.*, Chymase-like angiotensin II-generating activity in end-stage human autosomal dominant polycystic kidney disease. *Journal of the American Society of Nephrology : JASN* **15**, 493 (Feb, 2004).

84. P. J. Azurmendi *et al.*, Early renal and vascular changes in ADPKD patients with low-grade albumin excretion and normal renal function. *Nephrology, dialysis, transplantation : official publication of the European Dialysis and Transplant Association - European Renal Association* **24**, 2458 (Aug, 2009).

85. C. T. Itty, A. Farshid, G. Talaulikar, Spontaneous coronary artery dissection in a woman with polycystic kidney disease. *American journal of kidney diseases : the official journal of the National Kidney Foundation* **53**, 518 (Mar, 2009).

86. C. Boulter *et al.*, Cardiovascular, skeletal, and renal defects in mice with a targeted disruption of the Pkd1 gene. *Proceedings of the National Academy of Sciences of the United States of America* **98**, 12174 (Oct 9, 2001).

87. M. A. Arnaout, Molecular genetics and pathogenesis of autosomal dominant polycystic kidney disease. *Annual review of medicine* **52**, 93 (2001).

88. J. Neumann, G. Ligtenberg, I. H. Klein, P. J. Blankestijn, Pathogenesis and treatment of hypertension in polycystic kidney disease. *Current opinion in nephrology and hypertension* **11**, 517 (Sep, 2002).

89. I. H. Klein, G. Ligtenberg, P. L. Oey, H. A. Koomans, P. J. Blankestijn, Sympathetic activity is increased in polycystic kidney disease and is associated with hypertension. *Journal of the American Society of Nephrology : JASN* **12**, 2427 (Nov, 2001).

90. R. Zeltner, R. Poliak, B. Stiasny, R. E. Schmieder, B. D. Schulze, Renal and cardiac effects of antihypertensive treatment with ramipril vs metoprolol in autosomal dominant polycystic kidney disease. *Nephrology, dialysis, transplantation : official publication of the European Dialysis and Transplant Association - European Renal Association* **23**, 573 (Feb, 2008).

91. M. J. Koren, R. B. Devereux, P. N. Casale, D. D. Savage, J. H. Laragh, Relation of left ventricular mass and geometry to morbidity and mortality in uncomplicated essential hypertension. *Annals of internal medicine* **114**, 345 (Mar 1, 1991).

92. P. A. Gabow *et al.*, Factors affecting the progression of renal disease in autosomal-dominant polycystic kidney disease. *Kidney international* **41**, 1311 (May, 1992).

93. A. B. Chapman *et al.*, Left ventricular hypertrophy in autosomal dominant polycystic kidney disease. *Journal of the American Society of Nephrology : JASN* **8**, 1292 (Aug, 1997).

94. M. A. Cadnapaphornchai, K. McFann, J. D. Strain, A. Masoumi, R. W. Schrier, Increased left ventricular mass in children with autosomal dominant polycystic

kidney disease and borderline hypertension. *Kidney international* **74**, 1192 (Nov, 2008).

95. A. Bardaji *et al.*, Cardiac involvement in autosomal-dominant polycystic kidney disease: a hypertensive heart disease. *Clinical nephrology* **56**, 211 (Sep, 2001).

96. H. Oflaz *et al.*, Biventricular diastolic dysfunction in patients with autosomal-dominant polycystic kidney disease. *Kidney international* **68**, 2244 (Nov, 2005).

97. P. Verdecchia *et al.*, Circadian blood pressure changes and left ventricular hypertrophy in essential hypertension. *Circulation* **81**, 528 (Feb, 1990).

98. T. C. Li Kam Wa, A. M. Macnicol, M. L. Watson, Ambulatory blood pressure in hypertensive patients with autosomal dominant polycystic kidney disease. *Nephrology, dialysis, transplantation : official publication of the European Dialysis and Transplant Association - European Renal Association* **12**, 2075 (Oct, 1997).

99. F. A. Valero *et al.*, Ambulatory blood pressure and left ventricular mass in normotensive patients with autosomal dominant polycystic kidney disease. *Journal of the American Society of Nephrology : JASN* **10**, 1020 (May, 1999).

100. A. Lumiaho *et al.*, Insulin resistance is related to left ventricular hypertrophy in patients with polycystic kidney disease type 1. *American journal of kidney diseases : the official journal of the National Kidney Foundation* **41**, 1219 (Jun, 2003).

101. G. Lembo *et al.*, Abnormal sympathetic overactivity evoked by insulin in the skeletal muscle of patients with essential hypertension. *The Journal of clinical investigation* **90**, 24 (Jul, 1992).

102. T. Ecder, R. W. Schrier, Hypertension and left ventricular hypertrophy in autosomal dominant polycystic kidney disease. *Expert review of cardiovascular therapy* **2**, 369 (May, 2004).

103. P. M. Ruggieri *et al.*, Occult intracranial aneurysms in polycystic kidney disease: screening with MR angiography. *Radiology* **191**, 33 (Apr, 1994).

104. A. P. Rocchini, C. Moorehead, S. DeRemer, T. L. Goodfriend, D. L. Ball, Hyperinsulinemia and the aldosterone and pressor responses to angiotensin II. *Hypertension* **15**, 861 (Jun, 1990).

105. S. Graf *et al.*, Intracranial aneurysms and dolichoectasia in autosomal dominant polycystic kidney disease. *Nephrology, dialysis, transplantation : official publication of the European Dialysis and Transplant Association - European Renal Association* **17**, 819 (May, 2002).

106. M. M. Belz *et al.*, Recurrence of intracranial aneurysms in autosomal-dominant polycystic kidney disease. *Kidney international* **63**, 1824 (May, 2003).

107. M. M. Belz *et al.*, Familial clustering of ruptured intracranial aneurysms in autosomal dominant polycystic kidney disease. *American journal of kidney diseases : the official journal of the National Kidney Foundation* **38**, 770 (Oct, 2001).

108. H. Hadimeri, C. Lamm, G. Nyberg, Coronary aneurysms in patients with autosomal dominant polycystic kidney disease. *Journal of the American Society of Nephrology : JASN* **9**, 837 (May, 1998).

109. R. Torra *et al.*, Abdominal aortic aneurysms and autosomal dominant polycystic kidney disease. *Journal of the American Society of Nephrology : JASN* **7**, 2483 (Nov, 1996).

110. T. Ecder *et al.*, Reversal of left ventricular hypertrophy with angiotensin converting enzyme inhibition in hypertensive patients with autosomal dominant polycystic kidney disease. *Nephrology, dialysis, transplantation : official publication of the European Dialysis and Transplant Association - European Renal Association* **14**, 1113 (May, 1999).

111. M. Y. Chang, A. C. Ong, Mechanism-based therapeutics for autosomal dominant polycystic kidney disease: recent progress and future prospects. *Nephron. Clinical practice* **120**, c25 (2012).

112. M. Y. Chang, A. C. Ong, New treatments for autosomal dominant polycystic kidney disease. *British journal of clinical pharmacology*, (Apr 18, 2013).

113. G. Aguiari, L. Catizone, L. Del Senno, Multidrug therapy for polycystic kidney disease: a review and perspective. *American journal of nephrology* **37**, 175 (2013).

114. T. Yamaguchi, G. A. Reif, J. P. Calvet, D. P. Wallace, Sorafenib inhibits cAMP-dependent ERK activation, cell proliferation, and in vitro cyst growth of human

ADPKD cyst epithelial cells. *American journal of physiology. Renal physiology* **299**, F944 (Nov, 2010).

115. A. J. Streets, O. Wessely, D. J. Peters, A. C. Ong, Hyperphosphorylation of polycystin-2 at a critical residue in disease reveals an essential role for polycystin-1-regulated dephosphorylation. *Human molecular genetics* **22**, 1924 (May 15, 2013).

116. S. Terryn, A. Ho, R. Beauwens, O. Devuyst, Fluid transport and cystogenesis in autosomal dominant polycystic kidney disease. *Biochimica et biophysica acta* **1812**, 1314 (Oct, 2011).

117. S. Nagao *et al.*, Increased water intake decreases progression of polycystic kidney disease in the PCK rat. *Journal of the American Society of Nephrology : JASN* **17**, 2220 (Aug, 2006).

118. X. Wang, Y. Wu, C. J. Ward, P. C. Harris, V. E. Torres, Vasopressin directly regulates cyst growth in polycystic kidney disease. *Journal of the American Society of Nephrology : JASN* **19**, 102 (Jan, 2008).

119. V. H. Gattone, 2nd, X. Wang, P. C. Harris, V. E. Torres, Inhibition of renal cystic disease development and progression by a vasopressin V2 receptor antagonist. *Nature medicine* **9**, 1323 (Oct, 2003).

120. V. E. Torres *et al.*, Effective treatment of an orthologous model of autosomal dominant polycystic kidney disease. *Nature medicine* **10**, 363 (Apr, 2004).

121. V. H. Gattone, 2nd, R. L. Maser, C. Tian, J. M. Rosenberg, M. G. Branden, Developmental expression of urine concentration-associated genes and their altered expression in murine infantile-type polycystic kidney disease. *Developmental genetics* **24**, 309 (1999).

122. X. Wang, V. Gattone, 2nd, P. C. Harris, V. E. Torres, Effectiveness of vasopressin V2 receptor antagonists OPC-31260 and OPC-41061 on polycystic kidney disease development in the PCK rat. *Journal of the American Society of Nephrology : JASN* **16**, 846 (Apr, 2005).

123. V. E. Torres *et al.*, Tolvaptan in patients with autosomal dominant polycystic kidney disease. *The New England journal of medicine* **367**, 2407 (Dec 20, 2012).

124. C. Boehlke *et al.*, Primary cilia regulate mTORC1 activity and cell size through Lkb1. *Nature cell biology* **12**, 1115 (Nov, 2010).
125. O. Ibraghimov-Beskrovnaya, T. A. Natoli, mTOR signaling in polycystic kidney disease. *Trends in molecular medicine* **17**, 625 (Nov, 2011).

126. C. S. Bonnet *et al.*, Defects in cell polarity underlie TSC and ADPKD-associated cystogenesis. *Human molecular genetics* **18**, 2166 (Jun 15, 2009).

127. J. Huang, C. C. Dibble, M. Matsuzaki, B. D. Manning, The TSC1-TSC2 complex is required for proper activation of mTOR complex 2. *Molecular and cellular biology* **28**, 4104 (Jun, 2008).

128. J. M. Shillingford *et al.*, The mTOR pathway is regulated by polycystin-1, and its inhibition reverses renal cystogenesis in polycystic kidney disease. *Proceedings of the National Academy of Sciences of the United States of America* **103**, 5466 (Apr 4, 2006).

129. M. Wu *et al.*, Everolimus retards cyst growth and preserves kidney function in a rodent model for polycystic kidney disease. *Kidney & blood pressure research* **30**, 253 (2007).

130. P. R. Wahl *et al.*, Inhibition of mTOR with sirolimus slows disease progression in Han:SPRD rats with autosomal dominant polycystic kidney disease (ADPKD). *Nephrology, dialysis, transplantation : official publication of the European Dialysis and Transplant Association - European Renal Association* **21**, 598 (Mar, 2006).

131. G. Walz *et al.*, Everolimus in patients with autosomal dominant polycystic kidney disease. *The New England journal of medicine* **363**, 830 (Aug 26, 2010).

132. A. L. Serra *et al.*, Sirolimus and kidney growth in autosomal dominant polycystic kidney disease. *The New England journal of medicine* **363**, 820 (Aug 26, 2010).

133. N. N. Zheleznova, P. D. Wilson, A. Staruschenko, Epidermal growth factor-mediated proliferation and sodium transport in normal and PKD epithelial cells. *Biochimica et biophysica acta* **1812**, 1301 (Oct, 2011).

134. F. Zeng, A. B. Singh, R. C. Harris, The role of the EGF family of ligands and receptors in renal development, physiology and pathophysiology. *Experimental cell research* **315**, 602 (Feb 15, 2009).

135. F. Zeng, M. Z. Zhang, A. B. Singh, R. Zent, R. C. Harris, ErbB4 isoforms selectively regulate growth factor induced Madin-Darby canine kidney cell tubulogenesis. *Molecular biology of the cell* **18**, 4446 (Nov, 2007).

136. J. Du, P. D. Wilson, Abnormal polarization of EGF receptors and autocrine stimulation of cyst epithelial growth in human ADPKD. *The American journal of physiology* **269**, C487 (Aug, 1995).

137. P. D. Wilson, J. Du, J. T. Norman, Autocrine, endocrine and paracrine regulation of growth abnormalities in autosomal dominant polycystic kidney disease. *European journal of cell biology* **61**, 131 (Jun, 1993).

138. V. E. Torres *et al.*, EGF receptor tyrosine kinase inhibition attenuates the development of PKD in Han:SPRD rats. *Kidney international* **64**, 1573 (Nov, 2003).

139. G. Aguiari *et al.*, Polycystin-1 regulates amphiregulin expression through CREB and AP1 signalling: implications in ADPKD cell proliferation. *J Mol Med (Berl)* **90**, 1267 (Nov, 2012).

140. M. C. Hogan *et al.*, Randomized clinical trial of long-acting somatostatin for autosomal dominant polycystic kidney and liver disease. *Journal of the American Society of Nephrology : JASN* **21**, 1052 (Jun, 2010).

141. T. V. Masyuk, A. I. Masyuk, V. E. Torres, P. C. Harris, N. F. Larusso, Octreotide inhibits hepatic cystogenesis in a rodent model of polycystic liver disease by reducing cholangiocyte adenosine 3',5'-cyclic monophosphate. *Gastroenterology* **132**, 1104 (Mar, 2007).

142. L. van Keimpema *et al.*, Lanreotide reduces the volume of polycystic liver: a randomized, double-blind, placebo-controlled trial. *Gastroenterology* **137**, 1661 (Nov, 2009).

143. N. Perico *et al.*, Sirolimus therapy to halt the progression of ADPKD. *Journal of the American Society of Nephrology : JASN* **21**, 1031 (Jun, 2010).

144. V. E. Torres *et al.*, Analysis of baseline parameters in the HALT polycystic kidney disease trials. *Kidney international* **81**, 577 (Mar, 2012).

145. A. M. Sengul, Y. Altuntas, A. Kurklu, L. Aydin, Beneficial effect of lisinopril plus telmisartan in patients with type 2 diabetes, microalbuminuria and hypertension. *Diabetes research and clinical practice* **71**, 210 (Feb, 2006).

146. M. A. Cadnapaphornchai *et al.*, Effect of statin therapy on disease progression in pediatric ADPKD: design and baseline characteristics of participants. *Contemporary clinical trials* **32**, 437 (May, 2011).

147. R. W. Schrier, Optimal care of autosomal dominant polycystic kidney disease patients. *Nephrology (Carlton)* **11**, 124 (Apr, 2006).

148. J. Elliott, N. N. Zheleznova, P. D. Wilson, c-Src inactivation reduces renal epithelial cell-matrix adhesion, proliferation, and cyst formation. *American journal of physiology. Cell physiology* **301**, C522 (Aug, 2011).

149. S. J. Leuenroth, N. Bencivenga, H. Chahboune, F. Hyder, C. M. Crews, Triptolide reduces cyst formation in a neonatal to adult transition Pkd1 model of ADPKD. *Nephrology, dialysis, transplantation : official publication of the European Dialysis and Transplant Association - European Renal Association* **25**, 2187 (Jul, 2010).

150. S. J. Leuenroth, N. Bencivenga, P. Igarashi, S. Somlo, C. M. Crews, Triptolide reduces cystogenesis in a model of ADPKD. *Journal of the American Society of Nephrology : JASN* **19**, 1659 (Sep, 2008).

151. S. J. Leuenroth *et al.*, Triptolide is a traditional Chinese medicine-derived inhibitor of polycystic kidney disease. *Proceedings of the National Academy of Sciences of the United States of America* **104**, 4389 (Mar 13, 2007).

152. R. J. Kolb, S. M. Nauli, Ciliary dysfunction in polycystic kidney disease: an emerging model with polarizing potential. *Frontiers in bioscience : a journal and virtual library* **13**, 4451 (2008).

153. W. A. Abou Alaiwi, S. T. Lo, S. M. Nauli, Primary cilia: highly sophisticated biological sensors. *Sensors (Basel)* **9**, 7003 (2009).

154. S. Ratnam, S. M. Nauli, Hypertension in Autosomal Dominant Polycystic Kidney Disease: A Clinical and Basic Science Perspective. *Int J Nephrol Urol* **2**, 294 (2010).

Chapter 2

Abdul-Majeed, S., Moloney, B. C. and Nauli, S. M. (2012). Mechanisms regulating cilia growth and cilia function in endothelial cells. *Cell Mol Life Sci* **69**, 165-73.

AbouAlaiwi, W. A., Ratnam, S., Booth, R. L., Shah, J. V. and Nauli, S. M. (2011). Endothelial cells from humans and mice with polycystic kidney disease are characterized by polyploidy and chromosome segregation defects through survivin down-regulation. *Hum Mol Genet* **20**, 354-67.

AbouAlaiwi, W. A., Takahashi, M., Mell, B. R., Jones, T. J., Ratnam, S., Kolb, R. J. and Nauli, S. M. (2009). Ciliary polycystin-2 is a mechanosensitive calcium channel involved in nitric oxide signaling cascades. *Circ Res* **104**, 860-9.

Albrecht-Buehler, G. and Bushnell, A. (1980). The ultrastructure of primary cilia in quiescent 3T3 cells. *Exp Cell Res* **126**, 427-37.

Berselli, P., Zava, S., Sottocornola, E., Milani, S., Berra, B. and Colombo, I. (2006). Human GM3 synthase: a new mRNA variant encodes an NH2-terminal extended form of the protein. *Biochim Biophys Acta* **1759**, 348-58.

Cai, Y., Maeda, Y., Cedzich, A., Torres, V. E., Wu, G., Hayashi, T., Mochizuki, T., Park, J. H., Witzgall, R. and Somlo, S. (1999). Identification and characterization of polycystin-2, the PKD2 gene product. *J Biol Chem* **274**, 28557-65.

Cano, D. A., Murcia, N. S., Pazour, G. J. and Hebrok, M. (2004). Orpk mouse model of polycystic kidney disease reveals essential role of primary cilia in pancreatic tissue organization. *Development* **131**, 3457-67.

Cano, D. A., Sekine, S. and Hebrok, M. (2006). Primary cilia deletion in pancreatic epithelial cells results in cyst formation and pancreatitis. *Gastroenterology* **131**, 1856-69.

Dalen, H. (1981). An ultrastructural study of primary cilia, abnormal cilia and ciliary knobs from the ciliated cells of the guinea-pig trachea. *Cell Tissue Res* **220**, 685-97.

Delaine-Smith, R. M., Sittichokechaiwut, A. and Reilly, G. C. (2014). Primary cilia respond to fluid shear stress and mediate flow-induced calcium deposition in osteoblasts. *FASEB J* **28**, 430-9.

Dilly, P. N. (1977a). Further observations of transport within paddle cilia. *Cell Tissue Res* **185**, 105-13.

Dilly, P. N. (1977b). Material transport within specialised ciliary shafts on Rhabdopleura zooids. *Cell Tissue Res* **180**, 367-81.

Ehlers, U. and Ehlers, B. (1978). Paddle cilia and discocilia - genuine structures? Observations on cilia of sensory cells in marine turbellaria. *Cell Tissue Res* **192**, 489-501.

Elofsson, R., Andersson, A., Falck, B. and Sjoborg, S. (1984). The ciliated human keratinocyte. *J Ultrastruct Res* **87**, 212-20.

Gilula, N. B. and Satir, P. (1972). The ciliary necklace. A ciliary membrane specialization. *J Cell Biol* **53**, 494-509.

Harduin-Lepers, A., Mollicone, R., Delannoy, P. and Oriol, R. (2005). The animal sialyltransferases and sialyltransferase-related genes: a phylogenetic approach. *Glycobiology* **15**, 805-17.

Hidaka, S., Konecke, V., Osten, L. and Witzgall, R. (2004). PIGEA-14, a novel coiled-coil protein affecting the intracellular distribution of polycystin-2. *J Biol Chem* **279**, 35009-16.

Ishii, A., Ohta, M., Watanabe, Y., Matsuda, K., Ishiyama, K., Sakoe, K., Nakamura, M., Inokuchi, J., Sanai, Y. and Saito, M. (1998). Expression cloning and functional characterization of human cDNA for ganglioside GM3 synthase. *J Biol Chem* **273**, 31652-5.

Janich, P. and Corbeil, D. (2007). GM1 and GM3 gangliosides highlight distinct lipid microdomains within the apical domain of epithelial cells. *FEBS Lett* **581**, 1783-7.

Jensen, C. G., Davison, E. A., Bowser, S. S. and Rieder, C. L. (1987). Primary cilia cycle in PtK1 cells: effects of colcemid and taxol on cilia formation and resorption. *Cell Motil Cytoskeleton* **7**, 187-97.

Jensen, C. G., Jensen, L. C. and Rieder, C. L. (1979). The occurrence and structure of primary cilia in a subline of Potorous tridactylus. *Exp Cell Res* **123**, 444-9.

Jin, X., Mohieldin, A. M., Muntean, B. S., Green, J. A., Shah, J. V., Mykytyn, K. and Nauli, S. M. (2014). Cilioplasm is a cellular compartment for calcium signaling in response to mechanical and chemical stimuli. *Cell Mol Life Sci* **71**, 2165-78.

Koulen, P., Cai, Y., Geng, L., Maeda, Y., Nishimura, S., Witzgall, R., Ehrlich, B. E. and Somlo, S. (2002). Polycystin-2 is an intracellular calcium release channel. *Nat Cell Biol* **4**, 191-7.

Liu, W., Murcia, N. S., Duan, Y., Weinbaum, S., Yoder, B. K., Schwiebert, E. and Satlin, L. M. (2005). Mechanoregulation of intracellular Ca2+ concentration is attenuated in collecting duct of monocilium-impaired orpk mice. *Am J Physiol Renal Physiol* **289**, F978-88.

Mahone, M., Saffman, E. E. and Lasko, P. F. (1995). Localized Bicaudal-C RNA encodes a protein containing a KH domain, the RNA binding motif of FMR1. *EMBO J* **14**, 2043-55.

Masyuk, A. I., Masyuk, T. V., Splinter, P. L., Huang, B. Q., Stroope, A. J. and LaRusso, N. F. (2006). Cholangiocyte cilia detect changes in luminal fluid flow and transmit them into intracellular Ca2+ and cAMP signaling. *Gastroenterology* **131**, 911-20.

Matera, E. M. and Davis, W. J. (1982). Paddle cilia (discocilia) in chemosensitive structures of the gastropod mollusk Pleurobranchaea californica. *Cell Tissue Res* **222**, 25-40.

McGrath, J., Somlo, S., Makova, S., Tian, X. and Brueckner, M. (2003). Two populations of node monocilia initiate left-right asymmetry in the mouse. *Cell* **114**, 61-73.

Mitchell, K. A. (2013). Isolation of primary cilia by shear force. *Curr Protoc Cell Biol* **Chapter 3**, Unit 3 42 1-9.

Nauli, S. M., Alenghat, F. J., Luo, Y., Williams, E., Vassilev, P., Li, X., Elia, A. E., Lu, W., Brown, E. M., Quinn, S. J. et al. (2003). Polycystins 1 and 2 mediate mechanosensation in the primary cilium of kidney cells. *Nat Genet* **33**, 129-37.

Nauli, S. M., Kawanabe, Y., Kaminski, J. J., Pearce, W. J., Ingber, D. E. and Zhou, J. (2008). Endothelial cilia are fluid shear sensors that regulate calcium signaling and nitric oxide production through polycystin-1. *Circulation* **117**, 1161-71.

Nauli, S. M., Rossetti, S., Kolb, R. J., Alenghat, F. J., Consugar, M. B., Harris, P. C., Ingber, D. E., Loghman-Adham, M. and Zhou, J. (2006). Loss of polycystin-1 in human cyst-lining epithelia leads to ciliary dysfunction. *J Am Soc Nephrol* **17**, 1015-25.

Pazour, G. J., San Agustin, J. T., Follit, J. A., Rosenbaum, J. L. and Witman, G. B. (2002). Polycystin-2 localizes to kidney cilia and the ciliary level is elevated in orpk mice with polycystic kidney disease. *Curr Biol* **12**, R378-80.

Praetorius, H. A. and Spring, K. R. (2001). Bending the MDCK cell primary cilium increases intracellular calcium. *J Membr Biol* **184**, 71-9.

Qiu, N., Xiao, Z., Cao, L., Buechel, M. M., David, V., Roan, E. and Quarles, L. D. (2012). Disruption of Kif3a in osteoblasts results in defective bone formation and osteopenia. *J Cell Sci* **125**, 1945-57.

Roth, K. E., Rieder, C. L. and Bowser, S. S. (1988). Flexible-substratum technique for viewing cells from the side: some in vivo properties of primary (9+0) cilia in cultured kidney epithelia. *J Cell Sci* **89 (Pt 4)**, 457-66.

Rydholm, S., Zwartz, G., Kowalewski, J. M., Kamali-Zare, P., Frisk, T. and Brismar, H. (2010). Mechanical properties of primary cilia regulate the response to fluid flow. *Am J Physiol Renal Physiol* **298**, F1096-102.

Saffman, E. E., Styhler, S., Rother, K., Li, W., Richard, S. and Lasko, P. (1998). Premature translation of oskar in oocytes lacking the RNA-binding protein bicaudal-C. *Mol Cell Biol* **18**, 4855-62.

Seyfried, T. N., Ando, S. and Yu, R. K. (1978). Isolation and characterization of human liver hematoside. *J Lipid Res* **19**, 538-43.

Siroky, B. J., Ferguson, W. B., Fuson, A. L., Xie, Y., Fintha, A., Komlosi, P., Yoder, B. K., Schwiebert, E. M., Guay-Woodford, L. M. and Bell, P. D. (2006). Loss of primary cilia results in deregulated and unabated apical calcium entry in ARPKD collecting duct cells. *Am J Physiol Renal Physiol* **290**, F1320-8.

Su, S., Phua, S. C., DeRose, R., Chiba, S., Narita, K., Kalugin, P. N., Katada, T., Kontani, K., Takeda, S. and Inoue, T. (2013). Genetically encoded calcium indicator illuminates calcium dynamics in primary cilia. *Nat Methods* **10**, 1105-7.

Tobin, J. L. and Beales, P. L. (2009). The nonmotile ciliopathies. *Genet Med* **11**, 386-402.

Tran, U., Zakin, L., Schweickert, A., Agrawal, R., Doger, R., Blum, M., De Robertis, E. M. and Wessely, O. (2010). The RNA-binding protein bicaudal C regulates polycystin 2 in the kidney by antagonizing miR-17 activity. *Development* **137**, 1107-16.

Wang, L., Eckmann, C. R., Kadyk, L. C., Wickens, M. and Kimble, J. (2002). A regulatory cytoplasmic poly(A) polymerase in Caenorhabditis elegans. *Nature* **419**, 312-6.

Xu, C., Rossetti, S., Jiang, L., Harris, P. C., Brown-Glaberman, U., Wandinger-Ness, A., Bacallao, R. and Alper, S. L. (2007). Human ADPKD primary cyst epithelial cells with a novel, single codon deletion in the PKD1 gene exhibit defective ciliary polycystin localization and loss of flow-induced Ca2+ signaling. *Am J Physiol Renal Physiol* **292**, F930-45.

Yoder, B. K., Hou, X. and Guay-Woodford, L. M. (2002). The polycystic kidney disease proteins, polycystin-1, polycystin-2, polaris, and cystin, are co-localized in renal cilia. *J Am Soc Nephrol* **13**, 2508-16.

Yoshiba, S., Shiratori, H., Kuo, I. Y., Kawasumi, A., Shinohara, K., Nonaka, S., Asai, Y., Sasaki, G., Belo, J. A., Sasaki, H. et al. (2012). Cilia at the node of mouse embryos sense fluid flow for left-right determination via Pkd2. *Science* **338**, 226-31.

Chapter 3

Abdul-Majeed, S., Moloney, B. C. and Nauli, S. M. (2012). Mechanisms regulating cilia growth and cilia function in endothelial cells. *Cell Mol Life Sci* **69**, 165-73.

AbouAlaiwi, W. A., Ratnam, S., Booth, R. L., Shah, J. V. and Nauli, S. M. (2011). Endothelial cells from humans and mice with polycystic kidney disease are characterized by polyploidy and chromosome segregation defects through survivin down-regulation. *Hum Mol Genet* **20**, 354-67.

AbouAlaiwi, W. A., Takahashi, M., Mell, B. R., Jones, T. J., Ratnam, S., Kolb, R. J. and Nauli, S. M. (2009). Ciliary polycystin-2 is a mechanosensitive calcium channel involved in nitric oxide signaling cascades. *Circ Res* **104**, 860-9.

Albrecht-Buehler, G. and Bushnell, A. (1980). The ultrastructure of primary cilia in quiescent 3T3 cells. *Exp Cell Res* **126**, 427-37.

Berselli, P., Zava, S., Sottocornola, E., Milani, S., Berra, B. and Colombo, I. (2006). Human GM3 synthase: a new mRNA variant encodes an NH2-terminal extended form of the protein. *Biochim Biophys Acta* **1759**, 348-58.

Cai, Y., Maeda, Y., Cedzich, A., Torres, V. E., Wu, G., Hayashi, T., Mochizuki, T., Park, J. H., Witzgall, R. and Somlo, S. (1999). Identification and characterization of polycystin-2, the PKD2 gene product. *J Biol Chem* **274**, 28557-65.

Cano, D. A., Murcia, N. S., Pazour, G. J. and Hebrok, M. (2004). Orpk mouse model of polycystic kidney disease reveals essential role of primary cilia in pancreatic tissue organization. *Development* **131**, 3457-67.

Cano, D. A., Sekine, S. and Hebrok, M. (2006). Primary cilia deletion in pancreatic epithelial cells results in cyst formation and pancreatitis. *Gastroenterology* **131**, 1856-69.

Dalen, H. (1981). An ultrastructural study of primary cilia, abnormal cilia and ciliary knobs from the ciliated cells of the guinea-pig trachea. *Cell Tissue Res* **220**, 685-97.

Delaine-Smith, R. M., Sittichokechaiwut, A. and Reilly, G. C. (2014). Primary cilia respond to fluid shear stress and mediate flow-induced calcium deposition in osteoblasts. *FASEB J* **28**, 430-9.

Dilly, P. N. (1977a). Further observations of transport within paddle cilia. *Cell Tissue Res* **185**, 105-13.

Dilly, P. N. (1977b). Material transport within specialised ciliary shafts on Rhabdopleura zooids. *Cell Tissue Res* **180**, 367-81.

Ehlers, U. and Ehlers, B. (1978). Paddle cilia and discocilia - genuine structures? Observations on cilia of sensory cells in marine turbellaria. *Cell Tissue Res* **192**, 489-501.

Elofsson, R., Andersson, A., Falck, B. and Sjoborg, S. (1984). The ciliated human keratinocyte. *J Ultrastruct Res* **87**, 212-20.

Gilula, N. B. and Satir, P. (1972). The ciliary necklace. A ciliary membrane specialization. *J Cell Biol* **53**, 494-509.

Harduin-Lepers, A., Mollicone, R., Delannoy, P. and Oriol, R. (2005). The animal sialyltransferases and sialyltransferase-related genes: a phylogenetic approach. *Glycobiology* **15**, 805-17.

Hidaka, S., Konecke, V., Osten, L. and Witzgall, R. (2004). PIGEA-14, a novel coiled-coil protein affecting the intracellular distribution of polycystin-2. *J Biol Chem* **279**, 35009-16.

Ishii, A., Ohta, M., Watanabe, Y., Matsuda, K., Ishiyama, K., Sakoe, K., Nakamura, M., Inokuchi, J., Sanai, Y. and Saito, M. (1998). Expression cloning and functional characterization of human cDNA for ganglioside GM3 synthase. *J Biol Chem* **273**, 31652-5.

Janich, P. and Corbeil, D. (2007). GM1 and GM3 gangliosides highlight distinct lipid microdomains within the apical domain of epithelial cells. *FEBS Lett* **581**, 1783-7.

Jensen, C. G., Davison, E. A., Bowser, S. S. and Rieder, C. L. (1987). Primary cilia cycle in PtK1 cells: effects of colcemid and taxol on cilia formation and resorption. *Cell Motil Cytoskeleton* **7**, 187-97.

Jensen, C. G., Jensen, L. C. and Rieder, C. L. (1979). The occurrence and structure of primary cilia in a subline of Potorous tridactylus. *Exp Cell Res* **123**, 444-9.

Jin, X., Mohieldin, A. M., Muntean, B. S., Green, J. A., Shah, J. V., Mykytyn, K. and Nauli, S. M. (2014). Cilioplasm is a cellular compartment for calcium signaling in response to mechanical and chemical stimuli. *Cell Mol Life Sci* **71**, 2165-78.

Koulen, P., Cai, Y., Geng, L., Maeda, Y., Nishimura, S., Witzgall, R., Ehrlich, B. E. and Somlo, S. (2002). Polycystin-2 is an intracellular calcium release channel. *Nat Cell Biol* **4**, 191-7.

Liu, W., Murcia, N. S., Duan, Y., Weinbaum, S., Yoder, B. K., Schwiebert, E. and Satlin, L. M. (2005). Mechanoregulation of intracellular Ca2+ concentration is

attenuated in collecting duct of monocilium-impaired orpk mice. *Am J Physiol Renal Physiol* **289**, F978-88.

Mahone, M., Saffman, E. E. and Lasko, P. F. (1995). Localized Bicaudal-C RNA encodes a protein containing a KH domain, the RNA binding motif of FMR1. *EMBO J* **14**, 2043-55.

Masyuk, A. I., Masyuk, T. V., Splinter, P. L., Huang, B. Q., Stroope, A. J. and LaRusso, N. F. (2006). Cholangiocyte cilia detect changes in luminal fluid flow and transmit them into intracellular Ca2+ and cAMP signaling. *Gastroenterology* **131**, 911-20.

Matera, E. M. and Davis, W. J. (1982). Paddle cilia (discocilia) in chemosensitive structures of the gastropod mollusk Pleurobranchaea californica. *Cell Tissue Res* **222**, 25-40.

McGrath, J., Somlo, S., Makova, S., Tian, X. and Brueckner, M. (2003). Two populations of node monocilia initiate left-right asymmetry in the mouse. *Cell* **114**, 61-73.

Mitchell, K. A. (2013). Isolation of primary cilia by shear force. *Curr Protoc Cell Biol* **Chapter 3**, Unit 3 42 1-9.

Nauli, S. M., Alenghat, F. J., Luo, Y., Williams, E., Vassilev, P., Li, X., Elia, A. E., Lu, W., Brown, E. M., Quinn, S. J. et al. (2003). Polycystins 1 and 2 mediate mechanosensation in the primary cilium of kidney cells. *Nat Genet* **33**, 129-37.

Nauli, S. M., Kawanabe, Y., Kaminski, J. J., Pearce, W. J., Ingber, D. E. and Zhou, J. (2008). Endothelial cilia are fluid shear sensors that regulate calcium signaling and nitric oxide production through polycystin-1. *Circulation* **117**, 1161-71.

Nauli, S. M., Rossetti, S., Kolb, R. J., Alenghat, F. J., Consugar, M. B., Harris, P. C., Ingber, D. E., Loghman-Adham, M. and Zhou, J. (2006). Loss of polycystin-1 in human cyst-lining epithelia leads to ciliary dysfunction. *J Am Soc Nephrol* **17**, 1015-25.

Pazour, G. J., San Agustin, J. T., Follit, J. A., Rosenbaum, J. L. and Witman, G. B. (2002). Polycystin-2 localizes to kidney cilia and the ciliary level is elevated in orpk mice with polycystic kidney disease. *Curr Biol* **12**, R378-80.

Praetorius, H. A. and Spring, K. R. (2001). Bending the MDCK cell primary cilium increases intracellular calcium. *J Membr Biol* **184**, 71-9.

Qiu, N., Xiao, Z., Cao, L., Buechel, M. M., David, V., Roan, E. and Quarles, L. D. (2012). Disruption of Kif3a in osteoblasts results in defective bone formation and osteopenia. *J Cell Sci* **125**, 1945-57.

Roth, K. E., Rieder, C. L. and Bowser, S. S. (1988). Flexible-substratum technique for viewing cells from the side: some in vivo properties of primary (9+0) cilia in cultured kidney epithelia. *J Cell Sci* **89 (Pt 4)**, 457-66.

Rydholm, S., Zwartz, G., Kowalewski, J. M., Kamali-Zare, P., Frisk, T. and Brismar, H. (2010). Mechanical properties of primary cilia regulate the response to fluid flow. *Am J Physiol Renal Physiol* **298**, F1096-102.

Saffman, E. E., Styhler, S., Rother, K., Li, W., Richard, S. and Lasko, P. (1998). Premature translation of oskar in oocytes lacking the RNA-binding protein bicaudal-C. *Mol Cell Biol* **18**, 4855-62.

Seyfried, T. N., Ando, S. and Yu, R. K. (1978). Isolation and characterization of human liver hematoside. *J Lipid Res* **19**, 538-43.

Siroky, B. J., Ferguson, W. B., Fuson, A. L., Xie, Y., Fintha, A., Komlosi, P., Yoder, B. K., Schwiebert, E. M., Guay-Woodford, L. M. and Bell, P. D. (2006). Loss of primary cilia results in deregulated and unabated apical calcium entry in ARPKD collecting duct cells. *Am J Physiol Renal Physiol* **290**, F1320-8.

Su, S., Phua, S. C., DeRose, R., Chiba, S., Narita, K., Kalugin, P. N., Katada, T., Kontani, K., Takeda, S. and Inoue, T. (2013). Genetically encoded calcium indicator illuminates calcium dynamics in primary cilia. *Nat Methods* **10**, 1105-7.

Tobin, J. L. and Beales, P. L. (2009). The nonmotile ciliopathies. *Genet Med* **11**, 386-402.

Tran, U., Zakin, L., Schweickert, A., Agrawal, R., Doger, R., Blum, M., De Robertis, E. M. and Wessely, O. (2010). The RNA-binding protein bicaudal C regulates polycystin 2 in the kidney by antagonizing miR-17 activity. *Development* **137**, 1107-16.

Wang, L., Eckmann, C. R., Kadyk, L. C., Wickens, M. and Kimble, J. (2002). A regulatory cytoplasmic poly(A) polymerase in Caenorhabditis elegans. *Nature* **419**, 312-6.

Xu, C., Rossetti, S., Jiang, L., Harris, P. C., Brown-Glaberman, U., Wandinger-Ness, A., Bacallao, R. and Alper, S. L. (2007). Human ADPKD primary cyst epithelial cells with a novel, single codon deletion in the PKD1 gene exhibit defective ciliary polycystin localization and loss of flow-induced Ca2+ signaling. *Am J Physiol Renal Physiol* **292**, F930-45.

Yoder, B. K., Hou, X. and Guay-Woodford, L. M. (2002). The polycystic kidney disease proteins, polycystin-1, polycystin-2, polaris, and cystin, are co-localized in renal cilia. *J Am Soc Nephrol* **13**, 2508-16.

Yoshiba, S., Shiratori, H., Kuo, I. Y., Kawasumi, A., Shinohara, K., Nonaka, S., Asai, Y., Sasaki, G., Belo, J. A., Sasaki, H. et al. (2012). Cilia at the node of mouse embryos sense fluid flow for left-right determination via Pkd2. *Science* **338**, 226-31.

Chapter 3

1. Tobin, J.L. and P.L. Beales, *The nonmotile ciliopathies.* Genetics in Medicine, 2009. **11**(6): p. 386-402.

2. Roth, K.E., C.L. Rieder, and S.S. Bowser, *Flexible-substratum technique for viewing cells from the side: some in vivo properties of primary (9+0) cilia in cultured kidney epithelia.* J Cell Sci, 1988. **89 (Pt 4)**: p. 457-66.

3. Garcia-Gonzalo, F.R. and J.F. Reiter, *Scoring a backstage pass: mechanisms of ciliogenesis and ciliary access.* J Cell Biol, 2012. **197**(6): p. 697-709.

4. Gilula, N.B. and P. Satir, *The ciliary necklace. A ciliary membrane specialization.* J Cell Biol, 1972. **53**(2): p. 494-509.

5. Jin, X., et al., *Cilioplasm is a cellular compartment for calcium signaling in response to mechanical and chemical stimuli.* Cell Mol Life Sci, 2014. **71**(11): p. 2165-78.

6. Scherft, J.P. and W.T. Daems, *Single cilia in chondrocytes.* J Ultrastruct Res, 1967. **19**(5): p. 546-55.

7. AbouAlaiwi, W.A., A.M. Nauli, and S.M. Nauli, *Deciphering mechanosensory function of primary cilia in cardiovascular system.* Transworld Research Network Publisher, 2010. **Chapter 2**: p. 25-37.

8. Muntean, B.S., X. Jin, and S.M. Nauli, *Primary cilia are mechanosensory organelles with chemosensory roles.* Springer Publisher, 2012. **Chapter 9**: p. 201-22.

9. Nauli, S.M., *Primary cilia are mechanosensory organelles in vascular tissues.* Proceedings of the 15th World Congress on Heart Disease, 2011: p. 23-6.

10. Nauli, S.M., et al., *Primary Cilia are Mechanosensory Organelles in Vestibular Tissues.* Springer Publisher, 2010. **Chapter 14**: p. 317-50.

11. Nauli, S.M., X. Jin, and B.P. Hierck, *The mechanosensory role of primary cilia in vascular hypertension.* Int J Vasc Med, 2011. **2011**: p. 376281.

12. Abdul-Majeed, S. and S.M. Nauli, *Calcium-mediated mechanisms of cystic expansion.* Biochim Biophys Acta, 2011. **1812**(10): p. 1281-90.

13. Nauli, S.M. and J. Zhou, *Polycystins and mechanosensation in renal and nodal cilia.* Bioessays, 2004. **26**(8): p. 844-56.

14. AbouAlaiwi, W.A., et al., *Ciliary polycystin-2 is a mechanosensitive calcium channel involved in nitric oxide signaling cascades.* Circ Res, 2009. **104**(7): p. 860-9.

15. Praetorius, H.A. and K.R. Spring, *Bending the MDCK cell primary cilium increases intracellular calcium.* J Membr Biol, 2001. **184**(1): p. 71-9.

16. Satir, P., L.B. Pedersen, and S.T. Christensen, *The primary cilium at a glance.* J Cell Sci, 2010. **123**(Pt 4): p. 499-503.

17. AbouAlaiwi, W.A., et al., *Endothelial cells from humans and mice with polycystic kidney disease are characterized by polyploidy and chromosome segregation defects through survivin down-regulation.* Hum Mol Genet, 2011. **20**(2): p. 354-67.

18. AbouAlaiwi, W.A., et al., *Ciliary Polycystin-2 Is a Mechanosensitive Calcium Channel Involved in Nitric Oxide Signaling Cascades.* Circulation Research, 2009. **104**(7): p. 860-869.

19. Mohieldin, A.M., et al., *Protein composition and movements of membrane swellings associated with primary cilia.* Cell Mol Life Sci, 2015. **72**(12): p. 2415-29.

20. Berselli, P., et al., *Human GM3 synthase: a new mRNA variant encodes an NH2-terminal extended form of the protein.* Biochim Biophys Acta, 2006. **1759**(7): p. 348-58.

21. Nauli, S.M., et al., *Polycystins 1 and 2 mediate mechanosensation in the primary cilium of kidney cells.* Nat Genet, 2003. **33**(2): p. 129-37.

22. Masyuk, A.I., et al., *Cholangiocyte cilia detect changes in luminal fluid flow and transmit them into intracellular Ca2+ and cAMP signaling.* Gastroenterology, 2006. **131**(3): p. 911-20.

23. Delaine-Smith, R.M., A. Sittichokechaiwut, and G.C. Reilly, *Primary cilia respond to fluid shear stress and mediate flow-induced calcium deposition in osteoblasts.* FASEB J, 2014. **28**(1): p. 430-9.

24. McGrath, J., et al., *Two populations of node monocilia initiate left-right asymmetry in the mouse.* Cell, 2003. **114**(1): p. 61-73.

25. Cano, D.A., et al., *Orpk mouse model of polycystic kidney disease reveals essential role of primary cilia in pancreatic tissue organization.* Development, 2004. **131**(14): p. 3457-67.
26. Giles, R.H., H. Ajzenberg, and P.K. Jackson, *3D spheroid model of mIMCD3 cells for studying ciliopathies and renal epithelial disorders.* Nat Protoc, 2014. **9**(12): p. 2725-31.

27. Aboualaiwi, W.A., et al., *Survivin-induced abnormal ploidy contributes to cystic kidney and aneurysm formation.* Circulation, 2014. **129**(6): p. 660-72.

28. Nauli, S.M., et al., *Loss of polycystin-1 in human cyst-lining epithelia leads to ciliary dysfunction.* J Am Soc Nephrol, 2006. **17**(4): p. 1015-25.

Chapter 4

1. Gilula, N.B. & Satir, P. The ciliary necklace. A ciliary membrane specialization. *J Cell Biol* **53**, 494-509 (1972).

2. Jin, X. *et al.* Cilioplasm is a cellular compartment for calcium signaling in response to mechanical and chemical stimuli. *Cell Mol Life Sci* **71**, 2165-78 (2014).

3. Dilly, P.N. Material transport within specialised ciliary shafts on Rhabdopleura zooids. *Cell Tissue Res* **180**, 367-81 (1977).

4. Roth, K.E., Rieder, C.L. & Bowser, S.S. Flexible-substratum technique for viewing cells from the side: some in vivo properties of primary (9+0) cilia in cultured kidney epithelia. *J Cell Sci* **89 (Pt 4)**, 457-66 (1988).

5. Beninger, P.G., Potter, T.M. & Stjean, S.D. Paddle cilia fixation artifacts in pallial organs of adult Mytilus edulis and Placopecten magennanicus. *Canadian J Zool* **73**, 610-14 (1995).

6. Short, G. & Tamm, S.L. On the nature of paddle cilia and discocilia. *Biol Bull* **180**, 466-74 (1991).

7. Mohieldin, A.M. *et al.* Protein composition and movements of membrane swellings associated with primary cilia. *Cell Mol Life Sci* (2015).

8. Meryman, H.T. Replication of frozen liquids by vacuum evaporation. *Journal of Applied Physics (abstr.)* **21**, 68 (1950).

9. Hall, C.E. A low temperature replica method for electron micro-scopy. *Journal of Applied Physics* **21**, 61-2 (1950).

10. Meyer, H.W. & Richter, W. Freeze-fracture studies on lipids and membranes. *Micron* **32**, 615-44 (2001).

11. Moor, H. Endoplasmic reticulum as the initiator of bud formation in yeast (S. cerevisiae). *Arch Mikrobiol* **57**, 135-46 (1967).

12. Moor, H. & Muhlethaler, K. Fine Structure in Frozen-Etched Yeast Cells. *J Cell Biol* **17**, 609-28 (1963).

13. Gao, M. *et al.* Direct observation of liquid crystals using cryo-TEM: specimen preparation and low-dose imaging. *Microsc Res Tech* **77**, 754-72 (2014).

Chapter 5

1. Dilly, P.N., Further observations of transport within paddle cilia. Cell Tissue Res, 1977. 185(1): p. 105-13.

2. Dilly, P.N., Material transport within specialised ciliary shafts on Rhabdopleura zooids. Cell Tissue Res, 1977. 180(3): p. 367-81.

3. Nauli, S.M., et al., Loss of polycystin-1 in human cyst-lining epithelia leads to ciliary dysfunction. J Am Soc Nephrol, 2006. 17(4): p. 1015-25.

4. Nauli, S.M., et al., Polycystins 1 and 2 mediate mechanosensation in the primary cilium of kidney cells. Nat Genet, 2003. 33(2): p. 129-37.

5. AbouAlaiwi, W.A., et al., Ciliary polycystin-2 is a mechanosensitive calcium channel involved in nitric oxide signaling cascades. Circ Res, 2009. 104(7): p. 860-9.

6. Satir, P., L.B. Pedersen, and S.T. Christensen, The primary cilium at a glance. J Cell Sci, 2010. 123(Pt 4): p. 499-503.

7. Praetorius, H.A. and K.R. Spring, Removal of the MDCK cell primary cilium abolishes flow sensing. J Membr Biol, 2003. 191(1): p. 69-76.

8. Gherman, A., E.E. Davis, and N. Katsanis, The ciliary proteome database: an integrated community resource for the genetic and functional dissection of cilia. Nat Genet, 2006. 38(9): p. 961-2.

9. Francis, S.S., et al., A hierarchy of signals regulates entry of membrane proteins into the ciliary membrane domain in epithelial cells. J Cell Biol, 2011. 193(1): p. 219-33.

10. Yates, J.R., C.I. Ruse, and A. Nakorchevsky, Proteomics by mass spectrometry: approaches, advances, and applications. Annu Rev Biomed Eng, 2009. 11: p. 49-79.

11. Mitchell, K.A., Isolation of primary cilia by shear force. Curr Protoc Cell Biol, 2013. Chapter 3: p. Unit 3 42 1-9.

12. Mohieldin, A.M., et al., Protein composition and movements of membrane swellings associated with primary cilia. Cell Mol Life Sci, 2015.

13. Washburn, M.P., D. Wolters, and J.R. Yates, 3rd, Large-scale analysis of the yeast proteome by multidimensional protein identification technology. Nat Biotechnol, 2001. 19(3): p. 242-7.

14. Martin-Alonso, J.M., et al., Molecular cloning of the bovine CD9 antigen from ocular ciliary epithelial cells. J Biochem, 1992. 112(1): p. 63-7.

15. Matsuda, A., et al., Detection and immunolocalization of macrophage migration inhibitory factor in rat iris and ciliary epithelium. Immunol Lett, 1996. 53(1): p. 1-5.

16. Jersmann, H.P., Time to abandon dogma: CD14 is expressed by non-myeloid lineage cells. Immunol Cell Biol, 2005. 83(5): p. 462-7.

17. Iwanaga, T., Y. Hozumi, and H. Takahashi-Iwanaga, Immunohistochemical demonstration of dopamine receptor D2R in the primary cilia of the mouse pituitary gland. Biomed Res, 2011. 32(3): p. 225-35.

18. Christopher, G.K. and C.A. Sundermann, Isolation and partial characterization of the insulin binding sites of Tetrahymena pyriformis. Biochem Biophys Res Commun, 1995. 212(2): p. 515-23.

19. Al-Jamal, R.T. and T. Kivela, Prognostic associations of insulin-like growth factor-1 receptor in primary uveal melanoma. Can J Ophthalmol, 2011. 46(6): p. 471-6.

20. Yeh, C., et al., IGF-1 activates a cilium-localized noncanonical Gbetagamma signaling pathway that regulates cell-cycle progression. Dev Cell, 2013. 26(4): p. 358-68.

21. Gerdes, D., et al., Cloning and tissue expression of two putative steroid membrane receptors. Biol Chem, 1998. 379(7): p. 907-11.

22. Nutu, M., et al., Distribution and hormonal regulation of membrane progesterone receptors beta and gamma in ciliated epithelial cells of mouse and human fallopian tubes. Reprod Biol Endocrinol, 2009. 7: p. 89.

23. Teilmann, S.C. and S.T. Christensen, Localization of the angiopoietin receptors Tie-1 and Tie-2 on the primary cilia in the female reproductive organs. Cell Biol Int, 2005. 29(5): p. 340-6.

24. Bouley, R., et al., Bypassing vasopressin receptor signaling pathways in nephrogenic diabetes insipidus. Semin Nephrol, 2008. 28(3): p. 266-78.

25. Raychowdhury, M.K., et al., Vasopressin receptor-mediated functional signaling pathway in primary cilia of renal epithelial cells. Am J Physiol Renal Physiol, 2009. 296(1): p. F87-97.

26. Huang, J., et al., BCL10 as a new candidate gene for immune response in pigs: cloning, expression and association analysis. Int J Immunogenet, 2010. 37(2): p. 103-10.

27. Chardon, P., C. Renard, and M. Vaiman, The major histocompatibility complex in swine. Immunol Rev, 1999. 167: p. 179-92.

28. Yamada, Y., et al., [Studies on the concentration of surgical stress-related cytokines in exudate from operative wound or cavity: preliminary report]. Nihon Geka Gakkai Zasshi, 1991. 92(6): p. 760.

29. Pahl, J.H., et al., Expression of the immune regulation antigen CD70 in osteosarcoma. Cancer Cell Int, 2015. 15: p. 31.

30. Gustafsson, K., et al., Structure of miniature swine class II DRB genes: conservation of hypervariable amino acid residues between distantly related mammalian species. Proc Natl Acad Sci U S A, 1990. 87(24): p. 9798-802.

31. Kaur, S., et al., CD47 signaling regulates the immunosuppressive activity of VEGF in T cells. J Immunol, 2014. 193(8): p. 3914-24.

32. Ley, B., K.K. Brown, and H.R. Collard, Molecular biomarkers in idiopathic pulmonary fibrosis. Am J Physiol Lung Cell Mol Physiol, 2014. 307(9): p. L681-91.

33. Zhao, W.Q., et al., CD40 mutant expression and its clinical significance to prognosis in gastric cancer patients. World J Surg Oncol, 2014. 12: p. 167.

34. Wajant, H., The Fas signaling pathway: more than a paradigm. Science, 2002. 296(5573): p. 1635-6.

35. Pham, D.H., et al., Enhanced expression of transferrin receptor 1 contributes to oncogenic signalling by sphingosine kinase 1. Oncogene, 2014. 33(48): p. 5559-68.

36. Wang, S.K., et al., ITGB6 loss-of-function mutations cause autosomal recessive amelogenesis imperfecta. Hum Mol Genet, 2014. 23(8): p. 2157-63.

37. Hobiger, K. and T. Friedrich, Voltage sensitive phosphatases: emerging kinship to protein tyrosine phosphatases from structure-function research. Front Pharmacol, 2015. 6: p. 20.

38. Chengle, H., D. Kaihong, and B. Fuzhi, Association analysis of the poliovirus receptor related-2 gene in patients with nonsyndromic cleft lip with or without cleft palate. DNA Cell Biol, 2010. 29(11): p. 681-5.

39. Wessel, T., U. Schuchter, and H. Walt, Ciliary motility in bovine oviducts for sensing rapid non-genomic reactions upon exposure to progesterone. Horm Metab Res, 2004. 36(3): p. 136-41.

40. West, J., et al., Rescuing the BMPR2 signaling axis in pulmonary arterial hypertension. Drug Discov Today, 2014. 19(8): p. 1241-5.

41. O'Leary, D.D. and D.G. Wilkinson, Eph receptors and ephrins in neural development. Curr Opin Neurobiol, 1999. 9(1): p. 65-73.

42. Ikeo, K., et al., Junctional adhesion molecule-A promotes proliferation and inhibits apoptosis of gastric cancer. Hepatogastroenterology, 2015. 62(138): p. 540-5.

43. Mori, K., et al., Kidney produces a novel acylated peptide, ghrelin. FEBS Lett, 2000. 486(3): p. 213-6.

44. Nagaya, N., et al., Chronic administration of ghrelin improves left ventricular dysfunction and attenuates development of cardiac cachexia in rats with heart failure. Circulation, 2001. 104(12): p. 1430-5.

45. Wang, L., et al., Molecular cloning, characterization and three-dimensional modeling of porcine nectin-2/CD112. Vet Immunol Immunopathol, 2009. 132(2-4): p. 257-63.

46. Mayer, U., et al., Proteomic analysis of a membrane preparation from rat olfactory sensory cilia. Chem Senses, 2008. 33(2): p. 145-62.

47. Liu, Q., et al., The proteome of the mouse photoreceptor sensory cilium complex. Mol Cell Proteomics, 2007. 6(8): p. 1299-317.

48. Mayer, U., et al., The proteome of rat olfactory sensory cilia. Proteomics, 2009. 9(2): p. 322-34.

49. Ishikawa, H., et al., Proteomic analysis of mammalian primary cilia. Curr Biol, 2012. 22(5): p. 414-9.

Appendix A

Supplemental Data and Methods for Chapter 2

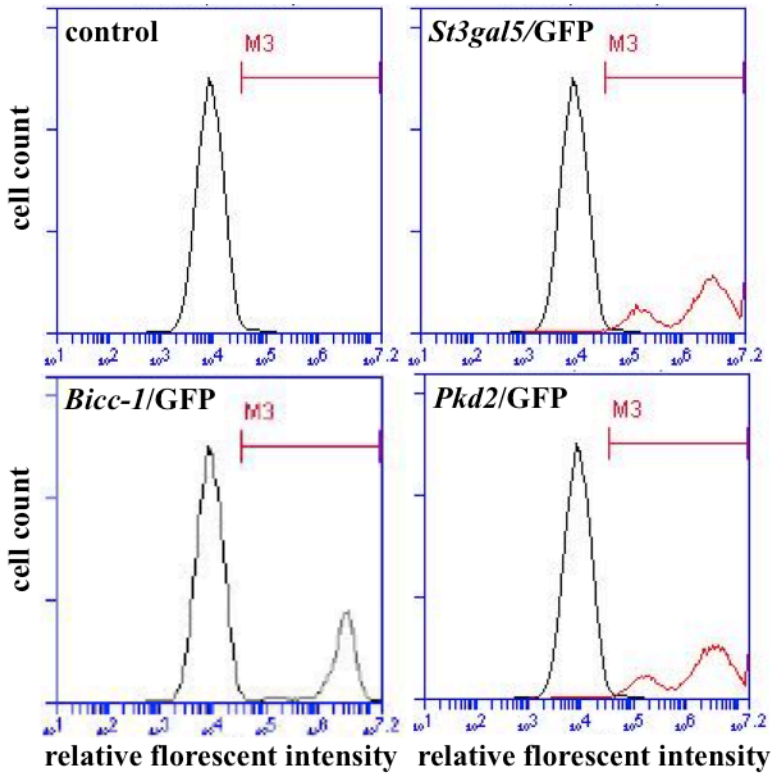

Supp Figure A-1 Stable *Bicc-1, St3gal5* and *Pkd2* knockdown cell lines were generated.

The shRNA-GFP knockdown efficiency in LLCPK cells was verified with flow cytometer. Stable *Bicc-1, St3gal5* and *Pkd2* cell lines showed a high knockdown efficiency as depicted by GFP signal intensity (M3 gated channel).

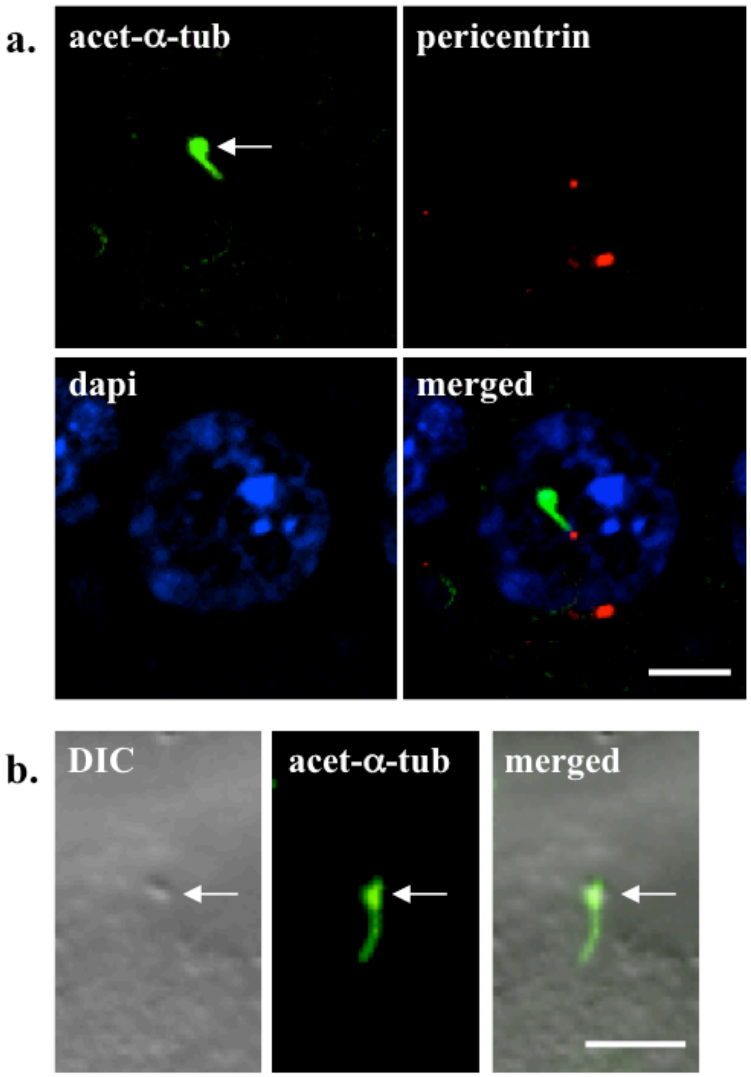

Supp Figure A-2 Ciliary membrane swelling was detected in mouse vascular endothelial cells.

Both standard (**a**) and formvar (**b**) techniques were used to show the presence of ciliary bulb in relatively short endothelial cilia. Acetylated-α-tubulin (green) was used as ciliary marker, whereas pericentrin (red) and DAPI (blue) were used as centrosomal and nuclear markers, respectively. Arrows indicate the presence of ciliary bulbs at the tip of cilia. Bar=3 mm.

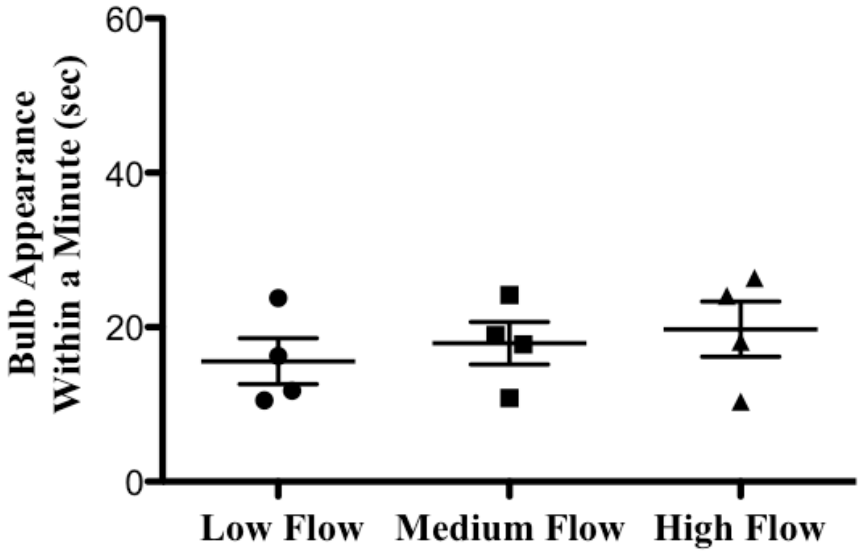

Supp Figure A-3 Flow-induced ciliary swelling formation was magnitude- and time-independent events.

To examine if the magnitude of shear stress would induce swelling formation differentially, we challenged the cells at low (10.3±2.1 mL/min), medium (21.6±2.4 mL/min) or high (35.3±1.1 mL/min) flow rate. Because the appearance of the swelling was so random (time-independent), we calculated those cells that responded to flow-induced bulb formation within a minute. All in all, flow-induced bulb formation was observed in about 80-90% of the cells. For those cells that responded to fluid-shear stress within a minute, there was no indication that magnitude of fluid-shear stress would differentially affect bulb formation (magnitude-independent).

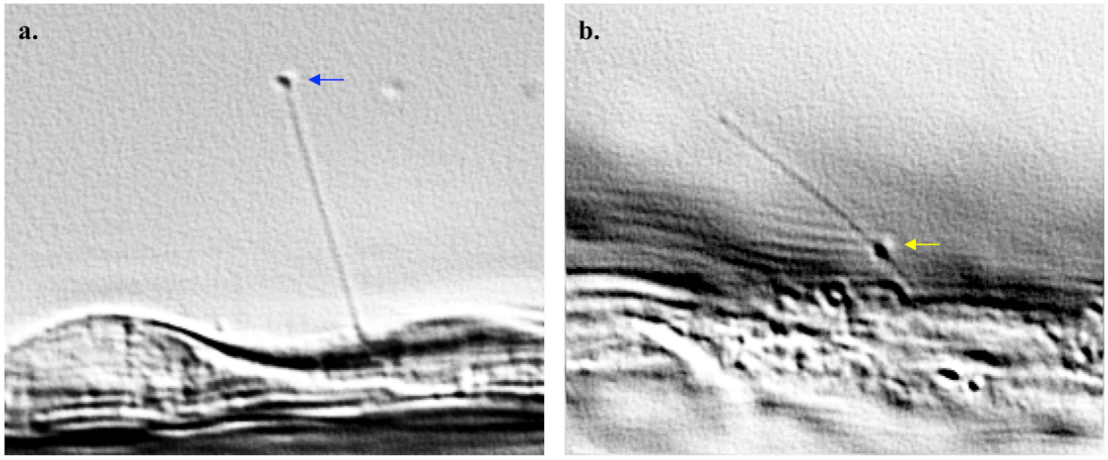

Supp Figure A-4 Ciliary membrane swelling was differentially positioned in static and flow conditions.

Most swellings were positioned around the mid of ciliary shaft in static no-flow condition, but they tended to move to the tip of cilia under fluid-shear stress (**Figure 2.2**). In about 10% of cases, however, the bulb would move to the tip of a cilium momentarily before move back along the ciliary shaft (**a**). Furthermore, in a very rare occasion the bulb could maintain at the bottom of a cilium under fluid-fluid flow (**b**).

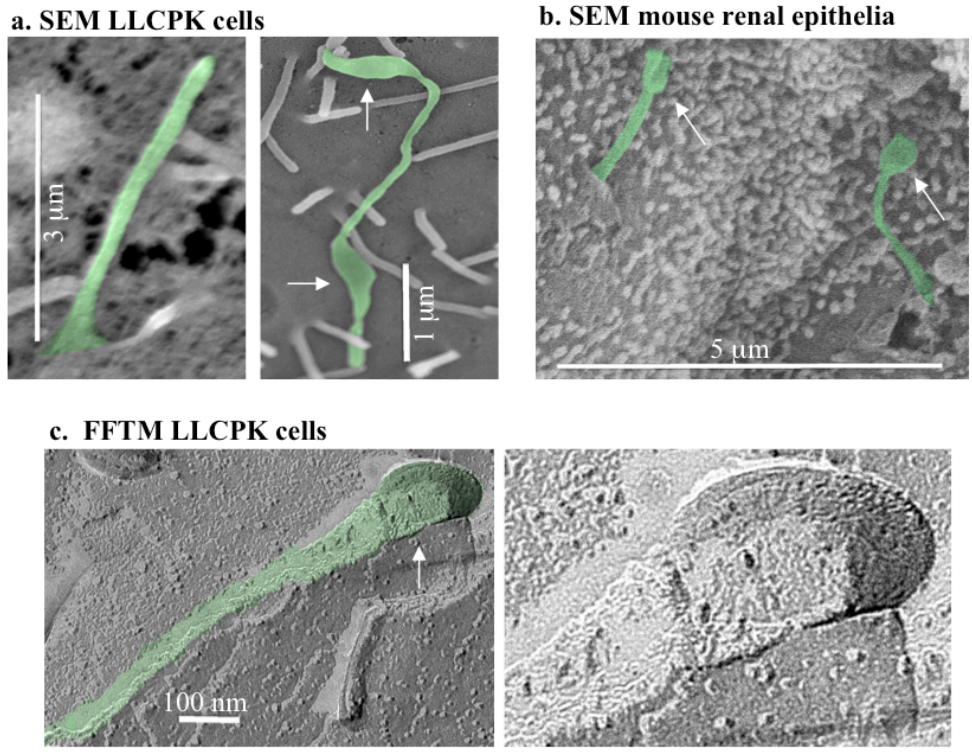

Supp Figure A-5 Ciliary membrane swelling was detected in renal epithelial cells *in vitro* and *in vivo*, and it contained integral proteins.

Scanning electron microscope revealed the absence (left panel) and presence (right panel) of ciliary swelling in LLCPK cells (**a**). The ciliary swelling was also seen in mouse renal epithelia (**b**). Two representative images were independently taken showing that the ciliary swelling was an integral structure of the ciliary membrane. Further studies with freeze fracture transmission microscopy (FFTM) further demonstrated the presence of ciliary swelling at the tip of cilium with residual integral proteins on the cilia and swelling region (**c**). Right panel shows an enlargement image from the left image. All primary cilia were pseudocolored with green, and white arrows point to ciliary bulbs.

Supplemental Movies

Movie A-6. Movement of ciliary membrane swelling under static condition

Primary cilium of an LLCPK renal epithelium showed the dynamic movement of ciliary swelling oscillating up and down along the ciliary shaft. The ciliary swelling never reached to the tip of the cilium. The black arrow points at the ciliary swelling. Time is shown in minute:second.

Movie A-7. The additional appearance of new ciliary bulb during flow-shear stress.

Primary cilium of an LLCPK renal epithelium showed the sensitivity of ciliary swelling in response to mechanical stimulus. A small pulse of fluid flow, enough to generate a small movement on the cilium, induced the appearance of another bulb (red arrow) along with the preexisting bulb (black arrow). Both ciliary swellings moved to the tip of the cilia during the course of the fluid-flow, but they returned to move dynamically along the ciliary shaft when fluid-flow was ceased. Time is shown in minute:second.

Movie A-8. The appearance of ciliary membrane swelling from the middle of the ciliary shaft.

Ciliary swelling could be induced by fluid-flow from the middle of ciliary shaft (red arrow) in an LLCPK renal epithelium. Time is shown in minute:second.

Supplemental Methods

Flow cytometer

All stable cell line *St3gal5-GFP*, *Bicc1-GFP* and *Pkd2-GFP* were further analyzed for GFP expression efficiency. Prior to analysis, cells were rinsed with 1X PBS, detached with trypsin, pelleted at 4000 rpm, resuspended in PBS and analyzed using C6 Flow Cytometer (*Accuri Cytometers*, MI, USA).

Scanning electron microscopy (SEM)

Briefly, cells were fixed with 2.5% of glutaraldehyde in 0.085 M cacodylate buffer for 1 hour and then washed with cacodylate buffer for 5 minutes. A 1% of osmium tetroxide in 0.085 M cacodylate buffer was used for 10 minutes and dehydrated the samples through a graded series of ethanol. The sample was then infiltrated with hexamethyldisilazane and left air dry overnight. The sample was then coated with gold particles and examined (*Hitachi* S-4800).

Freeze Fracture Transmission Electron Microscopy (FFTEM)

Sample was prepared on replica specimens prepared by combining high pressure freezing and freeze fracture. LLCPK cells were grown directly inside gold-plated FF carriers, and they were then cryo-fixed with the original culture media in a Leica EM Pact 2 high-pressure freezer. To optimize sample preparation, we also replaced the culture media in some of the carriers with 20% dextran solution (40K Mr) right before the freezing, which did not result in noticeable difference. After high pressure freezing, the carriers were

quickly transferred into a freeze-fracture vacuum chamber (*BalTec BAF060*) and fractured at -165°C. The topography of the fractured surface was then replicated by the deposition of a thin (~4 nm) Pt/C layer at 45° followed by a continuous carbon film (~20 nm) deposited normally to the surface. The replicas were collected by holey lacey carbon grids after dissolving all the culture media with water, and investigated in a FEI Tecnai F20 TEM operated at 200 KV.

Appendix B

Supplemental Data for Chapter 3

Movie B-1| Fluid-shear stress induces cilium bending and ciliary bulb movement. Recording of *LLC-PK* cell using DIC imaging to show cilia bending and movement of cilia bulb (green arrows) along the ciliary shaft in response to fluid shear stress (flow) conditions. Time is denoted in seconds.

Appendix C

List of Articles Published Based on this Dissertation

1. Mohieldin, Ashraf M. et al. "*Autosomal Dominant Polycystic Kidney Disease: Pathophysiology and Treatment*." Ed. Denis M. Lanza. Autosomal Dominant Disorders: New Research. Ed. Pietro Marciano. New York: Nova Science Publisher, 2013. 1-32. Print.

2. Mohieldin, A.M., et al., *Protein composition and movements of membrane swellings associated with primary cilia.* Cell Mol Life Sci, 2015. **72**(12): p. 2415-29.